
MASTER THESIS

STATISTICAL ENERGY ANALYSIS FOR ROOM ACOUSTICS

conducted at the
Signal Processing and Speech Communications Laboratory
Graz University of Technology, Austria

by
Nikolaus Fankhauser, 1073079

Supervisor:
Dipl.-Ing. Jamilla Balint

Assessor/Examiner:
Univ.-Prof. Dipl.-Ing. Dr. Gerhard Graber

Graz, October 2016

Statutory Declaration

I declare that I have authored this thesis independently, that I have not used other than the declared sources/resources, and that I have explicitly marked all material which has been quoted either literally or by content from the used sources. The text document uploaded to TUGonline is identical to the present master thesis.

date

(signature)

Abstract

The following master thesis deals with Statistical Energy Analysis for room acoustics. In the first chapters of the work SEA is introduced and the theory of SEA is described. Based on the energy equations of simple resonators for different excitation scenarios, the calculations are extended to coupled systems and it is presented how to determine the energy equations for complex systems. The goal of this thesis is to calculate the energy decay curves (that means temporally dependent and not stationary results) of different rooms with SEA: at first the easiest case of a rectangular room is described, then the energy decay curves of coupled rooms are dealt with and in the last experiment a rectangular room containing plates is discussed. Moreover it is shown how the reverberation time of the analysed rooms can be determined based on the decay curves. The three experiments are evaluated by comparing the results with methods used in literature and measurements respectively. Therefore a method is developed that can be used to simulate the reverberation time of rooms.

Kurzfassung

Die vorliegende Masterarbeit behandelt die Methode der statistischen Energieanalyse für Anwendungen der Raumakustik. In den ersten Kapiteln der Arbeit wird die Theorie der statistischen Energieanalyse beschrieben. Ausgehend von den Gleichungen, die die Energieverteilung in simplen Resonatoren für verschiedene Anregungen beschreiben, werden die Herleitungen auf gekoppelte Systeme erweitert. Schließlich werden Berechnungen, die die Energieverhältnisse in komplexen Systemen beschreiben, vorgestellt. Das Ziel der Arbeit ist es, Abklingkurven, das heißt keine stationären, sondern zeitabhängige Ergebnisse für verschiedene Raumvarianten mittels SEA zu ermitteln. Zu Beginn wird dazu ein rechteckiger Raum beschrieben, die Methoden werden danach auf gekoppelte Räume umgelegt und zum Schluss wird ein Raum, der Diffusoren enthält, diskutiert. Es wird auch gezeigt, dass basierend auf den Abklingzeiten von Räumen, die Nachhallzeit der behandelten Räume berechnet werden kann. Die drei erwähnten Experimente werden durch Vergleich der Resultate mit Methoden, die in der Literatur verwendet werden bzw. durch Vergleich mit Messergebnissen evaluiert. Somit wird ein Verfahren entwickelt, das zur Simulation von Nachhallzeiten verwendet werden kann.

Acknowledgement

At first I want to thank all the persons that made the writing of this master thesis possible:

Many thanks to Prof. Gerhard Graber who was primarily responsible for the supervision of this work. As I first asked him, if he could offer me a topic for a master thesis, he was always willing to find an interesting topic. He always supported me on organisational questions and had many nice inputs that definitely improved the thesis.

Jamilla Balint, who supervised from the day the topic was fixed, thank you very much for your great support. It was always possible to talk to you about all problems, no matter if they were organisational or technical questions. Thank you for all the meetings we had and emails we wrote and the time we spent together to discuss about the topic. We always had a clear goal and I really liked the pleasant atmosphere that characterized our cooperation. Once again, thank you very much for your help and support!

Thanks to my parents that made my studying possible and who did everything for me to get a good education. You also showed me that life is not always fun and that you have to fight sometimes to reach your targets. Thank you for all the things you enabled me, for your support in situations that were not so easy and for your forgiving when I made mistakes.

I also want to thank my brothers and my sister for the nice times we spent together. As youngest family member I had the chance to learn from you, but we also had lots of fun, e.g. when playing football together or drinking a glass of beer.

Last but not least I want to thank my girlfriend Anna: You always had an open ear for my problems, you had the ability to make me think on different topics, when I had to learn very much and you built me up and encouraged me in difficult situations. It is a good feeling to have you on my side and I really thank you for all the nice things we experienced together.

Contents

1	Introduction	1
1.1	Motivation and Overview	1
2	Statistical Energy Analysis	3
2.1	Basics of SEA	3
2.2	Historical Overview	4
2.3	The General Procedures of SEA	5
3	Energy Discription of Vibrating Systems	8
3.1	Modal Resonators	8
3.1.1	Free Vibration - No Damping	9
3.1.2	Free Vibration with Damping	10
3.1.3	Sinusoidal forced Vibration	11
3.1.4	Random Excitation	14
3.2	Modal Analysis of Distributed Systems	17
3.2.1	Response of System to Point Force Excitation	20
3.3	Dynamics of Infinite Systems	21
3.4	Mode-Wave Duality	26
4	Energy Sharing by Coupled Systems	32
4.1	Energy Sharing Among Resonators	32
4.2	Energy Exchange in Multi-Degree-of-Freedom Systems	37
4.3	Reciprocity and Energy Exchange in Wave Bearing Systems	41
5	The Estimation of Response Statistics in SEA	47
5.1	Mean Value Estimates of Dynamical Response	47
5.1.1	Single Mode Response	47
5.1.2	Multi-Modal Response	48
5.1.3	Wave Estimates	48
5.1.4	Strain Response	51
5.2	Calculation of Variance in Temporal Mean Square Response	52
5.2.1	Modal Power Flow and Response	53
5.3	Calculation of Confidence Interval	55
6	Procedures of SEA	58
6.1	General Approach of SEA	58
6.2	Defining the System Model	58
6.3	Evaluating the Subsystem Parameters	59
6.4	Evaluating the Response Variables	59
7	Calculation of Reverberation Time with SEA	61
7.1	Division of Room into Subsystems	61
7.2	Determination of Initial Conditions	62
7.3	Calculation of Damping Loss Factors	63
7.4	Calculation of Coupling Loss Factors	65
7.5	Calculation of Damping Factor of Air	68
7.6	Solving the System of Differential Equations	69
7.7	Calculation of T_{60} , T_{30} and T_{20}	70
7.8	Proof of Concept Experiment	72

8	Calculation of Decay Curves of Coupled Rooms with SEA	75
8.1	Calculation of Damping Loss Factors	75
8.2	Calculation of Coupling Loss Factors	76
8.3	Solving the System of Differential Equations	76
8.4	Proof of Concept Experiment	77
8.5	Decay Curves of Different Room Configurations	83
9	Calculation of Decay Curves of Rooms Containing Plates	88
9.1	Radiation Factor	88
9.1.1	Meaning of the Radiation Factor	88
9.1.2	Determination of the Radiation Factor	89
9.2	Calculation of Damping Loss Factors	92
9.3	Calculation of Coupling Loss Factors	93
9.4	Proof of Concept Experiment	94
10	Calculation of Energy Decay Curve of non-rectangular Rooms	97
10.1	Analysis of Energy Decay Curves of non-rectangular Rooms	97
10.2	Energy Decay Curve of non-rectangular Room with Diffusors	101
11	Summary and Outlook	104
11.1	Summary and Outlook	104
11.1.1	Summary of Chapters [2-5]	104
11.1.2	Summary of Chapters [6-10]	104
11.1.3	Outlook	105
12	List of symbols	107
13	Bibliography	111
14	Appendix	113
14.1	Description of Figures	113
14.2	Description of Matlab Files	114

1

Introduction

1.1 Motivation and Overview

This master thesis deals with the calculation of decay curves based on Statistical Energy Analysis. The calculation of reverberation times is an important discipline in room acoustics and can be done, if the energy decay curve of a given room is known. The theory of SEA was developed in the 1960s and since then SEA is used to analyse the acoustics of different situations. SEA can be used to analyse high-frequency vibro-acoustic problems and is also applied to problems where the main transmission paths of energy shall be discovered. The fields in which SEA is mainly used are: analysis of vehicle interior noise (also interior noise of ships and trains is analysed by SEA), vibrations of aircrafts and building acoustics as written in [Sarradj 2004].

SEA can be also used to determine the energy decay curve of a single, rectangular room as supposed in [Pfreundtner 2014] and [Pfreundtner et al. 2015]. The nice thing in these mentioned works is that the energy decay in a room can be calculated dependent on time. The results of this method are time dependent and not steady state results and therefore it is possible to calculate the reverberation time of the analysed room with this method.

In the following work the method presented in [Pfreundtner 2014] is extended to calculate the energy decay curve of coupled rooms and rooms that contain plates. Moreover it is examined if the method could be applied to non-rectangular rooms too. Based on the energy decay curve other variables of acoustics can be derived, e.g. the reverberation time, which is presented in the practical part of the work. The application of SEA for room acoustic problems makes sense because the effort is less compared to other methods used in room acoustics, e.g. ray tracing or FEM and the application of the method is very simple. In SEA the designer does not have to rebuild the room in detail, only the dimensions of the analysed room and the absorption values of the walls of the room have to be known.

This work shows that SEA can be used in different room acoustic scenarios and that the results obtained with SEA are promising. Based on measurement results the results obtained with SEA are evaluated and discussed and it can be seen that SEA is a good method to predict energy decay curves in room acoustics.

In the first five chapters of the work the main theory of SEA is described. The contents of chapters two to six are a summary of the book [Lyon and DeJong 1995] which is the main literature for SEA. The contents of each chapter are summarized in the following section.

Chapter 1: This chapter gives a short introduction in the topic of the master thesis and the contents of the chapters are presented.

Chapter 2: The basic principles of SEA are shortly described in this chapter. The historical overview and the reasons why SEA became famous are also discussed. The chapter is finished with an overview of the procedures used when applying SEA.

Chapter 3: The energy relations in a simple linear resonator are derived based on the solution

of the equation of motion of the resonator. The resonator is excited by different forces and the results are discussed. More complex systems can be described by modal analysis, therefore principles of modal analysis are presented. Then the relations between mode approaches and wave approaches are derived. Theory states that both methods should give the same results.

Chapter 4: The energy sharing of resonators is the basis for deriving the main statements of SEA. Based on the simplest case of energy sharing between two subsystems, the discussions are extended to multi-degree-of-freedom systems. Moreover the reciprocity principle is presented that can be useful when determining coupling loss factors.

Chapter 5: In this chapter the estimation of response statistics for SEA is derived. It is also stated why calculating the variance and the mean is important when dealing with SEA. Furthermore confidence intervals are described that are a tool of probability theory that is often used.

Chapter 6: The chapter gives a short description of how to use SEA in general. At first a system model has to be defined and the parameters that are used in this model have to be determined. It is also shown how the response variables can be obtained.

Chapter 7: The reverberation time of a single room can be obtained by using SEA. The SEA model for a single room is built up. Therefore the room has to be divided into seven subsystems where each subsystem belongs to a mode group. The damping loss factors, coupling loss factors and initial energies for the seven subsystems are derived. By solving a differential equation the energy decay curve of the rectangular room is given. Based on this curve the reverberation time can be calculated. The chapter is finished with a comparison between measurement results and results obtained with the SEA method.

Chapter 8: This chapter deals with the calculation of decay curves of coupled rooms. Equations are presented for the determination of the damping and coupling loss factors and the initial energies in the case of coupled rooms. Based on the knowledge of these values the system of differential equations can be solved and this leads to the result for the decay curve. The new SEA method is compared to a method presented in [Bradley and Wang 2005]. The advantages of the SEA method are highlighted and the SEA method is used for experiments, in which the double slope that is typical for decay curves of coupled rooms, is examined.

Chapter 9: The equations that are needed for the calculation of the decay curve of a room containing a plate are presented. One important factor when calculating the energy decay curve of a room coupled with a plate is the radiation factor of the plate. Therefore the meaning of this factor and analytical formulas for calculating this factor are shown. The results obtained with the SEA method in case of a room coupled with three plates are compared to measurement values.

Chapter 10: In this chapter the SEA method is used to calculate the energy decay curve of non-rectangular rooms. The results obtained with the SEA method are compared to measurement results that were made in a reverberation chamber. Finally the reverberation times for five different setups are presented in tables, where the measurement values are compared to the predicted values obtained with the SEA method.

2

Statistical Energy Analysis

2.1 Basics of SEA

The theory of Statistical Energy Analysis (SEA) was introduced in the early 1960s. The term describes important properties of the method.

- *Statistical* means that the results obtained with this method are expected values and that the variables are part of statistical populations of analogue design construction. The distributions of the dynamical parameters of these constructions are common.
- *Energy* emphasises that the variables of interest are energy variables. In SEA the system under test is evaluated in terms of stored, dissipated and exchanged energies of vibration. Other variables of acoustics, e.g. displacement or sound pressure can be determined based on the energy of vibration.
- *Analysis* denotes that SEA is not a specific technique but a general approach.

In dynamical systems statistical methods have been in use for a long time. In mechanics, statistical approaches are applied to describe deterministic systems that are excited by a vibration that is random in time, e.g. a plate that is excited by a point force. One basic aspect of SEA is that it treats the vibrating system as part of a statistical population or ensemble. The temporal behaviour of the system can be either random or deterministic. In conventional analysis of the mechanical vibration of systems the main focus lies on the analysis of the low frequency range. In most cases systems are excited by low frequencies which also cause the greatest displacement response¹. But with the introduction of large and lightweight structures in the aerospace industry the interest on higher order modal analysis has strongly increased. Goal of this analysis is to predict structural fatigue, equipment failure and noise production of the system under test. The analysis of higher order modes is difficult because the systems' resonance frequencies and mode shapes strongly depend on the accuracy of the modal parameters, i.e. geometry, construction, and material properties. Furthermore computer programs that calculate the mode shapes and frequencies² are not exact for higher order modes and therefore it makes sense to apply a statistical model for evaluating the modal parameters.

It is not only appropriate to use statistical methods from the nature of the dynamical problem, but there is also reason for statistical approaches from the viewpoint of application. Designers are often forced with the problem to predict systems' behaviour in stages at a project where the structural details are unknown. In these stages highly detailed analysis that requires specific knowledge of the system is not meaningful, it is better to analyse the systems with statistical methods at these stages of a project. In statistical approaches the knowledge of the exact parameters is less important.

Two disciplines of physics inspired the early developments of the SEA approach: (1) the theory

¹ In mechanics displacement is the result of the change of the configuration of a body

² FEM: Finite Element Method

of room acoustics and (2) statistical mechanics.

(1) In room acoustic systems many degrees of freedom are excited. It is no curiosity that a good sized room has over a million of modes in the audible frequency range. The theory of room acoustics also describes the interaction between systems of many degrees of freedom, e.g. sound transmission through a wall. The analysis that is done in room acoustics is based on both modal analysis and wave models. Because of the fact that room acoustic systems contain many degrees of freedom, it is highly justified to use statistical methods for the prediction of the behaviour of the system under test.

(2) In statistical mechanics the random motion of systems that are described can have a few or many degrees of freedom. All modes of these systems, independent of their resonance frequencies have nearly equal energies and nearly incoherent motions, i.e. equipartition of energy. Equipartition of energy means that all the modes have the same energy, i.e. the state of equal modal energy. In SEA the term equipartition of energy is sometimes used for modes that have their resonance frequencies in the same frequency band. A related discipline to statistical mechanics is heat transfer. The theory of heat transfer states that the thermal energy flows from hotter to cooler systems. It also says that the intensity of the flow is proportional to temperature difference. This theory can be used to describe dynamical systems where the excitation source is broad band noise. Narrow band sources have the same effects as broad band sources if system averages are calculated.

The greatest advantage of statistical analysis compared to other methods, e.g. modal or wave analysis is that the system under test can be described in a simpler way. In modal or wave analysis a number of input parameters must be known. This is not the case in statistical analysis. The disadvantage of statistical methods is that the results achieved with these approaches are always uncertain to some extent because the results are average values over an ensemble of systems and therefore differ from the results of the actually analysed system. This is not a big problem in systems with a large number of modes because in such systems the fluctuations will vanish. By calculating the mean, variance and the confidence intervals for predictions, the uncertainty of the results can be described and the designers can decide whether they trust the results or not.

2.2 Historical Overview

Two independent studies carried out by Lyon and Smith in 1959 set the basis for introducing the name SEA. Lyon's calculations dealt with two lightly coupled linear resonators. He described the power flow between these resonators when they were excited by independent white noise sources. His results showed that the power always went from the resonator with higher energy to the one with lower energy. His work also showed that the energy exchanged between the resonators was proportional to the uncoupled energies of the resonators. Smith's calculations [Smith 1962] dealt with a resonator that was excited by a diffuse and broad band sound field. When the radiation damping passed the internal damping of the resonator, the response of the system showed a limit. Smith's calculations also showed that this limit was not related to the exact value of the radiation damping. This is somehow strange because if a resonator without damping is excited by broad band noise its response should go to infinity. But the limit Smith found exists because of the reaction of the sound field on the resonator. This is called radiation damping. In 1960 Lyon and Smith began to work together and found out that their calculations described the same phenomenon: *Power flows between systems until equilibrium is reached*. Later Lyon and Maidanik [Lyon and Maidanik 1962] answered the question how the

findings by Smith and Lyon could be connected. In this work they found the basic parameters that are needed for SEA response predictions:

- modal density,
- damping loss factor and
- coupling loss factor.

Because of Smith's result the first applications of SEA dealt with sound-structure interaction, e.g. room connected with plate, but soon also structure-structure interactions, e.g. two connected plates, were described with this new method. In the beginning only two coupled systems (like two plates) could be described but an extension to three and then many coupled systems was developed. SEA became a famous method in the field of acoustics and therefore also many computer programs³ were developed that could deal with SEA calculations.

2.3 The General Procedures of SEA

SEA is a procedure for describing and calculating the energy flow and the storage of dynamical energy in a complex system. The general procedures of SEA shall be shortly described in the following section.

In SEA a complex system is divided into energy storage elements or so called "subsystems" that are groups of "similar modes". Each storage element can be described by energy input that usually comes from a random and external source. Moreover the energy dissipation from the system's damping and from the energy transfer between the subsystems describes the storage element. The SEA model is analogue to that of an electric R-C circuit. In the SEA model, energy is the equivalent to the electric charge in the R-C model and modal energy is the equivalent to electrical potential. In Fig. (2.1) a typical SEA model can be seen that consists of four subsystems. In Fig. (2.1) E_i stands for the energy that is stored in the i^{th} subsystem, N_i stands for the number of modes of the i^{th} subsystem, $\Pi_{i,in}$ describes the amount of energy that is fed into the subsystem, $\Pi_{i,j}$ stands for the energy that flows from subsystem i to subsystem j and $\Pi_{i,diss}$ says how much energy is dissipated in the i^{th} subsystem. By knowing the information on injected power and the system parameters, i.e. N_i , E_i , $\Pi_{i,j}$ and $\Pi_{i,diss}$ the energy flow through the complex system can be analysed. The equations that describe a complex system are linear equations that can be written down in matrix form and can be solved using the methods of linear algebra.

Subsystems are the fundamental elements of the SEA model and are defined as group of "similar" energy storage modes. Subsystems, e.g. an acoustic volume, a beam or a bulkhead are sections of the complex system under test that contain modes of the same type (flexural, torsional, and acoustical). Subsystems should fulfill the criteria of similarity and significance:

- Similarity says that the behaviour of the modes of a subsystem should be nearly equal. This means that they should be nearly equally excited by the sources, should have equal damping and equal coupling to modes of other subsystems.
- Significance means that only subsystems that play an important role in describing the general system are taken into consideration. Including subsystems that are not important in terms of transmission, dissipation and storage of energy into the analysis does not lead to errors but can complicate the calculations.

³ e.g. SEAM, VA One SEA Module or SEA+

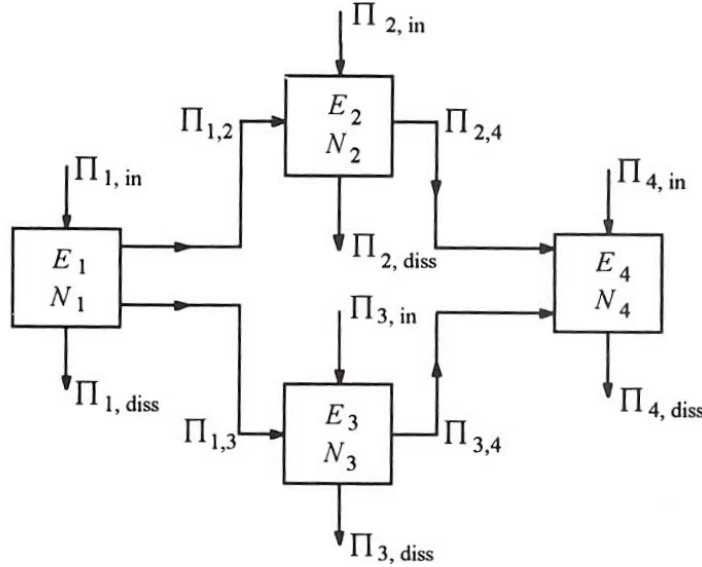


Figure 2.1: General SEA model containing of four subsystems [Lyon and DeJong 1995], p.10

The input power to a subsystem, defined as Π_{in} is usually computed for a one-third or a full octave band. The source of the input power can be a turbulent boundary layer, acoustical noise or mechanical excitation. The input power should not be sensitive to the coupling between subsystems. If this is the case the system that makes Π_{in} available with its internal dynamics has to be respected in the calculations.

The power that is dissipated by a subsystem named Π_{diss} is directly connected to the energy stored in that subsystem. Π_{diss} describes the energy that is lost because of the mechanical vibration of the subsystem. There are different reasons for energy losses, e.g. dissipation by friction or viscosity, radiation into the air, etc. Dissipated energy cannot be returned to the system, if it could, another subsystem or coupling path had to be added to the model. The power transmission between two subsystems defined as Π_{12} describes the amount of energy exchange between two subsystems. As described by the theory of heat transfer Π_{12} depends on the difference in modal energy of subsystems 1 and 2. Another influence to the values of Π_{12} is the strength of the coupling between the subsystems. SEA uses only time averaged energy quantities.

To evaluate the quantities that are shown in Fig. (2.1) the so called SEA parameters are needed. Most of them were defined before SEA was developed. The SEA parameters can be divided into a group of “energy storage” and “energy transfer” parameters.

- The group of energy storage parameters contains the number of modes N_1, N_2, \dots for each subsystem in a defined frequency band $\Delta\omega$. In SEA calculations the number of modes N_i is not always available and therefore often replaced by the modal density n that is defined by the quotient $\frac{N}{\Delta\omega}$.
- The group of energy transfer parameters consists of the input impedance to the system, the source impedances to calculate the input power, the loss factor and the coupling loss factor.

To evaluate the response of a system, the structure is divided into subsystems, then the mentioned parameters are determined and in the last step the overall system response is calculated. The first step in the computation of the system response is the solution of the linear algebraic equations to get the vibrational energy of each subsystem. In practice the number of these

equations, for every subsystem one equation is needed, is quite large and therefore computer programs are used to solve the calculations. Based on the vibrational energy other variables such as displacement, stress, pressure, etc. can be computed because the vibrational energy is related to the velocity of motion. It is important to know that all these variables are spatially averaged in SEA.

In the following chapter the energy conditions of a simple linear resonator that consists of a stiffness element, a mass and a mechanical resistance are derived and the results discussed. The energy equations of a simple linear resonator are the basis to extend the system to coupled resonators and describe the energy flow between resonators.

3

Energy Discription of Vibrating Systems

At the beginning of this chapter the energetics of a simple linear resonator are discussed. In Sec. (3.2) the resonator is used to describe the dynamics of the modal displacements in multi-degree-of-freedom (dof) systems.

3.1 Modal Resonators

The resonator that is shown in Fig. (3.1) consists of a mechanical resistance R , a mass M and a spring or stiffness element K . In the described system several forces occur:

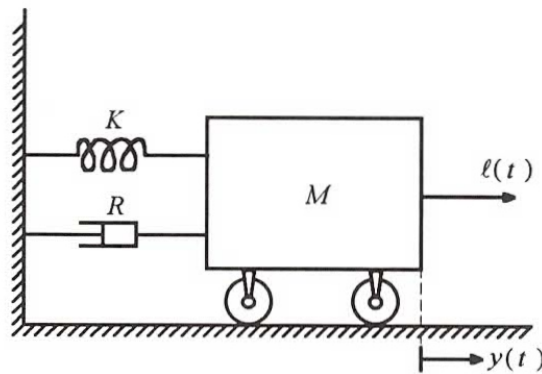


Figure 3.1: Linear Resonator [Lyon and DeJong 1995], p. 18

- R is the reason for the force $-R\dot{y}$ that acts in the opposite direction to the velocity \dot{y} of M
- the stiffness element K is the reason for a force $-Ky$ that points in the opposite direction to displacement $y(t)$ from the equilibrium position of the mass
- the third force is an external force $l(t)$.

The mass is accelerated because of the impact of all these forces. This can be described with the help of a differential equation:

$$l(t) - R\dot{y} - Ky = M\ddot{y}. \quad (3.1)$$

More often this equation is written as:

$$\boxed{\ddot{y} + \omega_0\eta\dot{y} + \omega_0^2y = \frac{l(t)}{M}}, \quad (3.2)$$

where $\omega_0 \equiv \sqrt{K/M}$ is the natural radian frequency and $\eta \equiv R/\omega_0 M$ is the loss factor. In the following sections, three different cases of vibration shall be determined: (1) free vibration without damping (Sec. 3.1.1), free vibration with damping (Sec. 3.1.2) and the case of sinusoidal forced vibration (Sec. 3.1.3).

3.1.1 Free Vibration - No Damping

For the analysis of the case *free vibration - no damping* the function $l(t) = 0$ in Eq. (3.1) and also the loss factor $\eta = 0$, i.e. no damping. By applying these two modifications Eq. (3.1) results in:

$$\ddot{y} + \omega_0^2 y = 0, \quad (3.3)$$

which is a homogeneous, linear differential equation of second order. Such equations can be solved by the so called ‘‘ansatz method’’. By using this method the general solution of Eq. (3.3) is:

$$y = A \cos(\omega_0 t) + B \sin(\omega_0 t) = C \sin(\omega_0 t + \Phi), \quad (3.4)$$

where $\omega_0 = 2\pi f_0$ describes the radian frequency of the free and undamped oscillation of the resonator. A and B (C and Φ) are the amplitudes and can take the value of any real number. The kinetic energy, KE for the mass element and the potential energy PE for the stiffness element at any time can be calculated with the following equations:

$$KE = \frac{1}{2} M \dot{y}^2 = \frac{1}{2} M C^2 \omega_0^2 \cos^2(\omega_0 t + \Phi) \quad (3.5)$$

$$PE = \frac{1}{2} K y^2 = \frac{1}{2} K C^2 \sin^2(\omega_0 t + \Phi). \quad (3.6)$$

The sum E of these two energies is given by

$$\boxed{E = KE + PE = \frac{1}{2} K C^2} \quad (3.7)$$

and depends only on the maximum amplitude of vibration. The system is isolated and not damped. Therefore the vibrational energy should be independent of time, which is fulfilled in the above equation. The period of the displacement and velocity is defined as $\frac{1}{f_0} = \frac{2\pi}{\omega_0}$. The kinetic and the potential energies can be averaged over one period. Averaging a squared sinusoidal function over one period leads to the following equation:

$$\langle \sin^2(\omega_0 t) \rangle_{\sim} = \frac{2\pi}{\omega_0} \int_0^{\frac{2\pi}{\omega_0}} \sin^2(\omega_0 t) dt. \quad (3.8)$$

With

$$1 - 2\sin^2(\omega_0 t) = \cos(2\omega_0 t) \quad (3.9)$$

Eq. (3.8) can be rewritten as:

$$\frac{2\pi}{\omega_0} \int_0^{\frac{2\pi}{\omega_0}} \left(\frac{1}{2} - \frac{1}{2} \cos(2\omega_0 t) \right) dt. \quad (3.10)$$

Solving this integral and simplifying it, the following result is obtained:

$$\frac{\omega_0}{2\pi} \left(\frac{\pi}{\omega_0} - \frac{1}{4\omega_0} \sin(4\pi) \right) = \frac{1}{2}. \quad (3.11)$$

By knowing the result of Eq. (3.11), the averaging of the potential and the kinetic energy over one period results in:

$$\boxed{\langle \text{KE} \rangle_{\sim} = \langle \text{PE} \rangle_{\sim} = \frac{1}{4} K C^2 = \frac{1}{2} E.} \quad (3.12)$$

Discussing this equation one finds out that time average kinetic and potential energies are equal. Furthermore one can see that they are equal to half of the total energy of vibration.

3.1.2 Free Vibration with Damping

In the case of free vibration with damping, $\eta \neq 0$ and respecting this in Eq. (3.2) leads to the following equation:

$$\ddot{y} + \omega_0 \eta \dot{y} + \omega_0^2 y = 0. \quad (3.13)$$

Again the “ansatz method” can be used, therefore y can be written as:

$$y(t) = C e^{\alpha t}. \quad (3.14)$$

Differentiating this equation with respect to time twice and inserting the results in Eq. (3.13) leads to:

$$C e^{\alpha t} (\alpha^2 + \omega_0 \eta \alpha + \omega_0^2) = 0 \quad (3.15)$$

The term in the brackets is called characteristic polynomial. Solving this quadratic equation, α can take two values:

$$\alpha = -\frac{1}{2} \omega_0 \eta \pm j \omega_d, \quad (3.16)$$

where $\omega_d \equiv \omega_0 \sqrt{1 - \eta^2/4}$. And the solution for Eq. (3.13) is:

$$\boxed{y(t) = C e^{-\frac{1}{2} \omega_0 \eta t} \sin(\omega_d t + \Phi).} \quad (3.17)$$

By analysing Eq. (3.17) it can be seen that in the case of free vibration with damping the amplitude of the oscillation decreases exponentially in time. The radian frequency ω_d is the frequency of oscillation and is nearly equal to ω_0 if the loss factor $\eta < 0.3$. If the loss factor fulfills this constraint then the damped oscillation is basically the same as the undamped oscillation. It should be mentioned that this limiting value of the loss factor is very large compared to typical values in most structures and spaces.

As in the case of free vibration without damping the potential energy and the kinetic energy are calculated for the case of free vibration with damping too. In this case the potential energy is:

$$\text{PE} = \frac{1}{2} K y^2 = \frac{1}{2} K C^2 e^{-\omega_0 \eta t} \sin^2(\omega_d t + \Phi) \quad (3.18)$$

For determining the kinetic energy, the derivative of y has to be calculated first:

$$\dot{y} = C \omega_d e^{-\frac{1}{2} \omega_0 \eta t} \cos(\omega_d t + \Phi) - \frac{1}{2} \omega_0 \eta C e^{-\frac{1}{2} \omega_0 \eta t} \sin(\omega_d t + \Phi) \quad (3.19)$$

The kinetic energy can be calculated as shown in Eq. (3.5). Substituting \dot{y} in this equation leads to:

$$\begin{aligned}
\text{KE} &= \frac{1}{2}M\dot{y}^2 \\
&= \frac{1}{2}MC^2e^{-\omega_0\eta t}\left(\omega_d^2\cos^2(\omega_d t + \Phi) - \omega_d\omega_0\eta\cos(\omega_d t + \Phi)\sin(\omega_d t + \Phi) + \frac{1}{4}\omega_0^2\eta^2\sin^2(\omega_d t + \Phi)\right) \\
&= \frac{1}{2}MC^2e^{-\omega_0\eta t}\omega_0^2\left(\frac{\omega_d^2}{\omega_0^2}\cos^2(\omega_d t + \Phi) - \frac{\omega_d}{\omega_0}\eta\cos(\omega_d t + \Phi)\sin(\omega_d t + \Phi) + \frac{1}{4}\eta^2\sin^2(\omega_d t + \Phi)\right) \\
&= \frac{1}{2}MC^2e^{-\omega_0\eta t}\omega_0^2\left(-\frac{\omega_d}{\omega_0}\cos(\omega_d t + \Phi) + \frac{1}{2}\eta\sin(\omega_d t + \Phi)\right)^2. \tag{3.20}
\end{aligned}$$

If these energy equations are averaged over period and if the little change in amplitude that arises because of the exponential multiplier is neglected, the result is much simpler:

$$\boxed{\langle\text{PE}\rangle_{\sim} \simeq \frac{1}{4}KC^2e^{-\omega_0\eta t} = \langle\text{KE}\rangle_{\sim} = \frac{1}{2}\langle E\rangle_{\sim}.} \tag{3.21}$$

The kinetic, potential and total energy in the case of free damped vibration is basically the same as in the case of undamped vibration if $\eta < 0.3$. The following relationship is valid for damped and undamped vibration:

$$\boxed{\langle y\rangle_{\sim} = \langle \dot{y}\rangle_{\sim}/\omega_0^2.} \tag{3.22}$$

In Eq. (3.17) the term in the exponential function is $-\pi\eta t/T$. This means that the amplitude decays with the logarithmic decrement, $\pi\eta$. The oscillations stop when the loss factor is twice the critical damping ratio, ζ , this is the case when $\eta \rightarrow 2$. From Eq. (3.21) it can be seen that:

$$\langle E\rangle_{\sim} = E_0e^{-\omega_0\eta t}. \tag{3.23}$$

A very well known measure of damping in acoustics is the reverberation time T_R . The reverberation time is the time the vibrational energy needs to decrease by a factor of 10^{-6} . By using the exponential term in the last equation, a formula for the reverberation time can be developed:

$$e^{-\omega_0\eta T_R} = 10^{-6}. \tag{3.24}$$

Solving Eq. (3.24) for T_R leads to:

$$\boxed{T_R = \frac{2.2}{f_0\eta},} \tag{3.25}$$

which is a well established formula in acoustics.

3.1.3 Sinusoidal forced Vibration

In the case of a sinusoidal forced vibration the force $l(t)$ applied to the linear resonator in Fig. (3.1) is sinusoidal at radian frequency ω and can be written in exponential form:

$$l(t) = \text{Re}[\mathbf{L}|e^{j(\omega t - \Psi)}], \tag{3.26}$$

where $\text{Re}[\]$ denotes the real part of the complex value. The dynamical equations are linear and the response to the excitation can be treated as the response to the complex excitation and

its complex conjugate. The response variables are therefore complex exponentials too. The complex force and complex velocity are:

$$\begin{aligned} l(t) &= \mathbf{L}e^{j\omega t} \\ \dot{y}(t) &= \mathbf{V}e^{j\omega t}, \end{aligned} \quad (3.27)$$

where \mathbf{L} and \mathbf{V} are complex numbers, i.e. $|\mathbf{L}|e^{-j\Psi}$ and $|\mathbf{V}|e^{-j\Psi}$. The goal is to derive and solve the differential equation in the case of a sinusoidal force. Therefore the velocity must be integrated and differentiated to get \ddot{y} and y :

$$\begin{aligned} \ddot{y}(t) &= \frac{d\dot{y}(t)}{dt} = j\omega\mathbf{V}e^{j\omega t} \\ y(t) &= \int \dot{y}(t)dt = \frac{1}{j\omega}\mathbf{V}e^{j\omega t}. \end{aligned} \quad (3.28)$$

In the next step these new values can be inserted in Eq. (3.2):

$$j\omega\mathbf{V}e^{j\omega t} + \omega_0\eta\mathbf{V}e^{j\omega t} + \omega_0^2\frac{\mathbf{V}e^{j\omega t}}{j\omega} = \frac{\mathbf{L}e^{j\omega t}}{M}. \quad (3.29)$$

Simplifying this equation leads to:

$$\mathbf{L} = \mathbf{V}(j\omega_0M)[(\omega/\omega_0 - \omega_0/\omega) - j\eta] \equiv \mathbf{V}\mathbf{Z}, \quad (3.30)$$

where \mathbf{Z} is the mechanical impedance of the resonator:

$$\mathbf{Z} = (j\omega_0M)[(\omega/\omega_0 - \omega_0/\omega) - j\eta]. \quad (3.31)$$

The reciprocal value of \mathbf{Z} is the mechanical mobility \mathbf{Y} :

$$\mathbf{Y} \equiv \frac{\mathbf{V}}{\mathbf{L}} = [\omega_0\eta M + j(\omega M - K/\omega)]^{-1} \quad (3.32)$$

with $K = M\omega_0^2$ and can be graphically represented as shown in Fig. (3.2). The power fed into the resonator because of the sinusoidal excitation is $\Pi = \langle l\dot{y} \rangle_t$. The time average of the product of complex variables can be written in terms of their complex amplitudes. By using this rule the power can be written as:

$$\begin{aligned} \Pi &= \langle l\dot{y} \rangle_t = \frac{1}{2}Re(\mathbf{L}\mathbf{V}^*) = \frac{1}{2}Re(\mathbf{L}\mathbf{L}^*\mathbf{Y}^*) \\ &= \frac{1}{2}|\mathbf{L}|^2Re(\mathbf{Y}^*) = \frac{1}{2}Re(\mathbf{V}\mathbf{V}^*\mathbf{Z}) = \frac{1}{2}|\mathbf{V}|^2Re(\mathbf{Z}), \end{aligned} \quad (3.33)$$

where * stands for the complex conjugate. The real part of \mathbf{Y} is:

$$Re(\mathbf{Y}) = Re(1/\mathbf{Z}) = Re(\mathbf{Z})/|\mathbf{Z}|^2 = \omega_0\eta M/|\mathbf{Y}|^2. \quad (3.34)$$

Eq. (3.34) shows that also the input power depends on the frequency as shown in Fig. (3.2). The maximum value of the power is:

$$\Pi = \frac{1}{2}|\mathbf{L}|^2/\omega_0\eta M = \langle l^2 \rangle_t/R.$$

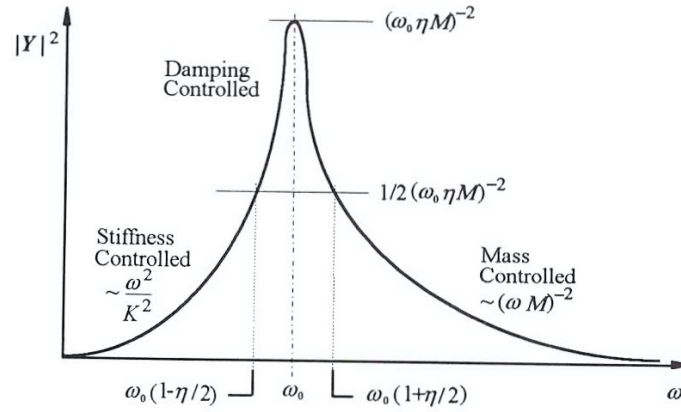


Figure 3.2: Mobility of a linear Resonator as a function of frequency [Lyon and DeJong 1995], p. 22

It is reached if the system has only a resistance i.e. when the imaginary part of the impedance is 0. The power decreases if the resonance frequency of the system is left. Half the value of the maximal power is reached at the frequencies $\omega = \omega_0 \pm \omega_0\eta/2$, when the assumption $\eta < 0.3$ is fulfilled. In the frequency region $\omega < \omega_0(1 - \eta/2)$ R and M can be neglected and the mobility can be described only by the stiffness term:

$$\mathbf{Y} \simeq j\frac{\omega}{K}, \quad (3.35)$$

defining the “stiffness controlled” region. For the frequencies $\omega > \omega_0(1 - \eta/2)$ R and K can be neglected and the mobility is approximated by keeping the mass term only:

$$\mathbf{Y} \simeq -\frac{j}{\omega M}. \quad (3.36)$$

This region is known as “mass controlled”. The region between the stiffness controlled and the mass controlled regions is called “damping controlled” (see Fig. 3.2). In systems with many degrees of freedom these simplified forms of behaviour of the resonator can be very helpful.

One important aspect in the case of sinusoidal excitation is that the resonance can often be better described by examination of the phase of the response than by the amplitude of the response. The phase of a complex variable is in general defined as $\text{Arg}\{\mathbf{X}\} = \tan^{-1}|\text{Im}(\mathbf{X})/\text{Re}(\mathbf{X})|$. The phase of the mobility function is the phase of the velocity with respect to the force and is the same as the phase of \mathbf{Z}^* :

$$\text{Arg}\{\mathbf{Z}^*\} = \tan^{-1}\{|\omega - \omega_0/\omega\}/\omega_0\eta\} = \tan^{-1}\{2(\omega - \omega_0)/\omega_0\eta\}. \quad (3.37)$$

There is a strong change in phase as the system passes through resonance. The smaller the damping the quicker this phase change happens. The behaviour of the phase is in contrast to the behaviour of the amplitude at resonance, because the amplitude has a horizontal slope at $\omega = \omega_0$. This is also the reason why resonance can be better described by the phase than by the amplitude. Another interesting point in discussing the resonator excited by a sinusoidal force is the mean square response at resonance:

$$\langle \dot{y}^2 \rangle = \frac{1}{2}|\mathbf{V}|^2 = \frac{1}{2}|\mathbf{L}|^2/\omega_0^2\eta^2M^2, \quad (\omega = \omega_0). \quad (3.38)$$

The average values of y and \ddot{y} at resonance result in:

$$\langle y^2 \rangle = \frac{1}{2} |\mathbf{V}|^2 / \omega_0^2 = \langle \dot{y}^2 \rangle / \omega_0^2 \quad (3.39)$$

and

$$\langle \dot{y}^2 \rangle = \frac{1}{2} |\mathbf{V}|^2 \omega_0^2 = \omega_0^2 \langle y^2 \rangle. \quad (3.40)$$

These relations that are derived from sinusoidal excitation show the same results as the relations for free vibration. It must be noted here that Eq. (3.39) and Eq. (3.40) are not valid outside the damping controlled region, but can be used with a high degree of accuracy in the bandwidth $|\omega - \omega_0| < \frac{1}{2} \omega_0 \eta$, known as half bandwidth.

3.1.4 Random Excitation

In most applications in which SEA is used the system under test is excited randomly. It should be noted here that the critical features of SEA ask for a statistical model of the system that is excited and not for the excitation itself. But the advantage of a random excitation is that much less averaging of the system parameters has to be done and that there is a smaller variability of the response from the mean. It is difficult to define a random signal accurately. Here, a stationary random signal is derived from an experimental viewpoint. A filter with the frequency response shown in Fig. (3.3) is assumed. The load function $l(t)$ acts as input to this filter.

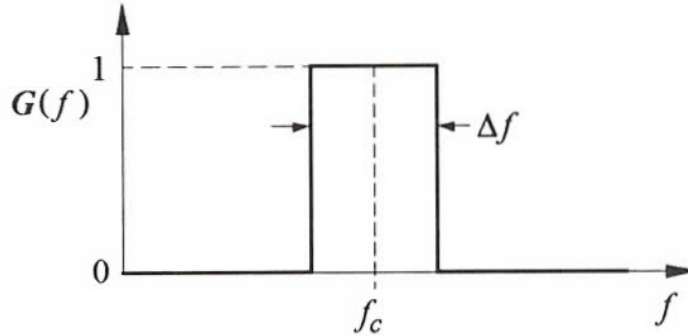


Figure 3.3: Frequency Response of a rectangular filter [Lyon and DeJong 1995], p. 24

The bandwidth Δf of the filter is assumed to be very small. The force applied to the filter can be said to be random if the mean square output of the filter is proportional to Δf . This constraint is not fulfilled by a pure tone, because if the frequency of the tone is a frequency that is contained in the pass band of the filter, the mean square output of the filter would not be dependent on the bandwidth. This last declaration is also true for any deterministic, periodic signal.

The mean square force that belongs to a band of frequencies is defined as:

$$\langle l^2 \rangle_{\Delta f} = \mathbf{S}_1 \Delta f, \quad (3.41)$$

where \mathbf{S}_1 is a proportionality factor. Usually this proportionality factor has a center frequency and is therefore a function of f , i.e. $\mathbf{S}_1(f)$. This function is known as the power spectral density (psd) of the random input force $l(t)$. It is assumed that the psd of $l(t)$ is calculated for each frequency f and the result is shown in Fig. (3.4). Then $l(t)$ is fed into two filters like the one discussed before. The filters have the center frequencies f_1 and f_2 . The mean square of

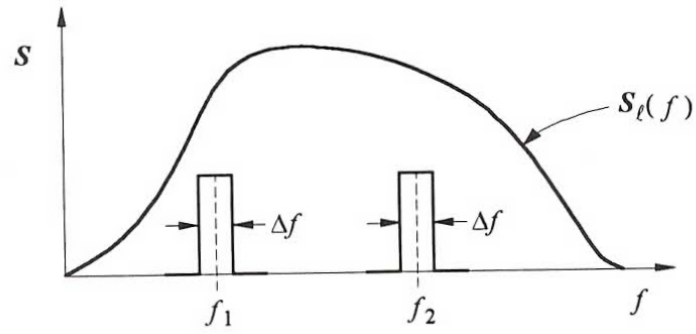


Figure 3.4: PSD of $l(t)$ sampled by two narrow band filters [Lyon and DeJong 1995], p. 25

the output of the system that consists of the two filters can be calculated by adding the mean squares of the two time functions that consist of different frequency components. So the overall output of the two filters is:

$$\langle l^2 \rangle = \mathbf{S}_1(f_1)\Delta f + \mathbf{S}_1(f_2)\Delta f. \quad (3.42)$$

This equation can be generalised, a filter with unity gain between the frequencies f_1 and f_2 has the mean square output

$$\langle l^2 \rangle = \int_{f_1}^{f_2} \mathbf{S}_1(f)df. \quad (3.43)$$

For a general gain $\mathbf{G}(f)$ the output becomes

$$\langle l^2 \rangle = \int_{f_1}^{f_2} \mathbf{S}_1(f)\mathbf{G}(f)df. \quad (3.44)$$

If $f_1 = 0$ and $f_2 = \infty$ then the total unfiltered mean square value of the filter is calculated. Noise excitations that have constant power spectral densities are known as “white noise” signals. White noise signals produce the following mean square forces in a narrow frequency band, here called df :

$$\langle l^2 \rangle_{df} = \mathbf{S}_1 df. \quad (3.45)$$

This force at frequency f produces a mean square velocity response of the resonator, since force and velocity are connected through mobility:

$$\langle \dot{y}^2 \rangle_{df} = \mathbf{S}_1 df |\mathbf{Y}|^2. \quad (3.46)$$

The total mean square velocity can be calculated analogue to Eq. (3.43), by integrating over the whole frequency range (for white noise):

$$\langle \dot{y}^2 \rangle = \int_0^{\infty} \mathbf{S}_1 |\mathbf{Y}|^2 df = \mathbf{S}_1 \int_0^{\infty} |\mathbf{Y}|^2 df. \quad (3.47)$$

Except for a constant the psd of \dot{y} has the form that is shown in Fig. (3.2). By looking at the form of the mobility in Fig. (3.2) it can be found out that the damping controlled region

contributes most to the integral in Eq. (3.47). Therefore it is meaningful to introduce the concept of “equivalent bandwidth” or “noise bandwidth”, called Δ_e . It is the bandwidth of a system that has a rectangular pass band. This pass band is characterised by a constant mobility that is defined only by damping, $\mathbf{Y}_{\max} = (\omega_0 \eta M)^{-1}$. The response of the pass band to white noise excitation is equal to the response of the actual system. In a mathematical sense this can be written as:

$$\langle \dot{y}^2 \rangle = \mathbf{S}_1 \Delta_e (\omega_0 \eta M)^{-2} = \frac{1}{2\pi} \mathbf{S}_1 (\omega_0 \eta M)^{-2} \int_0^{\infty} \frac{d\omega}{1 + (\omega^2 - \omega_0^2)/\eta^2 \omega^2 \omega_0^2}. \quad (3.48)$$

A change of variables can be helpful to solve this integral, i.e. $\xi = 2(\omega - \omega_0)/\eta\omega_0$ and it can be further simplified by using the knowledge that the biggest part of the integral is provided at $\omega = \omega_0$ or $\xi = 0$. These simplifications lead to:

$$\int_0^{\infty} \dots \rightarrow \frac{\eta\omega_0}{2} \int_{-\infty}^{\infty} \frac{d\xi}{1 + \xi^2} = \frac{\eta\omega_0}{2} (\tan^{-1}(\infty) - \tan^{-1}(-\infty)) = \frac{\pi\eta\omega_0}{2}. \quad (3.49)$$

By using this solution of the integral the noise bandwidth is defined as:

$$\Delta_e = \frac{\pi}{2} \eta \omega_0, \quad (\text{rad./sec.}) \quad (3.50)$$

or

$$\Delta_e = \frac{\pi}{2} \eta f_0, \quad (\text{Hz.}) \quad (3.51)$$

The equivalent bandwidth is the same as the “half power” bandwidth increased by the factor $\frac{\pi}{2}$. In many cases the description of the resonator by the equivalent filter can be useful. From Eq. (3.48) that describes the velocity of the system, it is simple to calculate the displacement. The mean square displacement is given by:

$$\langle y^2 \rangle = \frac{1}{2\pi} \mathbf{S}_1 (\omega_0 \eta M)^{-2} \int_0^{\infty} \frac{d\omega}{\omega^2 [1 + (\omega^2 - \omega_0^2)/\eta^2 \omega^2 \omega_0^2]}. \quad (3.52)$$

If it is supposed, as in the sections before that the level of damping is low, i.e. $\eta < 0.3$, the mean square displacement is:

$$\langle y^2 \rangle = \langle \dot{y}^2 \rangle / \omega_0^2. \quad (3.53)$$

If Eq. (3.48) is differentiated to get the mean square acceleration, a problem occurs because the integral

$$\langle \ddot{y}^2 \rangle = \frac{1}{2\pi} \mathbf{S}_1 (\omega_0 \eta M)^{-2} \int_0^{2\pi f_{\max}} \frac{\omega^2 d\omega}{1 + (\omega^2 - \omega_0^2)/\eta^2 \omega^2 \omega_0^2} \quad (3.54)$$

does not converge for $f_{\max} \rightarrow \infty$. But for large ω the integrand simplifies to $\omega_0^2 \eta^2$. The above described problem can therefore be solved by “subtracting out” this part, which leads to:

$$\langle \ddot{y}^2 \rangle = \omega_0^2 \langle \dot{y}^2 \rangle + \mathbf{S}_1 f_{\max} / M^2. \quad (3.55)$$

The second term of Eq. (3.55) describes the mass controlled acceleration whereas the first term stands for the damping controlled acceleration. In those cases of random excitation in which the resonant parts dominate, this is true for most but not for all situations, the mass controlled acceleration can be cancelled out and the equation for the acceleration simplifies to:

$$\langle \ddot{y}^2 \rangle = \omega_0^2 \langle \dot{y}^2 \rangle. \quad (3.56)$$

It was shown that free vibration and resonant response to either sinusoidal or random excitation related the mean square (m.s.) displacement, velocity and acceleration in the same way. This finding makes it possible to change from one response variable to another without concern for the accurate nature of excitation. But it has to be kept in mind that the requirements of resonant dominated response have to be fulfilled for these relations to be true ($\eta < 0.3$).

3.2 Modal Analysis of Distributed Systems

In practical applications a mechanical designer has to deal with much more complicated systems than that of a linear resonator. If there is a displacement in a distributed system⁴, that leads to an increase in the potential energy, then this increase is resisted by the elastic restoring forces. Damping forces resist changes of displacement of the system. The mass elements are accelerated based on these two forces together with the loading excitation. In this section it is found that modal density has two important functions: describing the energy capacity of a structure and to determine the power that the system absorbs in case of noise excitation. If the generalised displacement of the system is called y , the described relations can be mathematically written down as:

$$\rho \ddot{y} + r \dot{y} + \Lambda y = p, \quad (3.57)$$

where p stands for the distributed excitation, ρ describes the mass density, r is known as a viscous resistance coefficient and Λ is a linear operator that contains differentiations with respect to space. If such a system is bounded, the system's equations are often solved by using eigenfunctions Ψ_n . The boundary conditions must therefore be well defined. The eigenfunctions are solutions to the following equation:

$$\frac{1}{\rho} \Lambda \Psi_n = \omega_n^2 \Psi_n. \quad (3.58)$$

In Eq. (3.58) the boundary conditions that are satisfied by y also have to be fulfilled by Ψ_n . The term $\rho^{-1} \Lambda$ and the boundary conditions are responsible for the values ω_n^2 . The expansion of the response and excitation in these functions leads to:

$$\begin{aligned} y &= \sum_n \mathcal{Y}_n(t) \Psi_n(x) \\ p/\rho &= \frac{1}{M} \sum_n \mathcal{L}_n(t) \Psi_n(t). \end{aligned} \quad (3.59)$$

Eq. (3.58) is multiplied by Ψ_m and integrated over the region occupied by the structure. Then exactly the same equation is subtracted, but the indices of the subtracted equation are reversed.

⁴ This is a system, where mass, resistance and stiffness are distributed over the space that is filled by the structure.

This procedure leads to:

$$\int \{\Psi_m \Lambda \Psi_n - \Psi_n \Lambda \Psi_m\} dx = (\omega_n^2 - \omega_m^2) \int \Psi_m \rho(x) \Psi_n dx. \quad (3.60)$$

Of course this statement is true if $n = m$, but this is a trivial solution. Conditions exist where the above equation is fulfilled if $n \neq m$. Under these conditions the differential operator vanishes, this means that the term $\int \Psi_m \Lambda \Psi_n dx$ has to vanish. This happens if the eigenfunctions are orthogonal. If the amplitudes of the eigenfunctions are normalised by the mass, the result is known as mass density weighted average of the product $\Psi_m \Psi_n$. The normalisation can be written as:

$$\frac{1}{M} \int \Psi_m \rho \Psi_n dx \equiv \langle \Psi_m \Psi_n \rangle = \delta_{m,n}. \quad (3.61)$$

The expanded equations for the response and excitation can be inserted in Eq. (3.57) which leads to:

$$\rho \sum_n \left(\ddot{\mathcal{Y}}_n + \frac{r}{\rho} \dot{\mathcal{Y}}_n + \omega_n^2 \mathcal{Y}_n \right) \Psi_n = \frac{\rho}{M} \sum_m \mathcal{L}_m \Psi_m. \quad (3.62)$$

Multiplying Eq. (3.62) with $\Psi_n(x)$ and integrating it over the system domain results in:

$$\boxed{M\{\ddot{\mathcal{Y}}_n + \Delta \dot{\mathcal{Y}}_n + \omega_n^2 \mathcal{Y}_n\} = \mathcal{L}_n(t)}. \quad (3.63)$$

This result is very useful, because it means that each modal response amplitude can be described by the equation of a linear resonator that was discussed in Sec. (3.1) in detail. Based on this finding and the knowledge of the spatial orthogonality of the mode shapes, as shown in Eq. (3.61), a complex dynamical system can be treated as a group of independent resonators of mass M , stiffness $\omega_n^2 M$ and mechanical resistance $M\Delta = M\omega_n \eta_n$.

The modes and the ω_n 's correspond to each other, therefore the ω_n 's can be used to keep track of the modes. The equations for the mode shapes and the resonance frequencies of a rectangular plate are derived as an example.

The two dimensional plate has dimensions L_1 and L_2 and is isotropic and homogeneous. In this case the mode shapes of the plate for bending motion are defined as:

$$\Psi_{n_1, n_2} = 2 \sin \frac{n_1 \pi x_1}{L_1} \sin \frac{n_2 \pi x_2}{L_2}. \quad (3.64)$$

The resonance frequencies can be calculated with the following equation:

$$\omega_{n_1, n_2}^2 = \left[\left(\frac{n_1 \pi}{L_1} \right)^2 + \left(\frac{n_2 \pi}{L_2} \right)^2 \right] \kappa^2 c_1^2 \equiv (k_1^2 + k_2^2) \kappa^2 c_1^2 \equiv k^4 \kappa^2 c_1^2. \quad (3.65)$$

In Eq. (3.65) n_1 and n_2 stand for integers, κ for the radius of gyration of the plate cross-section. The longitudinal wavespeed in the plate material, c_1 can be calculated with the formula $c_1 = \sqrt{E/\rho_m}$, with E the Young's modulus and ρ_m the material density. Eq. (3.65) leads to a useful ordering of the modes. The modes can be drawn in a wavenumber lattice as shown in Fig. (3.5) in which every lattice point belongs to a mode. Another information that can be obtained from the wavenumber lattice is that the distance from the origin to a point of the lattice that corresponds to one mode, is the resonance frequency of the mode ω_n . The ordering makes mode counting possible: The number of modes that have resonance frequencies in a particular frequency interval can be determined. In Fig. (3.5) the ordering indices form a lattice and each lattice point belongs to an area, $\Delta A_k = \pi^2/A_p$ in the wavenumber plane where A_p is the plate's area. If the wavenumber is increased, e.g. by Δk a new area, i.e. $\frac{1}{2} \pi k \Delta k$ is introduced. The

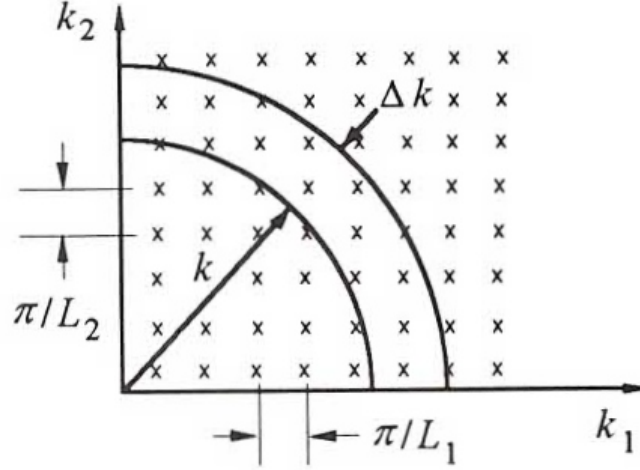


Figure 3.5: Wavenumber lattice for rectangular supported plate [Lyon and DeJong 1995], p. 31

number of new modes is on average

$$n(k) = \frac{\pi k \Delta k}{2\Delta A_k \Delta k} = \frac{\pi k}{2\Delta A_k}. \quad (3.66)$$

If the frequency is increased by 1 rad./sec. the average number of modes that result from this increase is known as modal density in radian frequency, $n(\omega)$. By reformulating the relation $n(\omega)\Delta\omega = n(k)\Delta k$ the equation for determining the modal density in radian frequency is obtained:

$$n(\omega) = \frac{\pi k}{2\Delta A_k} \cdot \frac{\Delta k}{\Delta\omega} = \frac{\pi k}{2c_g \Delta A_k}, \quad (3.67)$$

where $\Delta\omega/\Delta k$ is the group velocity c_g . This is valid in systems with phase velocities ω/k . The modal density in cycles per second (Hertz) for a flat plate in which the group velocity is twice the phase velocity, $c_g = 2c_p$ and the phase velocity is defined as $c_p = \omega/k = \sqrt{\omega\kappa c_1}$, can be calculated with the following equation:

$$n(f) = n(\omega) \frac{d\omega}{df} = \frac{2\pi^2 \omega A_p}{4c_p^2 \pi^2} = \frac{A_p}{2\kappa c_1} = \frac{\sqrt{3}A_p}{hc_1}. \quad (3.68)$$

To obtain this result it was used that the radius of gyration for a flat and homogeneous plate of thickness h is defined as $\kappa = h/2\sqrt{3}$. The modal density for the plate is independent of frequency and is for the same material higher if the area of the plate is increased or the thickness is decreased.

Using the orthogonality relation that was discussed before the kinetic energy of vibration is derived:

$$\boxed{\frac{1}{2} \int dx \rho \left(\frac{\partial y}{\partial t} \right)^2 = \frac{1}{2} \int dx \sum_{m,n} \dot{y}_m(t) \dot{y}_n(t) \rho \Psi_m(x) \Psi_n(x) = \frac{1}{2} M \sum_n \dot{y}_n(t)}. \quad (3.69)$$

The kinetic energy of the system is obtained by adding up the kinetic energies of the modes. The total energy of the system is the sum of the total energies of the modes because the kinetic and the potential energy of resonators at resonance are equal.

3.2.1 Response of System to Point Force Excitation

At location x_s on the structure a point force that has the amplitude l_0 is applied to the system. With the help of Eq. (3.59) the modal amplitudes are given as:

$$\mathcal{L}_m(t) = \int p \Psi_m dx = l_0(t) \Psi_m(x_s). \quad (3.70)$$

If the excitation has the form $l_0(t) = \mathbf{L}_0 e^{j\omega t}$ and is inserted in Eq. (3.63), the following equation is obtained:

$$M(\omega_n^2 + j\omega\omega_n\eta - \omega^2)\mathcal{Y}_n = \mathbf{L}_0 \Psi_n(x_s). \quad (3.71)$$

The formal result for the response of the system for this kind of excitation is:

$$y(x, t) = \frac{\mathbf{L}_0 e^{j\omega t}}{M} \sum_n \frac{\Psi_m(x_s) \Psi_n(x)}{\omega_n^2 - \omega^2 + j\omega\omega_n\eta}. \quad (3.72)$$

The input mobility of the system is given as the ratio of the velocity at the excitation point x_s ($j\omega y(x_s)$) to the applied force.

$$\mathbf{Y} = \frac{\mathbf{V}(x_s, \omega)}{\mathbf{L}_0} = \frac{j\omega}{M} \sum_n \frac{\Psi_n^2(x_s)}{\omega_n^2 - \omega^2 + j\omega\omega_n\eta} \equiv G + jB, \quad (3.73)$$

where the complex mobility can be divided into a real and an imaginary part. The real part of the mobility, termed conductance, is determined as G and the imaginary part termed susceptance is stated as B . The complex ratios can be rationalised and then G can be written as:

$$G = \sum_n a_n(x_s) g_n(\omega), \quad (3.74)$$

with $a_n = \Psi_n^2(x_s)/\omega\omega_n\eta M$ and $g_n = (\xi^2 + 1)^{-1}$. ξ is given in the paragraph below Eq. (3.48). The susceptance can be written as:

$$B = \sum_n a_n(x_s) b_n(\omega), \quad (3.75)$$

with $b_n = \xi(\xi^2 + 1)^{-1}$. The damping is supposed to be small for these equations to be true ($\eta < 0.3$).

The total mobility is a function of frequency and is quickly changing with frequency. The mobility can be simplified by calculating averages of \mathbf{Y} with respect to ξ . This can be justified if the system is described as a “random” system. This means that the mode shapes and resonance frequencies cannot be determined exactly. Therefore it is supposed that the resonance frequencies are random variables with uniform distribution over a frequency interval. This procedure can be said to be an example of statistical modelling that is widely used in SEA. But it is not only used in SEA, statistical modelling also appears in real world problems, because there are always variations in geometry and material properties that have an influence on the resonant frequencies and mode shapes. Therefore the analysis should include the statistical distributions of the system parameters.

If the interval in which the resonance frequency can vary is $\Delta\omega$, the averaging over ω_n leads to:

$$\langle g_n \rangle = \frac{\omega\eta}{2\Delta\omega} \int_{-\infty}^{\infty} \frac{d\xi}{\xi^2 + 1} = \frac{\pi\omega\eta}{2\Delta\omega}. \quad (3.76)$$

The interval $\Delta\omega$ provides $n(\omega)\Delta\omega$ modes that have an influence on the average value. Averaging leads to an average conductance:

$$\langle G \rangle_{\omega_n, y_s} = \frac{n(\omega)\Delta\omega}{\omega\eta M} \cdot \frac{\pi}{2\Delta\omega} \omega\eta \langle \Psi_n^2 \rangle = \frac{\pi n(\omega)}{2M} = (4M\bar{\delta}f)^{-1}. \quad (3.77)$$

Eq. (3.77) is a general result that is valid for multimodal systems, e.g. a flat plate. The average mobility of a finite system can often be found by using the results of infinite systems. This is very useful in practice and for example true for a flat plate. The average susceptance vanishes when the modal density is constant. In cases in which the modal density varies the average susceptance is the same as that of the same system infinitely extended.

The input force is changed to noise excitation. This means that the force in Eq. (3.70) has a flat spectrum over the band $\Delta\omega$ and the power that excites any mode can be derived from the dissipation $\omega_0\eta M \langle \dot{y}^2 \rangle$. \mathcal{S}_l describes the spectral density of the force $l(t)$ and can be calculated with $\mathcal{S}_l \Psi_n^2(x_s)/4M$. The noise acts in the bandwidth $\Delta\omega$ [rad/sec] and the modes that randomly result from this noise force are given as $n\Delta\omega$. This leads to an equation for the input power to the system, where averaging is done:

$$\langle \Pi \rangle = \frac{\pi}{2} \frac{\mathcal{S}_l \Delta\omega}{2\pi} \cdot \frac{n(\omega)}{M} = \langle l^2 \rangle \langle G \rangle \quad (3.78)$$

In this equation the conductance is again $\langle G \rangle = \pi n(\omega)/2M$. The conductance can be used to determine the number of modes that can be used to absorb energy from a noise force. This means that there is a strong relationship between conductance and modal density and conductance can be used to measure the modal density in systems where counting resonance peaks is not possible.

3.3 Dynamics of Infinite Systems

In the case of infinite systems, the systems analysed are greatly extended but the differential equation describing the motion of the system given by Eq. (3.57) is still valid. Some changes are made concerning the assumptions of the parameters: mass and damping distributions in the case of infinite systems are supposed to be uniform, i.e. ρ and r are constant and $\Lambda[\partial/\partial x_i]$ is assumed to be a polynomial with constant coefficients. Therefore the equation for unforced motion can be solved with a wave approach of the form:

$$y \sim e^{-j(\vec{k}\vec{x} - \omega t)}. \quad (3.79)$$

Using this relation and substituting it in the equation of motion the “dispersion relation” between frequency and wavenumber can be derived:

$$-\rho\omega^2 + j\omega r + \lambda[-jk_i] = 0. \quad (3.80)$$

In the case of an undamped string $r = 0$, $\rho =$ lineal density,

$$\Lambda[\partial/\partial x_i] = -T(\partial/\partial x)^2 = -Tj^2k^2 = T^2k^2,$$

where T is the tension of the string and the speed of free waves on the string is $c = \sqrt{T/\rho}$. With these definitions the equation of motion for the undamped string is:

$$Tk^2 = \rho\omega^2; \quad k^2 = \frac{\rho\omega^2}{T}; \quad k = \sqrt{\frac{\rho\omega^2}{T}} = \omega\sqrt{\frac{\rho}{T}} = \pm\omega/c. \quad (3.81)$$

In a second example the dispersion relation for undamped bending motions of a thin beam are derived. In this case

$$\Lambda[\partial/\partial x] = \mathbf{B}(\partial/\partial x)^4, \quad (3.82)$$

with \mathbf{B} the bending rigidity of the beam given by $\mathbf{B} = \rho c_1^2 \kappa^2$. The phase velocity for bending waves on a beam is frequency dependent:

$$c_\phi = \sqrt{\omega \kappa c_1} \quad (3.83)$$

and therefore the system is called dispersive. Using all these definitions the dispersion relation of the beam can be written as:

$$\rho \omega^2 = \mathbf{B} k^4 = \rho c_1^2 \kappa^2 k^4; \quad k^4 = \frac{\omega^2}{c_1^2 \kappa^2} \equiv (\omega/c_\phi)^4. \quad (3.84)$$

If damping would be included, this would result in a complex propagation constant k and the wave would be attenuated.

In infinite free wave systems energy variables are very important and the main focus of interest lies on the energy density that describes the energy of vibration per unit length, area or volume. Kinetic and potential energy densities of such systems can be proven to be equal. This means that the total energy density of the system equals the kinetic energy density multiplied with two, or $\rho(\partial y/\partial t)^2$. The power flowing through a unit width or area of a system resulting from a propagating wave has the same intensity \mathcal{I} as a free wave. The energy or group velocity $c_g = d\omega/dk$ describes the amount of structure that is filled with energy, if the power flow lasts for one second. \mathcal{E} is called energy density and $\mathcal{E} c_g = \mathcal{I}$ describes the energy that passed the reference location. Using Eq. (3.80) and setting $r = 0$ the energy velocity can be written as:

$$c_g = \frac{d\omega}{dk} = \frac{-j}{2\rho\omega} \Lambda'[-jk]. \quad (3.85)$$

With the relation $\mathcal{E} = \rho(\partial y/\partial t)^2$ the intensity becomes

$$\mathcal{I} = \frac{j\omega}{2} \langle y^2 \rangle_t \Lambda'[-jk]. \quad (3.86)$$

The intensities for the string and the thin beam are calculated as examples. In the case of the string $\Lambda[-jk] = -T(-jk)^2$ and $\Lambda'[-jk] = 2T(jk)$. Inserting these expressions in Eq. (3.86) leads to the intensity of the string:

$$\mathcal{I}_{string} = +\frac{j\omega}{2} \langle y^2 \rangle_t (+\rho c^2) 2jk = \rho c \left\langle \left(\frac{\partial y}{\partial t} \right)^2 \right\rangle_t. \quad (3.87)$$

For the beam $\Lambda = \rho \kappa^2 c_1^2 (-jk)^4$ and $\Lambda' = 4\rho \kappa^2 c_1^2 (-jk)^3$. And as before by inserting these expression in Eq. (3.86) the intensity of the beam becomes:

$$\mathcal{I}_{beam} = +\frac{-j}{2\omega} \left\langle \left(\frac{\partial y}{\partial t} \right)^2 \right\rangle_t 4\rho \kappa^2 c_1^2 (-jk)^3 = 2\rho c_\phi \left\langle \left(\frac{\partial y}{\partial t} \right)^2 \right\rangle_t. \quad (3.88)$$

In both examples string and beam, the intensity is a mean square velocity of motion of the system, multiplied by an impedance term. The impedance term is given by ρc , where ρ stands for the density and c for the wavespeed. The propagation constant becomes a complex value if the system is damped. In the case where damping is included the dispersion relation

can be written as:

$$k(\omega) \rightarrow k\left[\omega\left(1 + \frac{-j\eta}{2}\right)\right]. \quad (3.89)$$

This perturbation in frequency leads to a perturbation in wavenumber given by $\Delta k = \Delta\omega/c_g$ and results in a new wave function:

$$e^{-jkx} \rightarrow e^{-jkx}e^{-\Delta kx} = e^{-jkx}e^{-\omega\eta x/2c_g}. \quad (3.90)$$

The amplitude is decreased by 1 neper due to this factor after the wave passed the distance $2c_g/\omega\eta$.

In the last section the impedance of a finite plate was discussed, now the impedance of an infinite plate is calculated. The equation of motion for a two dimensional flat plate is given by Eq. (3.57). The linear differential operator is

$$\Lambda = \rho\kappa^2c_1^2\left[\left(\frac{\partial}{\partial x_1}\right)^2 + \left(\frac{\partial}{\partial x_2}\right)^2\right]^2. \quad (3.91)$$

The point force $\mathbf{L}_0e^{j\omega t}$ is applied to the system at position $x = 0$. The mobility of the plate can be calculated by the ratio of the velocity to the applied force. The difficulty is to determine the motion y at position $x = 0$, but y is needed for the calculation of the velocity $\partial y/\partial t$. The motion is calculated with the help of two-dimensional Fourier transforms:

$$\begin{aligned} p(\vec{x}) &= \frac{1}{(2\pi)^2} \int \int \mathcal{P}(\vec{k})e^{-j\vec{k}\cdot\vec{x}} dk_1 dk_2 \\ \mathcal{P}(\vec{k}) &= \int \int p(\vec{x})e^{j\vec{k}\cdot\vec{x}} dx_1 dx_2. \end{aligned} \quad (3.92)$$

The motion $y(\vec{x})$ and its transform $\mathcal{Y}(\vec{k})$ have the same relation as $p(\vec{x})$ and its transform $\mathcal{P}(\vec{k})$. The second integral in the last equation simplifies to $\mathcal{P}(\vec{k}) = \mathbf{L}_0$ because $p(\vec{x})$ is applied only at $x = 0$ with the force \mathbf{L}_0 . The introduced transform is used to arrange a new version of the equation of motion:

$$\left[-\omega^2(1 - j\eta)\rho + \Lambda(-jk_1, -jk_2)\right]\mathcal{Y}(\vec{k}) = \mathbf{L}_0. \quad (3.93)$$

Reformulating this equation leads to:

$$\mathcal{Y}(\vec{k}) = \frac{\mathbf{L}_0}{\Lambda[-jk_1, -jk_2] - \omega^2(1 - j\eta)\rho}. \quad (3.94)$$

Using Eq. (3.94) gives:

$$y(0) = \frac{\mathbf{L}_0}{(2\pi)^2} \int \int \frac{1}{\Lambda[-jk] - \omega^2(1 - j\eta)\rho} dk_1 dk_2. \quad (3.95)$$

The area element can be rewritten as $dk_1 dk_2 \rightarrow 2\pi k dk$ because there is no azimuthal dependence in the k_1, k_2 integration. This results in a simple integration over k :

$$y(0) = \frac{\mathbf{L}_0}{2\pi} \int_0^\infty \frac{1}{\rho\kappa^2c_1^2[k^4 - k_b^4(1 - j\eta)]} k dk. \quad (3.96)$$

Introducing a variable change $\xi = k^2 \rightarrow dk = d\xi/2k$ and $\xi_b = k_b^2$ the integral becomes:

$$y(0) = \frac{\mathbf{L}_0}{2\pi} \int_0^{\infty} d\xi \frac{1}{\xi^2 - \xi_b^2(1 - j\eta)}. \quad (3.97)$$

This integral can be rewritten:

$$y(0) = \frac{\mathbf{L}_0}{8\pi\rho\kappa^2c_1^2} \int_{-\infty}^{\infty} \frac{d\xi}{[\xi - \xi_b(1 - j\eta/2)][\xi + \xi_b(1 - j\eta/2)]}. \quad (3.98)$$

If the limit is assumed to be $\eta \rightarrow 0$ and the path of integration is the one shown in Fig. (3.6) then the result of this integral is:

$$y(0) = \frac{\mathbf{L}_0/(j\omega)}{8\rho\kappa c_1}. \quad (3.99)$$

The mobility of the infinite plate is the ratio of the velocity $j\omega y(0)$ to the force \mathbf{L}_0 :

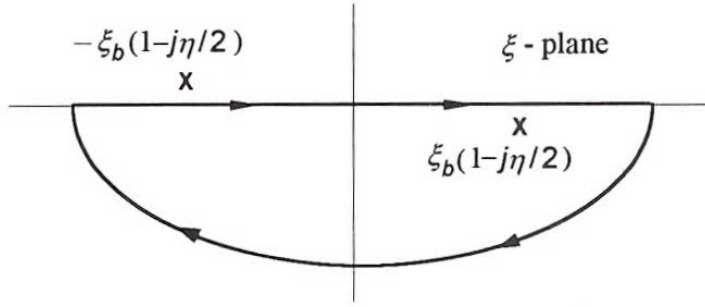


Figure 3.6: Contour for evaluation of integral [Lyon and DeJong 1995], p. 38

$$\boxed{\mathbf{Y}_\infty = (8\rho\kappa c_1)^{-1}}. \quad (3.100)$$

This result is exactly the same as the one for the mobility of the finite plate when it was averaged over the modal response and source location. The amount of power injected into an infinite plate due to a mean square force $\langle l^2 \rangle$ that is fed into the infinite plate at a point, is:

$$\boxed{\Pi_{\text{in}} = \langle l^2 \rangle \mathbf{Y}_\infty}. \quad (3.101)$$

This results in a circular wave that will propagate with the speed of the energy velocity starting from the point of excitation. If the wave reaches a boundary, it is reflected and propagates unobstructed until the next boundary is reached. The average distance between reflections covered by the wave is known as “mean free path”, d . The mean free path can be calculated by $d = \pi A_p / P$. P is the perimeter of the plate and A_p stands for the surface area of the plate. With the help of Eq. (3.90) the attenuation rate can be derived. The wave attenuates with $\omega\eta/2c_g$ nepers per unit length, which is the same as 4.34 $\omega\eta$ dB/sec. The reflections lead to rebounding energy and the vibration field resulting from this energy is called reverberant. The velocity spectrum of this field is termed $\mathbf{S}_{v,rev}(\omega)$ and the intensity in the range of the angle $d\Theta$ is described by the formula $d\mathcal{I} = \rho_s c_g \mathbf{S}_v(\omega) d\Theta / 2\pi$. Integrating only over the directions of the wave that fall onto the boundary and using only the component of the intensity that is

perpendicular to the boundary, the intensity on the boundary per unit length is:

$$\mathcal{I}_n(\omega) = \rho_s c_g \mathbf{S}_{v,rev}(\omega) / \pi. \quad (3.102)$$

The average modal energy can be introduced as

$$\mathcal{E}_{\text{modal}} = M \langle v^2 \rangle / n(\omega) \Delta\omega = \rho A \mathbf{S}_v(\omega) / n(\omega). \quad (3.103)$$

The modal density can be substituted by Eq. (3.67) which leads to:

$$\mathcal{I}_n(\omega) = k \mathcal{E}_{\text{modal}} / \pi. \quad (3.104)$$

Through this equation the modal energy is directly related to the intensity falling on the boundary. This is a useful result because it links the method of SEA with power-flow methods. The reverberation time can be calculated from Eq. (3.90) for systems in which the energy is stored in the propagation of free waves. The reverberation time is the time in which the energy of the system decays by 60 dB. By using Eq. (3.90) it is known that $4.34\omega\eta = 60$, and this leads to:

$$\boxed{T_R = \frac{2.2}{f\eta}}. \quad (3.105)$$

This is the same result as that derived earlier for the modal resonators and for a single dof system. The decay rate is often used to calculate the loss factor and can be applied for systems described by either modes or waves.

The interaction between a resonator that is composed of a mass M , a stiffness K , a dashpot resistance R and a finite plate as shown in Fig. (3.7) is discussed in the following section. The mean square velocity of the resonator that results from the random vibrations of the plate

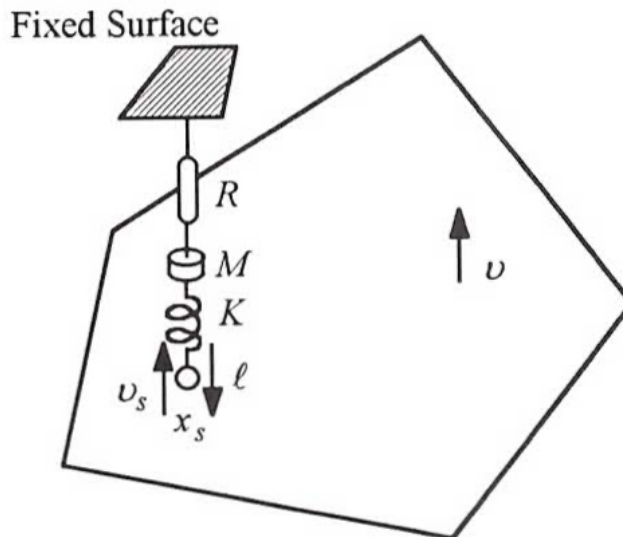


Figure 3.7: Interaction of a single resonator and a plate [Lyon and DeJong 1995], p. 40

is calculated. A transverse velocity v exists due to a diffuse reverberant vibrational field on the plate. The plate velocity at the point where the resonator and the plate are connected is termed v_s . The velocity that exists due to the resonator mass is called v_M . The difference of the velocities v_s and v_M combined with the compression of the spring K result in a force, called

reaction force:

$$l = K \int (v_s - v_M) dt = M \frac{dv_M}{dt} + Rv_M. \quad (3.106)$$

The velocity v_s is the same as the velocity v that would exist without a resonator, minus the velocity v_r that is called induced or reaction velocity. The induced velocity is defined as $l\langle G \rangle$, it depends on the reaction force. $\langle G \rangle$ stands for the plate admittance, given by $(8\rho_s \kappa c_l)^{-1}$. If we use $\langle G \rangle$ the modal density of the plate should be quite high, so that the following relation is true:

$$\frac{\pi}{2} \omega (\eta_p + \eta_0) n_p \gg 1. \quad (3.107)$$

This means that several plate modes exist in the combined equivalent bandwidth of the resonator and the plate modes. Eq. (3.106) is differentiated with respect to time and the relations described before are used resulting in the following differential equation:

$$M \frac{d^2 v_M}{dt^2} + R \frac{dv_M}{dt} + K v_M = K v - Kl \langle G \rangle. \quad (3.108)$$

Instead of writing l the relation given by Eq. (3.106) can be inserted to obtain:

$$\boxed{\frac{d^2 v_M}{dt^2} + \omega_0 (\eta_0 + \eta_{\text{coup}}) \frac{dv_M}{dt} + \omega_0^2 (1 + \eta_0 \eta_{\text{coup}}) v_M = \omega_0^2 v,} \quad (3.109)$$

with $\omega_0 \equiv \sqrt{K/M}$, $\eta_0 = R/\omega_0 M$ and $\eta_{\text{coup}} = \omega_0 M \langle G \rangle$. If a random excitation velocity is applied to a resonator, the response of the resonator is described by Eq. (3.109). If this velocity has a flat spectrum $\langle v^2 \rangle / (\Delta\omega)$ over the bandwidth $\Delta\omega$ then the response of the resonator becomes:

$$\langle v_M^2 \rangle = \frac{\pi}{2} \frac{\omega_0}{\eta_0 + \eta_{\text{coup}}} \frac{\langle v^2 \rangle}{\Delta\omega} \quad (3.110)$$

or

$$M \langle v_M^2 \rangle = \frac{\eta_{\text{coup}}}{\eta_0 + \eta_{\text{coup}}} \frac{M_p \langle v^2 \rangle}{n_p \Delta\omega}. \quad (3.111)$$

The last term in Eq. (3.111) specifies the ratio of the vibrational energy of the plate to the number of modes in the band $\Delta\omega$. Because of the fact that the ratio $\eta_{\text{coup}} / (\eta_{\text{coup}} + \eta_0)$ is always less than or equal to one, the average modal energy of the plate is always greater than or equal the average energy of vibration of the resonator. Only in case of a strong coupling, i.e. when the coupling loss factor η_{coup} is large compared to η_0 the energies are equal. If the energies are equal this is called “equipartition of energy”, a famous principal in statistical mechanics.

3.4 Mode-Wave Duality

Systems can be described by modal descriptions or wave descriptions as presented in the previous sections. These two ways of describing the motion of systems should give the same results but in some cases a wave approach makes more sense and in other cases it is more intelligent to use a modal approach. For example, the damping that occurs at the boundary of a plate can be nicely described by the method of wave reflections, whereas a modal description would be very difficult and complicated. But a description of the spatial variations in vibration amplitude in terms of wave analysis is very hard, whereas a modal analysis of this phenomenon is much easier.

It should be kept in mind that at least in theory both methods should give the same results. When discussing applications of Statistical Energy Analysis, certain quantities of the modal description can be found that equal other quantities of the wave description, e.g. modal energy and spatial energy density are connected through a proportionality factor. The coupling loss factors that are typical of modal systems and the junction impedances or transmissibilities that are typical of wave approaches are also equivalent quantities. The incident power on a junction between two plates is discussed as another example in the following section.

The junction between two plates a and b has the length L_{junct} . The incident power acts in the frequency band $\Delta\omega$. These definitions are graphically presented in Fig. (3.8). The incident

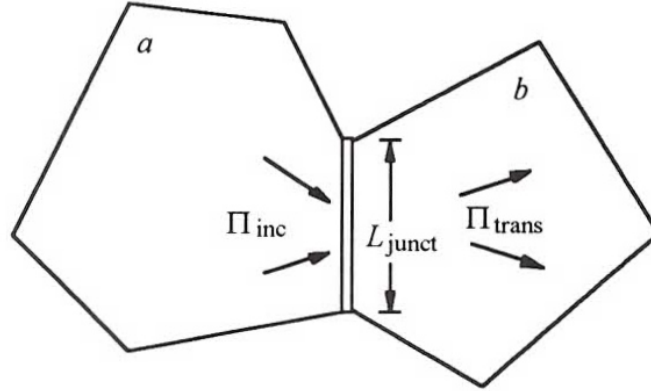


Figure 3.8: Connection of two plates [Lyon and DeJong 1995], p. 43

power is given by

$$\Pi_{\text{inc}} = \mathcal{I}_n(\omega)L_{\text{junct}}\Delta\omega, \quad (3.112)$$

with \mathcal{I}_n defined in Eq. (3.102). The transmitted power Π_{trans} can be expressed with the help of a variable that stands for the transmissibility τ :

$$\Pi_{\text{trans}} = \tau\Pi_{\text{inc}} = \tau\mathcal{I}_n(\omega)L_{\text{junct}}\Delta\omega = \tau kL_{\text{junct}}\mathcal{E}_{\text{modal}}\Delta\omega/\pi \quad (3.113)$$

when inserting Eq. (3.104) for \mathcal{I}_n . Another equation for the calculation of the power flow results by using Eq. (3.67) and introducing a coupling loss factor η_{ab} from plate a to plate b :

$$\Pi_{\text{trans}} = \omega\eta_{ab}n_p(\omega)\Delta\omega\mathcal{E}_{\text{modal}}. \quad (3.114)$$

The coupling loss factor is:

$$\eta_{ab} = \frac{c_g\tau}{\omega d}. \quad (3.115)$$

The variable d stands for the mean free path and describes how many energy packets in plate a arrive at the plate junction. It is defined as $d = \pi A_a/L_{\text{junct}}$.

The wave-mode duality can be used to divide wave fields in a plate in “coherent” and “incoherent” parts. At first this is discussed from the viewpoint of the wave description. A very large plate is excited by a point force in a bandwidth $\Delta\omega$ and the point force acts on location x_s . The power is injected into the plate at location x_s . The root mean square force of the source is l and therefore the injected power can be written as:

$$\Pi_{\text{in}} = l^2\mathbf{Y}_\infty = l^2\langle G \rangle. \quad (3.116)$$

The variable $\langle G \rangle$ was defined before and can be substituted. The mean square velocity at any point that lies in the distance r from the excitation point can be calculated using the intensity relation:

$$\rho_s c_g \langle v_D^2 \rangle 2\pi r = \Pi_{in}. \quad (3.117)$$

The power flow starts at point x_s and moves radially outward from this point. Eq. (3.117) is only valid for an infinite plate without damping. In the case where damping is present, an additional factor that describes the energy decay, has to be included to describe the mean square velocity:

$$\langle v_D^2 \rangle = \frac{\Pi_{in}}{2\pi\rho_s c_g r} e^{-\omega\eta r/c_g}. \quad (3.118)$$

Eq. (3.118) describes the “direct field” of the source and is characterised by an energy decay of 3 dB per double distance. The attenuation that results from the damping linearly increases with the distance r . If the analysed plate is infinite or η is so large that the vibration of the plate has stopped before the direct wave arrives at the boundary of the plate then the plate motion can be described only by the direct field. In the case where the direct field energy is reflected at boundaries, most of the time coherence between the reflected energy and the direct field is lost. This is especially true in cases where the boundaries are not perfectly regular or a high number of reflections exist. The motion resulting from these reflections of energy is termed v_r and describes the “reverberant field”. The power that is dissipated by the reverberant field is defined as:

$$\Pi_R = \Pi_{in} e^{-\omega\eta d/2c_g} = M \langle v_R^2 \rangle \omega\eta. \quad (3.119)$$

Reformulating this expression by making use of the assumption that the average distance from the source to the boundary is half the mean free path $d/2$ gives:

$$\langle v_R^2 \rangle = \Pi_{in} e^{-\omega\eta d/2c_g} / \omega\eta M. \quad (3.120)$$

The total mean square velocity can be obtained by summing up the direct and reverberant velocity parts due to the assumption made before that they are incoherent,

$$\langle v^2 \rangle = \langle v_D^2 \rangle + \langle v_R^2 \rangle. \quad (3.121)$$

It is clear that next to the excitation point the direct field provides the main part to the total mean square velocity and that at large distances the reverberant field outweighs the direct field (see Fig. (3.9)). There is also one special distance at which the direct field and the reverberant field are equal. This distance is termed r_D and is given by:

$$r_D = \frac{\omega\eta M}{2\pi\rho c_g} = \eta_p \Delta_e \frac{\lambda}{\pi^2}. \quad (3.122)$$

The same example that was analysed by a wave approach, can also be discussed by a modal description. According to Sec. (3.2) the velocity that results by exciting a plate by a point force is:

$$v(x, \omega) = \frac{j\omega L_0}{M} \sum_m \frac{\Psi_m(x)\Psi_m(x_s)}{\omega^2(1+i\eta) - \omega_m^2}. \quad (3.123)$$

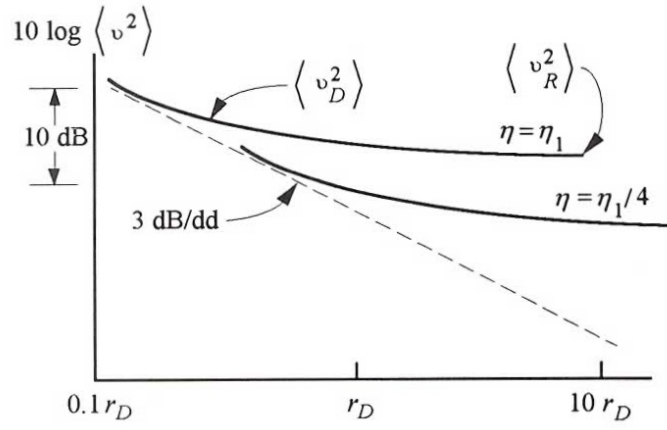


Figure 3.9: Direct and reverberant field of plate [Lyon and DeJong 1995], p. 45

The mode shapes of a simply supported plate can be written as:

$$\Psi_m(x)\Psi_m(x_s) = \frac{1}{4} \prod_{i=1}^2 \left(e^{jk_i x_i} - e^{-jk_i x_i} \right) \left(e^{jk_i x_{s_i}} - e^{-jk_i x_{s_i}} \right). \quad (3.124)$$

The product in Eq. (3.124) consists of 16 terms when expanded, where each term describes a plane wave, having one of the phase vectors that are presented in Fig. (3.10). The inner

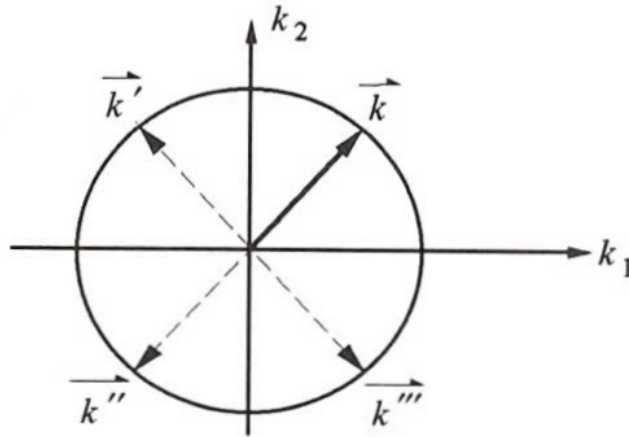


Figure 3.10: Construction of four wave vectors corresponding to a single mode [Lyon and DeJong 1995], p. 46

product between the wave vectors and the four position vectors that are graphically presented in Fig. (3.11) leads to the phase factors. If a point is excited by a force that acts at frequency ω , only the modes within the bandwidth $\Delta\omega = \pi\omega\eta/2$ are excited. The summation is made over the excited modes in k -space, therefore there are terms with strong fluctuations in phase and terms that will be combined to small fluctuations in phase. The smaller the vector $\vec{x} - \vec{x}_s$ the smaller the phase variation. Only terms with small phase variation are considered when describing the “coherent“ part of the summation. By only taking care of the coherent part Eq. (3.124) becomes:

$$\Psi_m(x)\Psi_m(x_s) \simeq \frac{1}{4} e^{-j\vec{k}\vec{r}}, \quad (3.125)$$

with $\vec{r} \equiv \vec{x} - \vec{x}_s$ and \vec{k} varying over a whole circle. Assuming that the phase varies less than $\pi/2$ between two lattice points the summation over m can be substituted by an integration over the angles in the k-space:

$$v(x) = \frac{j\omega \mathbf{L}_0}{M\kappa^2 c_1^2} \sum_m \frac{e^{-jkrcos(\Theta)}}{k^4 - k_p^4(1 - j\eta)}, \quad (3.126)$$

where Θ represents the angle between \vec{r} and \vec{k} ; $k_p = \omega/\kappa c_1$. The mass can be replaced by $M = \rho A_p = \rho\pi^2/\Delta A_k$. By using $\Delta A_k = k\Delta k\Delta\Theta$, the summation becomes an integral:

$$v(x) = \frac{-j\omega \mathbf{L}_0}{4\pi^2 \rho\kappa^2 c_1^2} \int_0^\infty \frac{kdk}{k^4 - k_p^4(1 - j\eta)} \int_0^{2\pi} e^{-jkrcos(\Theta)} d\Theta. \quad (3.127)$$

The solution to the second integral is $2\pi J_0(kr)$, and the final integral that has to be solved is therefore:

$$v(x) = \frac{j\omega \mathbf{L}_0}{\pi^2 \rho\kappa^2 c_1^2} \int_0^\infty \frac{J_0(kr)}{k^4 - k_p^4(1 - j\eta)} kdk, \quad (3.128)$$

which is a standard integral in the tables of Hankel transforms. For $\eta \rightarrow 0$ the result of Eq. (3.128) is:

$$v(x) = \frac{\mathbf{L}_0}{8\rho\kappa c_1} \{H_0^{(1)}(k_p r) - H_0^{(1)}(-jk_p r)\}. \quad (3.129)$$

Assuming that $k_p r > 1$ Eq. (3.129) leads to:

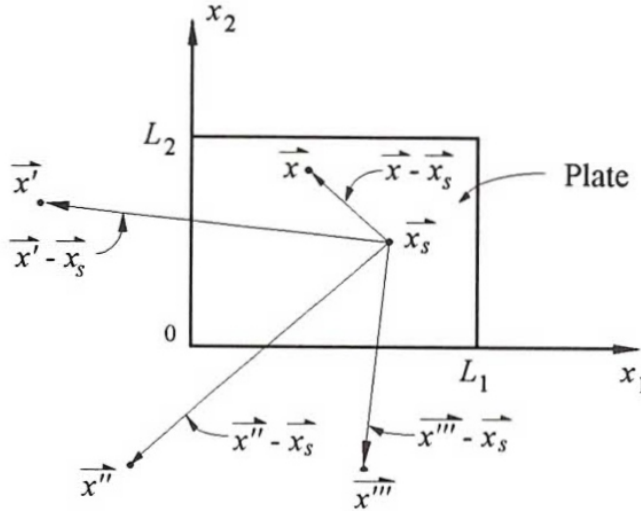


Figure 3.11: Configuration of source point and observation point [Lyon and DeJong 1995], p. 46

$$v(x) = \frac{\mathbf{L}_0}{8\rho\kappa c_1} \sqrt{\frac{2}{\pi k_p r}} \{e^{-jk_p r} - e^{j\pi/2} e^{-k_p r}\}. \quad (3.130)$$

The first term describes a cylindrically spreading wave with a reduction of the amplitude by the factor $1/\sqrt{r}$, whereas the second term represents an exponential decay. The vibrational energy

is represented by the first term, the velocity can be written as:

$$\langle v_0^2 \rangle = \frac{\langle \mathbf{L}_0 \rangle}{8\rho\kappa c_l} \frac{1}{4\pi\rho\kappa c_l k_p r} = \Pi_{\text{in}}/2\pi\rho c_g r, \quad (3.131)$$

which is the same result as in the wave analysis for the direct field. To get the incoherent part the summation in Eq. (3.123) only takes care of the incoherent modes, then the mean square value can be written as:

$$\frac{\omega^2 \mathbf{L}_0^2}{2M^2} \cdot \frac{pi}{2} \omega \eta n_s \cdot 1 \omega^2 \eta^2 = \frac{\mathbf{L}_0}{2} \cdot \frac{1}{\omega \eta M} \cdot \frac{pi}{2} \cdot n_s M = \frac{1}{2} \mathbf{L}_0 G / \omega \eta M. \quad (3.132)$$

This is again the same result as the one obtained in the wave analysis for the reverberant field (see Eq. (3.120)), assuming that the direct field is not very much dissipated before the first reflection from a boundary occurs.

It was shown that the description in the wave analysis, where the field contains a direct and a reverberant part, leads to the same results as in the modal analysis, in which the field is divided into a coherent and an incoherent part. The duality of the wave analysis and modal analysis can be very useful because phenomena described by waves can be interpreted by their effects on modal analysis.

4

Energy Sharing by Coupled Systems

In the following chapter the energy exchange of coupled resonators is discussed. At first two simple linear resonators are coupled and the energy flow between these resonators is discussed. Then the systems are extended to multi-modal systems and again the energy exchange between the systems is analysed. By discussing the energy flow between resonators some basic theorems of SEA can be found.

In SEA systems under test are divided into subsystems and analysed in terms of dissipated and coupled energies. In this chapter the main principles of the coupling of subsystems are derived, based on the analysis of coupled resonators. The basic theorems found by these discussions are also true in real world applications of SEA and therefore it is important to know these theorems.

4.1 Energy Sharing Among Resonators

The energy interaction of a system that couples two linear resonators with conservative elements is discussed (see Fig. (4.1)). Based on the results of this simple system, later on more complex

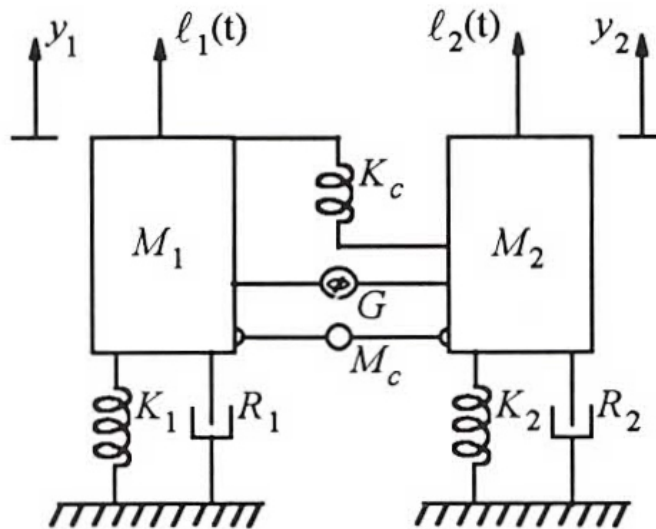


Figure 4.1: Two coupled, linear resonators [Lyon and DeJong 1995], p. 51

systems can be studied and analysed. To calculate the equation of motion for mass M_1 all forces that operate on this mass must be taken in account. Also the forces that act on M_1 because of a motion of mass M_2 must be included, in mathematics this is done by Langrange operators. The kinetic energy is given by:

$$\text{KE} = \frac{1}{2}M_1\dot{y}_1^2 + \frac{1}{2}M_2\dot{y}_2^2 + \frac{1}{8}M_c(\dot{y}_1 + \dot{y}_2)^2 \quad (4.1)$$

and the potential energy of the system can be written as:

$$\text{PE} = \frac{1}{2}K_1y_1^2 + \frac{1}{2}K_2y_2^2 + \frac{1}{2}K_c(y_2 - y_1)^2. \quad (4.2)$$

If there are no velocity dependent forces, the equations of motion are:

$$\frac{d}{dt} \frac{\partial \text{KE}}{\partial \dot{y}_i} - \frac{\partial \text{PE}}{\partial y_i} = l_i. \quad (4.3)$$

Eq. (4.1) and Eq. (4.2) are introduced in Eq. (4.3), the damping force $R\dot{y}$ and the gyroscopic coupling force $G\dot{y}$ are included in the independent equation of motion, resulting in:

$$(M_1 + \frac{1}{4}M_c)\ddot{y}_1 + R_1\dot{y}_1 + (K_1 + K_c)y_1 = l_1 + K_cy_2 + G\dot{y}_2 - \frac{1}{4}M_c\ddot{y}_2 \quad (4.4)$$

$$(M_2 + \frac{1}{4}M_c)\ddot{y}_2 + R_2\dot{y}_2 + (K_2 + K_c)y_2 = l_2 + K_cy_1 + G\dot{y}_1 - \frac{1}{4}M_c\ddot{y}_1. \quad (4.5)$$

These equations show that forces in one system are caused due to motion in the other system. In real systems also uncoupled structures exist. They can be described by Eq. (4.4) and Eq. (4.5), if the terms y_1, \dot{y}_1 and \ddot{y}_1 are set to 0 in Eq. (4.5) and the terms y_2, \dot{y}_2 and \ddot{y}_2 are set to 0 in Eq. (4.4). This means that system (2) is clamped⁵ in Eq. (4.4) and system (1) is clamped in Eq. (4.5). Eq. (4.4) and Eq. (4.5) can be made more symmetric by introducing new terms:

$$\ddot{y}_1 + \Delta_1\dot{y}_1 + \omega_1^2y_1 + \frac{1}{\lambda}[\mu\ddot{y}_2 - \gamma\dot{y}_2 - \kappa y_2] = \mathcal{L}_1 \quad (4.6)$$

$$\ddot{y}_2 + \Delta_2\dot{y}_2 + \omega_2^2y_2 + \lambda[\mu\ddot{y}_1 - \gamma\dot{y}_1 - \kappa y_1] = \mathcal{L}_2, \quad (4.7)$$

with

$$\begin{aligned} \Delta_i &= R_i/(M_i + M_c/4), \\ \omega_i^2 &= (K_i + K_c)/(M_i + M_c/4), \\ \mu &= (M_c/4)(M_1 + M_c/4)^{1/2}(M_2 + M_c/4)^{-1/2}, \\ \gamma &= G/(M_1 + M_c/4)^{1/2}(M_2 + M_c/4)^{1/2}, \\ \kappa &= K_c/(M_1 + M_c/4)^{1/2}(M_2 + M_c/4)^{1/2}, \\ \lambda &= (M_1 + M_c/4)^{1/2}(M_2 + M_c/4)^{-1/2} \end{aligned}$$

and

$$\mathcal{L}_i = l_i/(M_i + M_c/4).$$

If the parameters are set as $\Delta_1 = \Delta_2 = \Delta$, $\omega_1 = \omega_2 = \omega$, $\lambda = 1$ and $\mu = \gamma = 0$, the system described contains of two identical resonators that are only stiffness coupled. Then Eq. (4.6) is added to and subtracted from Eq. (4.7). This procedure leads to:

$$\ddot{z}_1 + \Delta\dot{z}_1\Omega_1^2z_1 = g_1 \quad (4.8)$$

⁵ Here clamped means that the response variables of a system are set to 0.

and

$$\ddot{z}_2 + \Delta \dot{z}_2 \Omega_2^2 z_2 = g_2, \quad (4.9)$$

with $z_1 = y_1 + y_2$, $z_2 = y_1 - y_2$, $g_1 = \mathcal{L}_1 + \mathcal{L}_2$, $g_2 = \mathcal{L}_1 - \mathcal{L}_2$, $\Omega_1^2 = \omega_0^2 + \kappa$ and $\Omega_2^2 = \omega_0^2 - \kappa$. The free vibration response for each of the masses in the case where no damping is present, obeys the following equation:

$$y(t) = A \sin(\Omega_1 t + \Phi_2) + B \sin(\Omega_2 t + \Phi_2). \quad (4.10)$$

If A and B have nearly the same values then motion of each of the masses is described by:

$$y_1(t) \simeq C \sin\left(\frac{\kappa}{\omega_0} + \Theta_a\right) \sin(\omega_0 t + \Theta_b). \quad (4.11)$$

This means that the oscillation is modulated by an envelope that changes with κ/ω_0 . This is well known as beating phenomenon, which is one of the most interesting features of coupled resonators. By introducing a damping Δ , a decaying factor $e^{-\Delta t/2}$ has to be included in Eq. (4.11). In the case of a strong damping compared to the coupling the energy sharing will not take place, because the vibrational energy will be dissipated before the beating oscillations can start. In case of a light damping compared to coupling, the beating oscillations and therefore the energy sharing exist. Exciting the resonators with white noise lead to similar conclusions.

In Eq. (4.8) and Eq. (4.9) l_2 is assumed to be 0 to discuss the power obtained in the indirectly excited resonator. Inserting $l_2 = 0$ it is found that $g_1 = g_2$ and that y_1 and y_2 are identical, noting that their responses are shifted as presented in Fig. (4.2). Three cases are presented:

- Damping strong compared to coupling

- Damping equal coupling

- Coupling stronger than damping

Assuming that there is no coupling means that $z_1 = z_2$ and $\dot{y}_2 = \frac{1}{2}(\dot{z}_1 - \dot{z}_2) = 0$. If the damping is strong compared to the coupling, i.e. $\kappa/\omega_0 < \Delta$, then the difference between $\mathcal{S}_{\dot{z}_1}$ and $\mathcal{S}_{\dot{z}_2}$ is nearly the same as the spectrum of \dot{y}_2 (see Fig. (4.2.a)). Although y_2 is weak in this scenario, its spectrum has a slight double peak that stands for a little beating effect. If the coupling is nearly equal the damping then $\langle \dot{y}_2^2 \rangle$ is increasing. This leads to a more distinct double peak and a stronger beating. It can be seen in Fig. (4.2.b) that the spectra $\mathcal{S}_{\dot{z}_1}$ and $\mathcal{S}_{\dot{z}_2}$ are moved further apart and that their difference is bigger as in the first case, resulting in the mentioned increase in the spectrum of \dot{y}_2 . In the third case shown in Fig. (4.2.c) the coupling is much stronger than the damping, i. e. $\kappa/\omega_0 \gg \Delta$. This means that \dot{y}_1 and \dot{y}_2 do not share common frequencies any longer and become statistically independent. The power that is given from the white noise source is dissipated to one half in resonator “1” and to the other half in the second resonator, i.e. $\langle \dot{y}_1^2 \rangle = \langle \dot{y}_2^2 \rangle = \langle \dot{z}_1^2 \rangle$. In this case the beating activities will be quite strong and the energy flows from one resonator to the other and vice versa.

In the experiment discussed before, the excitation force l_2 was assumed to be 0. Now independent white noise sources l_1 and l_2 are applied to the system and the resulting behaviour of the system is discussed in the following section. Introducing the power $\langle l_1 \dot{y}_1 \rangle$ that is provided by l_1 in Eq. (4.4) leads to:

$$\langle l_1 \dot{y}_1 \rangle = (M_1 + \frac{1}{4} M_c) \langle \ddot{y}_1 \dot{y}_1 \rangle + R_1 \langle \dot{y}_1^2 \rangle + (K_1 + K_c) \langle y_1 \dot{y}_1 \rangle - K_c \langle y_2 \dot{y}_1 \rangle - G \langle \dot{y}_2 \dot{y}_1 \rangle + \frac{1}{4} M_c \langle \ddot{y}_2 \dot{y}_1 \rangle. \quad (4.12)$$

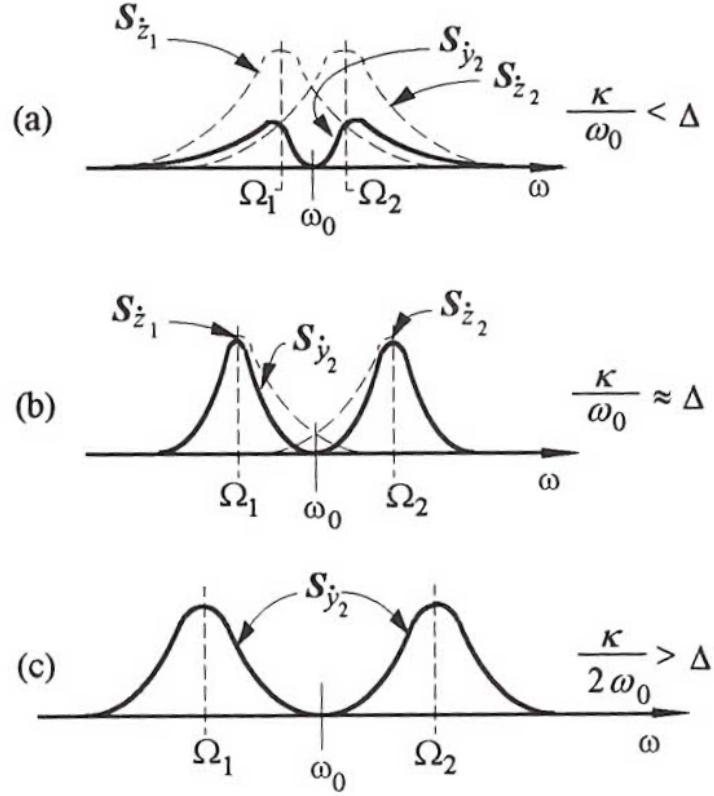


Figure 4.2: Spectral density of indirectly excited resonator velocity as a function of the degree of coupling [Lyon and DeJong 1995], p. 54

If stationary processes are assumed then $\langle d\dot{y}_1^2/dt \rangle$ and $\langle dy_1^2/dt \rangle$ are equal to 0. By inserting this in Eq. (4.12), the equation simplifies to:

$$\langle l_1 \dot{y}_1 \rangle = R_1 \langle \dot{y}_1^2 \rangle - K_c \langle y_2 \dot{y}_1 \rangle - G \langle \dot{y}_2 \dot{y}_1 \rangle + \frac{1}{4} M_c \langle \ddot{y}_2 \dot{y}_1 \rangle. \quad (4.13)$$

The first term on the right hand side stands for the energy that is dissipated by the damper and all the other terms on the right hand side stand for power flow into coupling elements. The same calculations as for source l_1 can be done for l_2 resulting in the final equation:

$$\langle l_2 \dot{y}_2 \rangle = R_2 \langle \dot{y}_2^2 \rangle - K_c \langle y_1 \dot{y}_2 \rangle - G \langle \dot{y}_1 \dot{y}_2 \rangle + \frac{1}{4} M_c \langle \ddot{y}_1 \dot{y}_2 \rangle. \quad (4.14)$$

It is supposed that

$$\left\langle \frac{d}{dt} y_1 y_2 \right\rangle = \langle \dot{y}_1 y_2 \rangle + \langle \dot{y}_2 y_1 \rangle = 0$$

and

$$\left\langle \frac{d}{dt} \dot{y}_1 \dot{y}_2 \right\rangle = \langle \ddot{y}_1 \dot{y}_2 \rangle + \langle \ddot{y}_2 \dot{y}_1 \rangle = 0.$$

Using these assumptions by inserting them in Eq. (4.13) and Eq. (4.14) and finally adding these equations up, gives:

$$\langle l_1 \dot{y}_1 \rangle + \langle l_2 \dot{y}_2 \rangle = R_1 \langle \dot{y}_1^2 \rangle + R_2 \langle \dot{y}_2^2 \rangle. \quad (4.15)$$

This means that the injected power is only dissipated by the damping elements and that the coupling elements can be said to be non-dissipative, if the presented simplifications are valid for stationary processes.

The power flow from resonator 1 to resonator 2 is described by the last three terms on the right hand side of Eq. (4.13):

$$\boxed{\Pi_{12} = -K_c \langle y_2 \dot{y}_1 \rangle - G \langle \dot{y}_2 \dot{y}_1 \rangle + \frac{1}{4} M_c \langle \ddot{y}_2 \dot{y}_1 \rangle.} \quad (4.16)$$

Calculating these averages is very exhausting and as it is done in the literature [Lyon and DeJong 1995], it is not executed here but the result is discussed. The evaluation of these averages is achieved in time or frequency domain resulting in:

$$\boxed{\Pi_{12} = A \left[\frac{\pi \mathbf{S}_{l_1}}{\Delta_1 (M_1 + \frac{1}{4} M_c)} - \frac{\pi \mathbf{S}_{l_2}}{\Delta_2 (M_2 + \frac{1}{4} M_c)} \right],} \quad (4.17)$$

where A can be looked up in the literature [Lyon and DeJong 1995], too. Assuming that $y_2 = \dot{y}_2 = 0$, the second term on the rhs of Eq. (4.17) vanishes and the first term defines the uncoupled or blocked energy of resonator 1:

$$E_1^{(b)} \equiv \frac{\pi \mathbf{S}_{l_1}(\omega)}{\Delta_1 (M_1 + \frac{1}{4} M_c)} = \frac{\pi \mathbf{S}_{l_1}(f)}{4\omega_1 \eta_1 (M_1 + \frac{1}{4} M_c)} = \left(M_1 + \frac{1}{4} M_c \right) \langle \dot{y}_1^2 \rangle. \quad (4.18)$$

In the same way $E_2^{(b)}$ can be defined, if $y_1 = \dot{y}_1 = 0$:

$$E_2^{(b)} \equiv \frac{\pi \mathbf{S}_{l_2}(\omega)}{\Delta_2 (M_2 + \frac{1}{4} M_c)} = \left(M_2 + \frac{1}{4} M_c \right) \langle \dot{y}_2^2 \rangle. \quad (4.19)$$

Eq. (4.17) describes the power flow from resonator 1 to resonator 2 and can be written in the form $\Pi_{12} = \mathcal{A}(E_1^{(b)} - E_2^{(b)})$. Using this form of describing the power flow, some important remarks can be made:

- (1) The main part of the power flow comes from the resonant interaction between the two resonators. If the resonance frequencies ω_1 and ω_2 are within a resonant bandwidth of the other resonance frequency \mathcal{A} is large, otherwise it is small.
- (2) The power flow is directly proportional to the difference of the blocked energies of the resonators.
- (3) The power always flows from the resonator with greater energy to the one with lesser energy due to the fact that \mathcal{A} is positive definite.
- (4) Because of the symmetry of \mathcal{A} in the system parameters the power flow is reciprocal. This means that the power flow from resonator 1 to resonator 2 is equal to the power flow from resonator 2 to resonator 1, if an equality in the difference of the resonator energies in each direction is given.

The power flow can also be expressed by resonator energies, showing that the difference in kinetic, potential or total energy of the resonators is proportional to the power flow. Therefore the power flow can be written as:

$$\boxed{\Pi_{12} = \mathcal{B}(E_1 - E_2),} \quad (4.20)$$

where E_i stands for the average energy of the resonator i and \mathcal{B} is a proportionality constant defined in the literature [Lyon and DeJong 1995] and therefore not given here. Assuming that resonator 2 is only indirectly excited, this means that $\mathcal{S}_{l_2} = 0$. The power that is flown from resonator 1 to resonator 2 has to be equal the dissipated power in resonator 2 in this case: $\Pi_{2,diss} = \Pi_{12} = \Delta_2 E_2 = \mathcal{B}(E_1 - E_2)$ which leads to:

$$\boxed{\frac{E_1}{E_2} = \frac{\mathcal{B}}{\Delta_2 + \mathcal{B}}}. \quad (4.21)$$

This relation states that the largest energy value in system 2 is reached when the coupling is strong compared to the damping. In this case $E_2 \simeq E_1$. Now the additional remarks to the presented ones can be made:

- (5) A proportionality between the vibrational energies of the system and the power flow exists. The factor of proportionality is \mathcal{B} .
- (6) Because of the symmetry in the parameters of the system and the positive definiteness of the proportionality factor, the power flows from the resonator that contains more energy to the one with less energy. Furthermore the system is said to be reciprocal.
- (7) If one resonator is directly excited, whereas the other is only indirectly excited, the maximal amount of energy in the indirectly excited resonator is the energy of the directly excited resonator.

These seven statements are the basis of energy flow studies in acoustical and mechanical systems. The power flow between resonators as discussed, is the basis of the description of more complex systems.

4.2 Energy Exchange in Multi-Degree-of-Freedom Systems

The development of a theory of multi-modal interactions is based on the results of Sec. (3.2), in which distributed systems were discussed and the results of Sec. (4.1) in which the energy sharing between two resonators was derived.

In this section two subsystems are connected and their response to the direct excitation p_i and the interaction “forces”, as shown in Fig. (4.3) is analysed. Assuming that one subsystem is

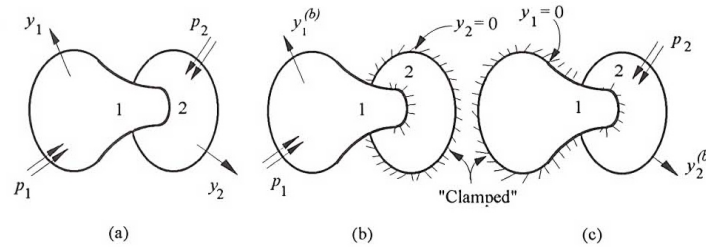


Figure 4.3: Analysis of coupled multi-DOF system (a) systems of interest; (b) system 2 is blocked; (c) system 1 is blocked [Lyon and DeJong 1995], p. 59

blocked, the other one vibrates because of the excitation p_i . This situation leads to the same results as presented in Sec. (3.2), where the equation of motion was:

$$\ddot{y}_i^{(b)} + (r_i/\rho_i)\dot{y}_i^{(b)} + \rho_i^{-1}\Lambda_i y_i^{(b)} = p_i/\rho_i, \quad i = 1, 2. \quad (4.22)$$

The eigenfunctions and eigenvalues of the operator $\rho_i^{-1}\Lambda_i$ are related through (as found in Sec. (3.2)):

$$\rho_i^{-1}\Lambda_i\Psi_{i\alpha} = \omega_{i\alpha}^2\Psi_{i\alpha}. \quad (4.23)$$

Using the orthogonality and normalisation leads to:

$$\langle\Psi_{i\alpha}\Psi_{i\beta}\rangle_{\rho_i} = \delta_{\alpha,\beta}. \quad (4.24)$$

The condition for blocking subsystem j if subsystem i is analysed, i.e. $y_j \equiv 0$, is part of the boundary conditions fulfilled for $\Psi_{i\alpha}$. It is assumed that the modal excitation of the system is white, according to the fact that the spectral densities are flat over the range of frequency $\Delta\omega$. The modal density in this finite frequency band for each subsystem is termed as $n_i(\omega)$ and the modes of the i^{th} subsystem are given by $N_i = n_i\Delta\omega$. The modes in the cases of coupled and uncoupled subsystems are shown in Fig. (4.4), where each mode group stands for a subsystem model. This model has some interesting properties that are important by applying SEA to real world problems:

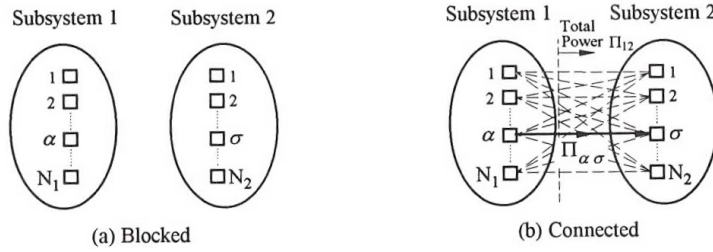


Figure 4.4: Model coupling in connected subsystems, (a) modal groups with blocked subsystems; (b) modal pairs with connected subsystems [Lyon and DeJong 1995], p. 60

(1) The resonance frequency $\omega_{i\alpha}$ of each mode of a subsystem is supposed to be equally probable over the frequency interval $\Delta\omega$. Therefore the subsystems belong to a population of systems that have in general similar physical features but differ enough so that their parameters can be said to be randomly distributed. For example acoustical spaces will have fluctuations in their modal parameters, especially in higher frequency regions.

(2) All the modes of a subsystem are supposed to have the same energy. Moreover the assumption is made that the modal amplitudes $\mathcal{Y}_{i\alpha}(t) = \int(\rho_i y_i \Psi_{i\alpha}/M) dx_i$ are incoherent, i.e.

$$\langle\mathcal{Y}_{i\alpha}\mathcal{Y}_{i\beta}\rangle_t = \delta_{\alpha,\beta}\langle\mathcal{Y}_{i\alpha}^2\rangle. \quad (4.25)$$

This means that the mode groups should be selected in such a way that this assumption is true. Furthermore this statement says that the modal excitation functions \mathcal{L}_i should be taken from random populations of functions with particular similarities, e.g. equal frequency and wave number, but are however incoherent.

(3) For reasons of simplicity the damping of each mode in a subsystem is supposed to be the same. This assumption is not essential but simplifies the discussions and is quite true for complex systems.

These three remarks are the basis for the term “statistical” in SEA.

So far only the blocked system was discussed. The system is now unblocked and the equations

of motion become:

$$\ddot{y}_i(r_i/\rho_i)\dot{y}_i + \Lambda_i y_i = \left[p_i + \mu_{ij}(x_i, x_j)\ddot{y}_j + (-)^j \gamma_{ij}(x_i, x_j)\dot{y}_j + \kappa_{ij} y_j \right] / \rho_i \quad [i \neq j; i, j = 1, 2]. \quad (4.26)$$

Expanding these two equations by using the eigenfunctions $\Psi_{1\alpha}(x_1)$ and $\Psi_{2\sigma}(x_2)$ leads to:

$$M_1[\ddot{\mathcal{Y}}_\alpha + \Delta_1 \dot{\mathcal{Y}}_\alpha + \omega_\alpha^2 \mathcal{Y}_\alpha] = \mathcal{L}_\alpha + \sum_\sigma [\mu_{\alpha\sigma} \ddot{\mathcal{Y}}_\sigma + \gamma_{\alpha\sigma} \dot{\mathcal{Y}}_\sigma + \kappa_{\alpha\sigma} \mathcal{Y}_\sigma] \quad (4.27)$$

$$M_2[\ddot{\mathcal{Y}}_\sigma + \Delta_2 \dot{\mathcal{Y}}_\sigma + \omega_\sigma^2 \mathcal{Y}_\sigma] = \mathcal{L}_\sigma + \sum_\alpha [\mu_{\sigma\alpha} \ddot{\mathcal{Y}}_\alpha + \gamma_{\sigma\alpha} \dot{\mathcal{Y}}_\alpha + \kappa_{\sigma\alpha} \mathcal{Y}_\alpha]. \quad (4.28)$$

The indices α, β, \dots are used for subsystem 1 and σ, τ, \dots for subsystem 2. The mass of subsystem i is termed M_i , $\Delta_i = r_i/\rho_i$ and $\mu_{\alpha\sigma}$ and $\mu_{\sigma\alpha}$ are the coupling factors. The coupling is termed conservative if the following conditions are fulfilled: $\mu_{\alpha\sigma} = \mu_{\sigma\alpha}$, $\gamma_{\alpha\sigma} = \gamma_{\sigma\alpha}$ and $\kappa_{\alpha\sigma} = \kappa_{\sigma\alpha}$. In Fig. (4.4.b) two coupled subsystems are shown, where the connections show the energy flow due to the coupling. If the subsystems are excited by white noise, the modes α of subsystem 1 and σ of subsystem 2 have the energies E_α and E_σ . Previous findings showed that all modes of a subsystem have the same modal energies, therefore $E_\alpha = \mathcal{E}_1 = const.$ and $E_\sigma = \mathcal{E}_2 = const..$ According to that, the inter-modal power flow is (see Eq. (4.20)):

$$\Pi_{\alpha\sigma} = \langle \mathcal{B}_{\alpha\sigma} \rangle_{\omega_\alpha \omega_\sigma} (\mathcal{E}_1 - \mathcal{E}_2), \quad (4.29)$$

with (not derived here)

$$\langle \mathcal{B}_{\alpha\sigma} \rangle_{\omega_\alpha \omega_\sigma} = \frac{\pi}{2} \frac{\Delta_1 \Delta_2}{\Delta \omega} \langle \lambda \rangle_{\alpha, \sigma} \quad (4.30)$$

and

$$\lambda \equiv [\mu^2 \omega^2 + (\gamma^2 + 2\mu\kappa) + \kappa^2/\omega^2] / \Delta_1 \Delta_2. \quad (4.31)$$

All modes N_1 of subsystem 1 provide a power flow to mode σ of subsystem 2, that is:

$$\Pi_{1, \alpha} = \langle \mathcal{B}_{\alpha\sigma} \rangle N_1 (\mathcal{E}_1 - \mathcal{E}_2). \quad (4.32)$$

The total power flow from subsystem 1 to subsystem 2 is obtained by summing over all modes of subsystem 2:

$$\Pi_{1, 2} = \langle \mathcal{B}_{\alpha\sigma} \rangle N_1 N_2 (\mathcal{E}_1 - \mathcal{E}_2). \quad (4.33)$$

For deriving the coupling loss factors η_{12} and η_{21} the total energy of the subsystems are termed $E_{1,tot}$ and $E_{2,tot}$, where $\mathcal{E}_1 = E_{1,tot}/N_1$ and $\mathcal{E}_2 = E_{2,tot}/N_2$. Then the total power flow from subsystem 1 to subsystem 2 expressed in these terms can be written as:

$$\Pi_{12} = \langle \mathcal{B}_{\alpha, \sigma} \rangle N_1 N_2 \left[\frac{E_{1,tot}}{N_1} - \frac{E_{2,tot}}{N_2} \right] \equiv \omega \eta_{12} \left[E_{1,tot} - \frac{N_1}{N_2} E_{2,tot} \right], \quad (4.34)$$

with $\eta_{12} \equiv \langle \mathcal{B}_{\alpha\sigma} \rangle N_2 / \omega$. The power that is lost by subsystem 1 because of coupling, is $\omega \eta_{12} E_{1,tot}$ and the power that is fed from subsystem 2 with energy $E_{2,tot}$ into subsystem 1, is $\omega \eta_{21} E_{2,tot}$. In the equation

$$\boxed{N_1 \eta_{12} = N_2 \eta_{21}} \quad (4.35)$$

the number of modes N_i can be replaced by the modal densities $n_i\Delta\omega$. This equation can be used to calculate an unknown loss factor from a known one.

The system represented in Fig. (4.4.b) is shown in a simpler version in Fig. (4.5). From this

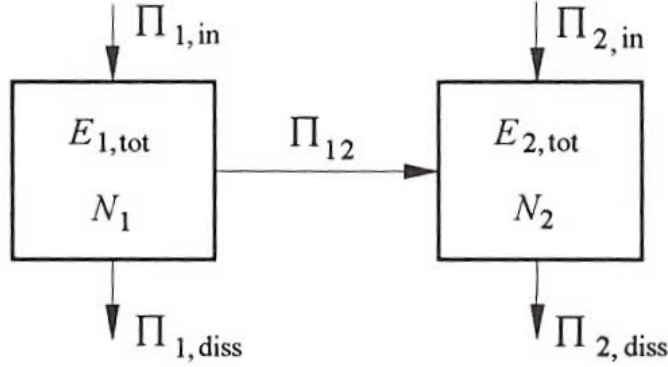


Figure 4.5: Energy transfer and storage in the case of two connected subsystems [Lyon and DeJong 1995], p. 64

figure the power flow equations for the whole system can be derived:

$$\Pi_{1,in} = \Pi_{1,diss} + \Pi_{12} = \omega \left[\eta_1 E_{1,tot} + \eta_{12} E_{1,tot} - \eta_{21} E_{2,tot} \right] \quad (4.36)$$

$$\Pi_{2,in} = \Pi_{2,diss} + \Pi_{21} = \omega \left[\eta_2 E_{2,tot} + \eta_{21} E_{2,tot} - \eta_{12} E_{1,tot} \right]. \quad (4.37)$$

If only system 1 is excited by an external source, $\Pi_{2,in} = 0$ and this leads to:

$$\frac{E_{2,tot}}{E_{1,tot}} = \frac{\eta_{12}}{\eta_2 + \eta_{21}} = \frac{N_2}{N_1} \frac{\eta_{21}}{\eta_2 + \eta_{21}}. \quad (4.38)$$

If both subsystems are excited by external sources, the total power of the subsystems is:

$$E_{1,tot} = \{ \Pi_{1,in}(\eta_2 + \eta_{21}) + \Pi_{2,in}\eta_{21} \} / \omega D \quad (4.39)$$

$$E_{2,tot} = \{ \Pi_{2,in}(\eta_1 + \eta_{12}) + \Pi_{1,in}\eta_{12} \} / \omega D \quad (4.40)$$

where D is introduced as

$$D = (\eta_1 + \eta_{12})(\eta_2 + \eta_{21}) - \eta_{12}\eta_{21}. \quad (4.41)$$

The coupling loss factor defines the inter-modal forces at the junctions between subsystems. It is an average not only over frequency but also over the modes of the systems that interact with each other.

At the end of this section it should be mentioned that in complex systems both local and global modes exist. If two resonators are connected global modes effect motions in both resonators, whereas local modes only effect substantial motion in one of the subsystems. Global modes are responsible for a significant energy flow between the subsystems.

4.3 Reciprocity and Energy Exchange in Wave Bearing Systems

In systems that contain linear, passive and bilateral elements, a general principle that is useful to describe wave interactions is reciprocity. For the following definitions it is assumed that the system is divided into a large number of tiny masses, springs and dampers:

(a) linear: This means that the force that acts on an element is directly proportional to the mechanical response of the element.

(b) passive: The term passive states that the only operating sources are those that are explicitly defined as sources in the equations of motion. Energy cannot be produced by elements of the system.

(c) bilateral: Forces are transmitted from one neighbour to the next one. The roles between the neighbours are reversed because of force interactions. These reversed roles will lead to an exact reversal of the relative motions.

In Fig. (4.6) a system is presented in which the principle of reciprocity can be applied. At terminal pair 1 of a reciprocal system a drop l is produced and the flow U due to this drop is measured through a wire that connects terminal pair 2. In Fig. (4.6.b) the drop p' is generated at terminal pair 2, resulting in a short circuit flow v' at terminal pair 1. In this scenario the

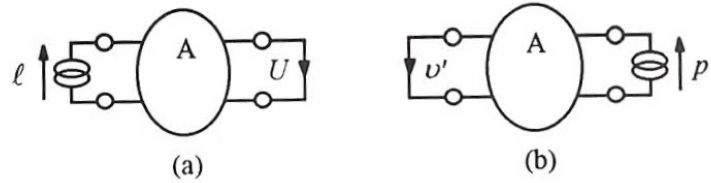


Figure 4.6: Reciprocal system A [Lyon and DeJong 1995], p. 70

reciprocity principle gives:

$$\frac{v'}{p'} = \frac{U}{l}. \quad (4.42)$$

The only limitation when using this principle is that p' , U , and l , v' have to be conjugate variables. This means that

$$\left| \frac{v'}{p'} \right| = \left| \frac{U}{l} \right|. \quad (4.43)$$

If p' and l are noise signals that have the same spectral shapes, it follows that:

$$\frac{\langle v'^2 \rangle}{\langle p'^2 \rangle} = \frac{\langle U^2 \rangle}{\langle l^2 \rangle}. \quad (4.44)$$

For the systems in Fig. (4.7) and Fig. (4.8) the reciprocity statements are:

$$\frac{\langle p^2 \rangle}{\langle v^2 \rangle} = \frac{\langle l'^2 \rangle}{\langle U'^2 \rangle} \quad (4.45)$$

and

$$\frac{\langle U^2 \rangle}{\langle v^2 \rangle} = \frac{\langle l'^2 \rangle}{\langle p'^2 \rangle}. \quad (4.46)$$

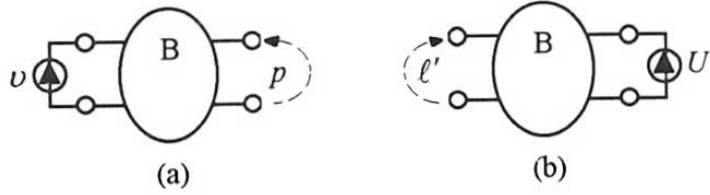


Figure 4.7: Reciprocal system B [Lyon and DeJong 1995], p. 71

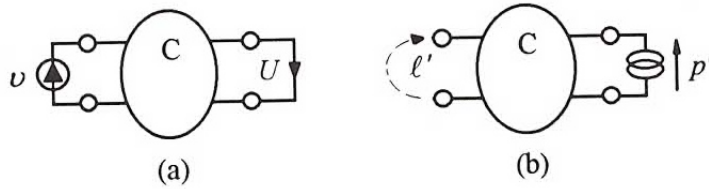


Figure 4.8: Reciprocal system C [Lyon and DeJong 1995], p. 71

The differences between Fig. (4.6), Fig. (4.7) and Fig. (4.8) are the used variables. In Fig. (4.6) a drop force is applied at terminal pair 1 and a flow measured at terminal pair 2. In Fig. (4.7) a flow is generated at terminal pair 1 and a drop measured at terminal pair 2. In Fig. (4.8.a) a flow is applied at terminal pair 1 and a drop measured at terminal pair 2, whereas in Fig. (4.8.b) a drop is generated at terminal pair 2 and a flow measured at terminal pair 1.

The force that arises on a point clamp at the edge of the plate because of the vibration of the plate is discussed as an example of reciprocity. A band limited noise source $l_1(t)$ acts on a point x_s on the surface of the plate and the dynamic load resulting to this excitation on the clamp is termed l_B , as shown in Fig. (4.9). The power $\langle l_1^2 \rangle G_{1,\infty}$ is injected into the plate because of the

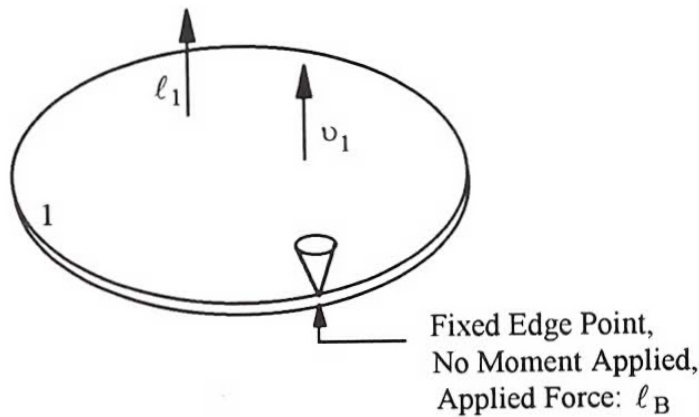


Figure 4.9: Plate driven by a point load noise source [Lyon and DeJong 1995], p. 71

load l_1 . This power leads to the following mean square velocity $\langle v_1^2 \rangle$ in the plate:

$$\langle v_1^2 \rangle = \alpha \langle l_1^2 \rangle G_{1,\infty} \quad (4.47)$$

where α relates the mean square velocity to the input power. Because of the linearity of the system it can be written:

$$\langle l_B^2 \rangle = \Theta \langle v_1^2 \rangle \quad (4.48)$$

where Θ is the unknown parameter. If the clamp is driven with a noise velocity $v'_B(t)$ then this procedure describes the reciprocal situation. It has to be noted that $v'_B(t)$ must have the same band limited spectrum that $l_1(t)$ has. The power produced by $v'_B(t)$ is $\langle v_B'^2 \rangle R_1$ and the resulting plate velocity is:

$$\langle v_1'^2 \rangle = \alpha \langle v_B'^2 \rangle R_1. \quad (4.49)$$

The system in Fig. (4.9) has the same structure as the one in Fig. (4.8) and therefore with the help of Eq. (4.46) the following can be written:

$$\langle l_B^2 \rangle / \langle l^2 \rangle = \langle v_1'^2 \rangle / \langle v_B'^2 \rangle, \quad (4.50)$$

and Θ becomes:

$$\Theta = R_1 / G_{1,\infty}. \quad (4.51)$$

This example is extended by introducing a second plate that is connected to plate 1 at the edge point that was analysed before, as seen in Fig. (4.10). It is assumed that they are connected

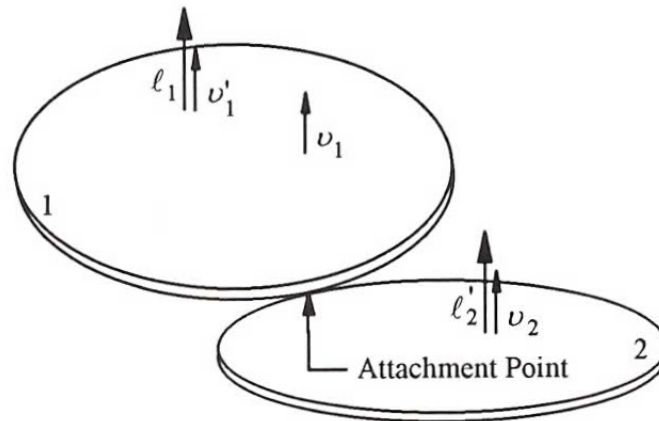


Figure 4.10: Two plates connected at one point along the edge [Lyon and DeJong 1995], p. 72

in a transverse way and that no moments are transmitted, to keep the problem simple. The mean square velocity in plate 1 is given by $\langle v_1^2 \rangle$ and a result of the band limited noise $l_1(t)$. This motion of plate 1 leads to a velocity in plate 2 $\langle v_2^2 \rangle = \Theta \langle v_1^2 \rangle$. This can be expressed in the form:

$$\langle v_2^2 \rangle = \Gamma \langle v_1^2 \rangle = \Gamma \beta \langle l_1^2 \rangle G_{1,\infty}. \quad (4.52)$$

The load $l_2'(t)$ that has the same spectrum as l_1 acts at the position where the velocity v_2 due to the force l_1 was measured. A part of the power that results from l_2 will be dissipated and another part, $\langle l_2'^2 \rangle G_{2,\infty}$ will be injected into plate 1 through the junction and is termed Π'_{12} . By

using the coupling loss factors defined earlier the following can be written:

$$\Pi'_{12} = \langle l_2^2 \rangle G_{2,\infty} \eta_{12} / (\eta_{21} + \eta_2). \quad (4.53)$$

Because of the power that is transmitted into plate 1 through the junction, a mean square velocity results in plate 1:

$$\langle v_1^2 \rangle = \Pi'_{12} \beta. \quad (4.54)$$

Using the reciprocity condition that $\langle l_1^2 \rangle / \langle l_2^2 \rangle = \langle v_2^2 \rangle / \langle v_1^2 \rangle$, the unknown factor Γ becomes:

$$\Gamma = \frac{G_{2,\infty}}{G_{1,\infty}} \frac{\eta_{21}}{\eta_2 + \eta_{21}} = \frac{\langle v_2^2 \rangle}{\langle v_1^2 \rangle}. \quad (4.55)$$

In finite systems it can be used that $G_{2,\infty} = (\pi/2)(n_2/M_2)$ and $G_{1,\infty} = (\pi/2)(n_1/M_1)$. Substituting this in the equation for Γ leads to:

$$\frac{M_2 \langle v_2^2 \rangle}{n_2} = \frac{M_1 \langle v_1^2 \rangle}{n_1} \frac{\eta_{21}}{\eta_2 + \eta_{21}}. \quad (4.56)$$

This is another representation of Eq. (4.38), which states power flow relations of Statistical Energy Analysis.

The power flow between plate 1 and plate 2 can also be described in terms of a blocked force as used in Eq. (4.48) and (4.50), respectively (4.51). Then the system shown in Fig. (4.11a) must be divided in parts as in Fig. (4.11b). The blocked force l_B minus the force resulting due to the

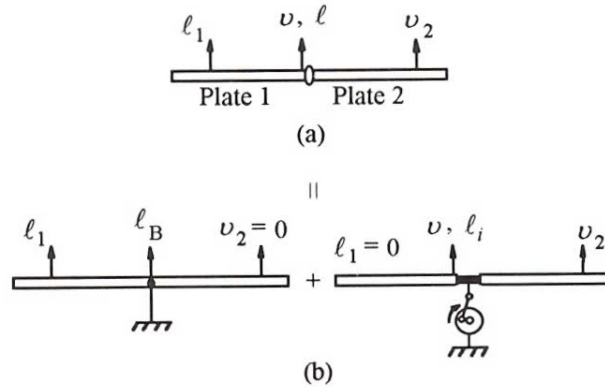


Figure 4.11: Superposition used to analyse 2-plate system, a) actual system; b) system divided into 2 idealised problems [Lyon and DeJong 1995], p. 74

velocity, ($l_i = vZ_i$) gives the actual force that the junction applies to plate 1. Upward forces and velocities are positive, whereas downward forces and velocities are negative. The velocity at the boundary will create an upward force on the edge of plate 1 and also on plate 2 there will be an upward force because of the motion v and therefore a downward reaction force on the edge of plate 1. This leads to:

$$l = -vZ_2 = l_B + vZ_1 \quad (4.57)$$

and according to that

$$\langle l_B^2 \rangle = \langle v^2 \rangle |Z_1 + Z_2|^2. \quad (4.58)$$

The relation between $\langle I_B^2 \rangle$ and $\langle v_1^2 \rangle$ is given through Eq. (4.48). The power into plate 2 is defined as $\langle v^2 \rangle R_2$ and the velocity in plate 2 is related to $\langle v^2 \rangle$ by the loss factor of plate 2:

$$\langle v_2^2 \rangle = \langle v^2 \rangle R_2 / \omega M_2 \eta_2. \quad (4.59)$$

Combining Eq. (4.48, 4.50, 4.51, 4.57, 4.58, 4.59) leads to:

$$\frac{M_2 \langle v_2^2 \rangle}{n_2} = \frac{M_1 \langle v_1^2 \rangle}{n_1} \left\{ \frac{2}{\pi} \frac{R_1 R_2}{|\mathbf{Z}_1 + \mathbf{Z}_2|^2} \right\} \frac{1}{\omega \eta_2 n_2}. \quad (4.60)$$

This can be seen as the multi-dof equivalent of Eq. (4.17). The power that is injected into system 1 is given by $M \langle v_1^2 \rangle$ and the coefficient in the above relation that describes the power flow, can be called the ‘‘coupling loss factor’’ for the case of uncoupled system energies. It is defined as:

$$\alpha_{12} = \frac{2}{\pi \omega n_1} \frac{R_1 R_2}{|\mathbf{Z}_1 + \mathbf{Z}_2|^2}. \quad (4.61)$$

The reciprocity condition that is fulfilled by η_{12} is also valid for α_{12} , this means that:

$$n_1 \alpha_{12} = n_2 \alpha_{21}. \quad (4.62)$$

Since there is a relation between α_{12} and η_{12} the coupling loss factor can be calculated by junction impedances or averages over impedances. The relation between α_{12} and η_{12} depends on the system that is analysed. The impedances \mathbf{Z}_1 and \mathbf{Z}_2 can be calculated based on a wave or modal analysis. In some cases they can be easily evaluated by a wave model and therefore wave analysis is important in SEA for the evaluation of junction impedances.

The coupling loss factor can be calculated relatively easy, if systems are connected through a line in the two dimensional case or through a surface in a three dimensional case. The constraint is that the dimensions of the line or the surface must be large in comparison to the free wave length of the system. As it can be seen in Fig. (4.12), waves that have the intensity \mathcal{I}_0 in the interval $d\Omega$ are partly transmitted and partly reflected at the junction. The transmission

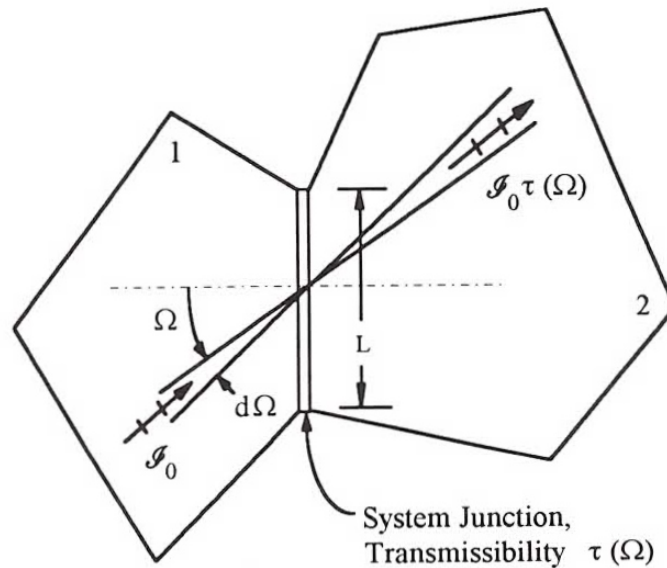


Figure 4.12: Transmission of power between two systems through a line junction [Lyon and DeJong 1995], p. 72

coefficient $\tau(\Omega)$ determines the ratio of the transmitted to the incident power. It is a function of the angle between the junction line or surface and the incident waves. In the same way as presented in Eq. (3.113), the transmitted power can be calculated by:

$$\Pi_{12} = \int_{\Omega_{\text{inc}}} \tau(\Omega) L_p(\Omega) d(\Delta\mathcal{I}). \quad (4.63)$$

In this equation $d(\Delta\mathcal{I})$ is given by:

$$d(\Delta\mathcal{I}) = \Delta\mathcal{E} c_g D(\Omega) d\Omega / \Omega_{\text{tot}}, \quad (4.64)$$

with $d(\Delta\mathcal{I})$ being the intensity of wave energy, $D(\Omega)$ stands for a weighting function, $d\Omega$ describes the interval of directions of the waves and Ω_{tot} is the total range of Ω . In Eq. (4.63) L_p is a projection of the boundary length or area for the waves that propagate in the direction Ω , and Ω_{inc} is the range of angles of the waves reaching the boundary. The energy that leads to the transmitted power is $A_1 \Delta\mathcal{E}_1$ with A_1 defining the area of system 1. Therefore the coupling loss factor is:

$$\eta_{12} = \frac{\Pi_{12}}{\omega A_1 \Delta\mathcal{E}_1} = \frac{c_g}{\omega A_1 \Omega_{\text{trans}}} \int_{\Omega_{\text{inc}}} \tau(\Omega) L_p(\Omega) D(\Omega) d\Omega. \quad (4.65)$$

As an example a two dimensional isotropic system is analysed. In this case L_{junct} is the length of the transmitting boundary (straight line). The variable Ω defines the angle of the incident waves. With these assumptions $D(\Omega) = 1$, $\Omega_{\text{inc}} = \pi$ and $\Omega_{\text{tran}} = \pi$. The coupling loss factor becomes:

$$\eta_{12} = \frac{c_g L_{\text{junct}}}{\pi \omega A_1} \int_{-\pi/2}^{\pi/2} \tau(\Omega) \cos\Omega d\Omega = \frac{c_g L_{\text{junct}}}{\omega A_1} \langle \tau(\Omega) \cos\Omega \rangle_{\Omega_{\text{inc}}}. \quad (4.66)$$

To calculate the coupling loss factor with the presented formula the transmissibility must be known. This value can be either calculated or is even available in the literature. In a three dimensional case, e.g. in acoustics, the coupling loss factor becomes:

$$\eta_{12} = \frac{c A_{\text{junct}}}{4\omega V_1} \langle \tau(\Omega) \cos\Theta \rangle_{\Omega_{\text{inc}}}, \quad (4.67)$$

with c the speed of sound, V_1 the room volume, A_{junct} the area of the boundary and Θ the angle between the panel and the wave vector.

5

The Estimation of Response Statistics in SEA

5.1 Mean Value Estimates of Dynamical Response

Using average energy quantities can be very advantageous because sound, vibration and other resonant systems can be analysed by the same variables. It has to be kept in mind that all those variables are averages and that the actual energy of the system that is analysed will not be exactly equal the averaged energy that was calculated based on an ensemble of similar systems. The difference between the actual system and the average system can be expressed by defining a standard deviation (σ) or variance (σ^2) of the system energy. If σ is small that means that the actual system is described quite well by the mean value but if σ is big, the probability that one realisation will have a response that is close to the mean is small. In this case a confidence interval or confidence coefficient is used that defines an interval of response amplitudes that will be reached by an actual realisation with some probability.

5.1.1 Single Mode Response

System 1 is assumed to be a multi-modal system and the force that acts on the system is supposed to be a noise force of bandwidth $\Delta\omega$. The total energy of that system is $E_{1,\text{tot}}$ and the system has N_1 modes in the bandwidth of the source. For system 2 the assumption is made that it has only one mode with mode shape $\Psi_2(x)$. By using the coupling loss factor η_{12} that was defined in chapter 3, the energy of the mode of system 2 can be written as:

$$E_2 = \mathcal{E}_1 \frac{\eta_{21}}{\eta_2 + \eta_{21}}. \quad (5.1)$$

The actual response of system two at location x_2 should be found, assuming that the coupling loss factor has been calculated yet. With the help of Eq. (3.59) it can be written that:

$$y_2(x, t) = \mathcal{Y}_2(t) \Psi_2(x). \quad (5.2)$$

The general result for the energy E_2 is:

$$E_2 = \int dx \rho \langle \dot{y}^2 \rangle_t = M_2 \langle \dot{\mathcal{Y}}_2^2(t) \rangle_t = M_2 \omega_2^2 \langle \mathcal{Y}_2^2(t) \rangle_t. \quad (5.3)$$

In Eq. (5.3) M_2 stands for the mass of system 2 and ω_2 stands for the resonance frequency of system 2 but ω_2 can be replaced by ω because it is assumed that ω_2 is in $\Delta\omega$. So the average response becomes:

$$\langle y_2^2(x, t) \rangle = \frac{E_2}{\omega^2 M_2} \Psi_2^2(x) = \left[\frac{E_{1,\text{tot}}}{N_1} \frac{\eta_{21}}{\eta_2 + \eta_{21}} \right] \frac{1}{\omega^2 M_2} \Psi_2^2(x). \quad (5.4)$$

This last equation shows that even if a statistical model is used, the spatial distribution of the response can be calculated. By normalising the mode shape, it is still valid that

$$\langle y_2^2 \rangle_{\rho,t} = E_2 / \omega^2 M_2. \quad (5.5)$$

5.1.2 Multi-Modal Response

In the case in that several modes N_2 exist in system 2 due to the indirect excitation of system 1 in the band $\Delta\omega$ the energy of system 2 is:

$$\frac{E_{2,\text{tot}}}{N_2} \equiv \mathcal{E}_2 = \frac{E_{1,\text{tot}}}{N_1} \frac{\eta_{21}}{\eta_2 + \eta_{21}}. \quad (5.6)$$

The mean square response of system 2 due to this energy is given by:

$$\langle y_2^2 \rangle_{\rho,t} = E_{2,\text{tot}} / \omega^2 M_2. \quad (5.7)$$

In the case of a clamped free beam the response estimate would be a poor estimate, because the actual value of $\langle y_2^2 \rangle_t$ would only be equivalent to $\langle y_2^2 \rangle_{\rho,t}$ at a finite number of points. At most of the points $\langle y_2^2 \rangle_t$ would oscillate around the estimate. Therefore the variance of the response should be estimated in the described example to analyse the system properly.

In Sec. (4.2) a model for system interaction was derived. The following three statements can be made for the response of system 2:

(1) Based on Eq. (5.2) the response of the multi-modal system can be written as:

$$y_2(x, t) = \sum_{\sigma} \mathcal{Y}_{\sigma}(t) \Psi_{\sigma}(x). \quad (5.8)$$

(2) The incoherence of the modal response amplitudes leads to:

$$\langle \mathcal{Y}_{\sigma}(t) \mathcal{Y}_{\tau}(t) \rangle_t = \langle \mathcal{Y}_{\sigma}^2(t) \rangle_t \delta_{\sigma,\tau}. \quad (5.9)$$

(3) All the modes of system 2 have the same energy:

$$\langle \mathcal{Y}_{\sigma}^2(t) \rangle_t = \langle \mathcal{Y}_{\tau}^2(t) \rangle_t = \mathcal{E} / \omega^2 M_2. \quad (5.10)$$

The values that are valid for σ are defined by the modes of system 2 in the frequency band $\Delta\omega$. This result can be used for describing the multi-modal temporal mean square response of a rectangular plate.

5.1.3 Wave Estimates

The most important use of wave analysis in SEA is the calculation of average impedance functions for deriving coupling loss factors at the boundaries of a system. As an example the system of Fig. (5.1) is analysed, where a beam is cantilevered to a plate.

The displacement along the connection of the systems will be very small, because the systems have very high impedances. But there will be a transmission of power due to torques and rotational motion of the junction. For the determination of the coupling loss factor, the power

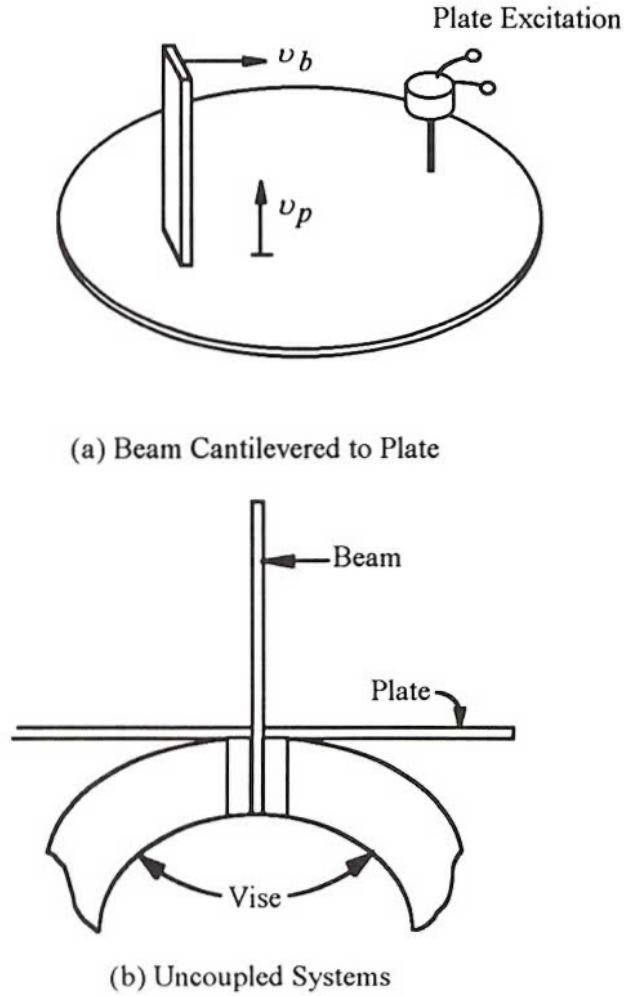


Figure 5.1: Beam plate system, beam indirectly excited [Lyon and DeJong 1995], p. 87

transmission between the systems must be evaluated. If the rotation force of the contact line is left out (see Fig. (5.1)) they are uncoupled. Then the modes of the beam are known, in this case the beam has clamped-free boundary conditions. To evaluate the modes of the plate a finite element model would be needed because of the complicated boundary conditions of the plate. Applying the reciprocity principle for coupling loss factors and by assuming that the plate is infinite, the problem can be solved. The reciprocity of the coupling loss factor allows to determine the plate to beam coupling loss factor η_{pb} , if the beam to plate coupling loss factor η_{bp} is known:

$$N_p \eta_{pb} = N_b \eta_{bp}. \quad (5.11)$$

The moment impedance that looks into the plate can be replaced by the one that belongs to an infinite plate. The infinite system moment impedance is known and equals the averaged moment impedance, as shown in Sec. (3.2) and Sec. (3.3). The advantage of this procedure is that the energy of the plate that returns to the junction is omitted.

In Sec. (4.3) the power flow between systems was described by using the boundary impedances, resulting in:

$$\Pi_{bp} = \omega \alpha_{bp} E_{b,tot}^{(b)}, \quad (5.12)$$

with

$$\omega\alpha_{\text{bp}} = \frac{2}{\pi n_{\text{b}}} \frac{R_{\text{b}}R_{\text{p}}}{|\mathbf{Z}_{\text{b}} + \mathbf{Z}_{\text{p}}|^2}. \quad (5.13)$$

In Eq. (4.34) a second version for describing the transmitted power from subsystem 1 into subsystem 2 was found that can be adapted here to:

$$\Pi_{\text{bp}} = \omega\eta_{\text{bp}} \left(E_{\text{b,tot}} - \frac{N_{\text{b}}}{N_{\text{p}}} E_{\text{p,tot}} \right). \quad (5.14)$$

In general α_{bp} in Eq. (5.12) is not the same as η_{bp} in Eq. (5.14). By expanding the receiving system (in this case the plate), and not changing the loss factor η_{p} , the term $N_{\text{b}}E_{\text{p,tot}}/N_{\text{p}}$ will vanish. Introducing the infinite plate impedances in Eq. (5.12) and using the last statements, leads to:

$$\alpha_{\text{bp}} = \frac{2}{\pi\omega n_{\text{b}}} \frac{R_{\text{b}}R_{\text{p}}^{\infty}}{|\mathbf{Z}_{\text{b}} + \mathbf{Z}_{\text{p}}^{\infty}|^2}. \quad (5.15)$$

The junction does not influence the input power to the system:

$$\Pi_{1,\text{in}} = E_{1,\text{tot}}^{(b)} \Delta_1 = E_{1,\text{tot}} \Delta_1 + \omega\alpha_{12} E_{1,\text{tot}}^{(b)} \quad (5.16)$$

and

$$\omega\eta_{\text{bp}} E_{\text{b,tot}} = \omega\eta_{\text{bp}} \left[1 - \frac{\omega\alpha_{\text{bp}}}{\Delta_{\text{b}}} \right] E_{\text{b,tot}}^{(b)} = \omega\alpha_{\text{bp}} E_{\text{b,tot}}^{(b)}. \quad (5.17)$$

Accordingly, η_{bp} and α_{bp} can be related:

$$\eta_{\text{bp}} = \alpha_{\text{bp}} (1 - \omega\alpha_{\text{bp}}/\Delta_{\text{b}})^{-1}. \quad (5.18)$$

For a beam that has only one single mode $\Delta_{\text{b}} = R_{\text{b}}/M_{\text{b}}$ and averaging α_{bp} over Δ_{ω} leads to:

$$\langle \alpha_{\text{bp}} \rangle_{\Delta_{\omega}} = \frac{2}{\pi\omega} \frac{R_{\text{b}}R_{\text{p}}^{\infty}}{(R_{\text{b}} + R_{\text{p}})^2} \cdot \frac{\pi}{2} \frac{R_{\text{b}} + R_{\text{p}}}{M_{\text{b}}}. \quad (5.19)$$

Expressing η_{bp} in Eq. (5.18) in terms of the averaged α_{bp} of Eq. (5.19) leads to:

$$\omega\eta_{\text{bp}} = \frac{R_{\text{p}}^{\infty}}{M_{\text{b}}}. \quad (5.20)$$

Discussing a beam that has very dense modes, i.e. $n_{\text{b}}\Delta_{\text{b}} \gg 1$, then the beam looks infinite and it can be written that:

$$\frac{\omega\alpha_{\text{bp}}}{\Delta_{\text{b}}} = \frac{2}{\pi} \frac{R_{\text{b}}^{\infty} + R_{\text{p}}^{\infty}}{|\mathbf{Z}_{\text{b}}^{\infty} + \mathbf{Z}_{\text{p}}^{\infty}|^2} \frac{1}{n_{\text{b}}\Delta_{\text{b}}} \ll 1. \quad (5.21)$$

Therefore, the term in brackets in Eq. (5.18) is nearly 1 and this means that $\eta_{\text{bp}} \rightarrow \alpha_{\text{bp}}$:

$$\eta_{\text{bp}} \rightarrow \alpha_{\text{bp}} = \frac{2}{\pi\omega n_{\text{b}}} \frac{R_{\text{b}}^{\infty} + R_{\text{p}}^{\infty}}{|\mathbf{Z}_{\text{b}}^{\infty} + \mathbf{Z}_{\text{p}}^{\infty}|^2}. \quad (5.22)$$

η_{bp} can be described in terms of a mode-mode coupling coefficient $\langle \mathcal{B}_{\alpha\sigma} \rangle$:

$$\omega\eta_{\text{bp}} = \langle \mathcal{B}_{\text{bp}} \rangle n_{\text{p}} \Delta_{\omega}. \quad (5.23)$$

The value of $\langle \mathcal{B}_{bp} \rangle$ is indirectly proportional to the plate area of the receiving system whereas n_p is directly proportional to the plate area. This means that the extension of the receiving system does not change the value of η_{bp} but it affects the value of α_{bp} . This leads to the fact that applying Eq. (5.18) is only correct, if the parameters of the receiving systems are infinite but Eq. (5.15) is correct in any situation.

In the system shown in Fig. (5.1) the infinite impedances for beam and plate are defined as:

$$\mathbf{Z}_b^M = \rho_b c_b^2 S_b \kappa_b^2 c_{fb}^{-1} (1 - j) \quad (5.24)$$

$$\mathbf{Z}_p^M = 16 \rho_s \kappa_p^2 c_p^2 / \omega (1 + j\Gamma). \quad (5.25)$$

The variables ρ , c and κ stand for the material density, longitudinal wave speed and radius of gyration of the beam (with subscript b), respectively plate (with subscript p). The cross-sectional area of the beam is termed S_b , the flexural phase speed of the beam is defined as $c_{fb} = \sqrt{\omega \kappa_b c_b}$ and ρ_s stands for the mass per unit area of the plate. The shape of the junction is responsible for the susceptance parameter Γ . If it is assumed that the plate and the beam are of same material thickness and that the coupling factor is not depending on Γ , this is true if, $\mathbf{Z}_p^M \gg \mathbf{Z}_b^M$, then it can be written that:

$$\eta_{bp} \rightarrow w/4L. \quad (5.26)$$

In Eq. (5.26) w describes the width of the beam and L stands for the length of the beam. The modal density of the beam is given by:

$$n_b(\omega) = L/2\pi c_{fb}. \quad (5.27)$$

Using Eq. (5.11) the coupling loss factor from plate to beam can be written as:

$$\eta_{pb} = n_b \eta_{bp} / n_p, \quad (5.28)$$

with $n_p = A_p / 4\pi \kappa_p c_p$. With these definitions the average response of the beam can be calculated:

$$\langle v_b^2 \rangle = \langle v_p^2 \rangle \frac{M_p n_b}{M_b n_p} \frac{\eta_{bp}}{\eta_b + \eta_{bp}}. \quad (5.29)$$

5.1.4 Strain Response

The energy response of a system that is strained or stressed is described in this section. The pressure in a sound field obeys the relation:

$$\frac{\langle p^2 \rangle V_R}{\rho_0 c^2} = \langle v^2 \rangle M_R, \quad (5.30)$$

with $\langle v^2 \rangle$ describing the mean square velocity of fluid particles. M_R stands for the mass of the fluid that is contained in the analysed room and given by $M_R = \rho_0 V_R$. The volumetric stiffness or bulk modulus of the fluid is defined as $\mathbf{K}_0 = \rho_0 c^2$ and by using this relation, Eq. (5.30) can be rewritten:

$$\frac{\langle p^2 \rangle}{(\mathbf{K}_0)^2} = \left\langle \left(\frac{\partial \rho}{\rho_0} \right)^2 \right\rangle = \frac{\langle v^2 \rangle}{c^2}, \quad (5.31)$$

with the volumetric strain or dilatation $\partial \rho / \rho_0$. This equation states that the mean square mach number, i.e. the ratio of particle velocity to sound speed, is equivalent to the mean square strain

of the particles. In the case of plates a similar result can be found. The strain distribution in the case of a plate of thickness h is given as:

$$\epsilon(z) = \frac{2z}{h} \epsilon_{\max} \quad (5.32)$$

where ϵ_{\max} describes the maximum of the strain that is given at the free surface of the plate. If only a layer of plate material with thickness dz is considered, the energy density of this layer is $1/2 \int \mathbf{E} \epsilon^2(z) dz$, with the Young's modulus \mathbf{E} . The total strain energy density for the plate is given by the following equation:

$$\text{PE}_{\text{density}} = \mathbf{E} \int_{-h/2}^{h/2} \frac{1}{2} z^2 \frac{4}{h^2} \epsilon_{\max}^2 dz = \frac{2\kappa^2}{h} \mathbf{E} \langle \epsilon_{\max}^2 \rangle. \quad (5.33)$$

If the kinetic energy density $\frac{1}{2} \rho_p h \langle v^2 \rangle$ is set equal to the potential energy density (Eq. (5.33)), and using that $\mathbf{E} = \rho c^2$ and that for a homogeneous plate $\kappa^2 = h^2/12$, Eq. (5.33) can be written as:

$$\langle \epsilon_{\max}^2 \rangle = \frac{h^2}{4\kappa^2} \frac{\langle v^2 \rangle}{c_1^2} = 3 \frac{\langle v^2 \rangle}{c_1^2}. \quad (5.34)$$

In the special case of a sandwich plate, all the stiffness is at the surface of the plate and $\kappa = h/2$. Accordingly

$$\langle \epsilon_{\max}^2 \rangle = \frac{\langle v^2 \rangle}{c_1^2} \quad (5.35)$$

which is the same relation as presented in Eq. (5.31). Therefore it is valid to calculate the mean square strain estimates from energy or velocity estimates.

5.2 Calculation of Variance in Temporal Mean Square Response

The goal of this section is to derive the standard deviation that is the square root of the variance of the analysed system from the mean square response. Here, the variance that is dealt with, is not a temporal variance but the variance from one "similar" system to another. Or it can also be the variance from one location to another. The time averaging is assumed to vanish because of long noise signals that work as input. Four aspects, described below, make it necessary to calculate the variance between the mean and any member of the population:

- (1) The irregularity of the spatial distribution of the excitation sources and the internal coupling of the blocked system is not big enough and therefore equipartition is not guaranteed. This means that the modal energies of the system that is directly excited can be unequal.
- (2) The actual realisations of coupled systems will be different compared to the average of the population. Thus, the actual number of resonant interacting modes will be different in each realisation.
- (3) The modal shape at the junction of the systems is responsible for the strength of the coupling. Even due to small differences in the modal shape of the actual realisation to another, the value of the coupling parameters will fluctuate.

(4) The mode shapes will be different for each realisation of a system. Therefore the response at the selected analysis position will fluctuate because the analysis position is randomly chosen.

The variance of a system can only be calculated based on the modal analysis, because in wave analysis spatial coherence effects are not taken into account. Nevertheless these effects are essential for variance determination.

5.2.1 Modal Power Flow and Response

For the calculation of the variance in the modal energies again the system in Fig. (4.4) is discussed. It is assumed that only system 1 is excited by an external force and the resulting power flow from the resonators of system 1 to the resonator σ of system 2 therefore is:

$$\Pi_{1\sigma} = \sum_{\alpha} \mathcal{A}_{\alpha\sigma} E_{\alpha}^{(b)} = \sum_{\alpha} \mathcal{B}_{\alpha\sigma} (E_{\alpha} - E_{\sigma}), \quad (5.36)$$

with \mathcal{A} and \mathcal{B} defined in [Lyon and DeJong 1995]. The dissipation of energy of mode σ can be written as $E_{\sigma}\Delta_{\sigma}$ if the damping of the mode is Δ_{σ} . Then the energy E_{σ} becomes:

$$E_{\sigma} = \sum_{\alpha} E_{\alpha}^{(b)} (\mathcal{A}_{\alpha\sigma} / \Delta_{\sigma}) = \left(\sum_{\alpha} E_{\alpha} \mathcal{B}_{\alpha\sigma} \right) (\Delta_{\sigma} + \sum_{\alpha} \mathcal{B}_{\alpha\sigma})^{-1}. \quad (5.37)$$

If the focus of interest lies in the velocity response, it can be written that:

$$\langle v_{\sigma}^2 \rangle_t = (E_{\sigma} / M_2) \Psi_{\sigma}^2(x_2), \quad (5.38)$$

with x_2 defining the observation position. The mean square velocity response of system 2 at this position is therefore:

$$\langle v_{\sigma}^2(x_2, t) \rangle_t = \frac{1}{M_2} \sum_{\sigma} \Psi_{\sigma}^2(x_2) \sum_{\alpha} E_{\alpha}^{(b)} \mathcal{A}_{\alpha\sigma} / \Delta_{\sigma} = \frac{1}{M_2} \sum_{\sigma} \Psi_{\sigma}^2(x_2) \left(\sum_{\alpha} E_{\alpha} \mathcal{B}_{\alpha\sigma} \right) / \left(\Delta_{\sigma} + \sum_{\alpha} \mathcal{B}_{\alpha\sigma} \right). \quad (5.39)$$

Each of the four aspects listed above can be found in Eq. (5.39): variance in modal energies is included in $E_{\alpha}^{(b)}$ respectively E_{α} (1), the summation in α incorporates the variance of the number of interacting modes (2), variance in coupling strength can be found in $\mathcal{A}_{\alpha\sigma}$ or $\mathcal{B}_{\alpha\sigma}$ (3) and the variance of the mode shapes is presented by Ψ_{σ}^2 (4).

The variance of the sum in Eq. (5.39) should be found in the next step. This is a difficult problem and therefore some simplifications are needed. At first it is assumed that the coupling damping is much larger than the internal damping, i.e. $\sum_{\alpha} \mathcal{B}_{\alpha\sigma} \gg \Delta_{\sigma}$. With this assumption Eq. (5.39) becomes:

$$\langle v_{\sigma}^2 \rangle_t = (\Psi_{\sigma}^2(x_2) / M_2) \sum_{\alpha} E_{\alpha} \mathcal{B}_{\alpha\sigma} / \sum_{\alpha} \mathcal{B}_{\alpha\sigma}. \quad (5.40)$$

This means that the weighed, averaged energy of the modes of system 1 define the energy of the σ -mode. The weighting factor in this case is $b_{\alpha\sigma} = \mathcal{B}_{\alpha\sigma} / \sum_{\alpha} \mathcal{B}_{\alpha\sigma}$. The second case in which the variance can be calculated is the one, when it is assumed that $\Delta_{\sigma} \gg \sum_{\alpha} \mathcal{B}_{\alpha\sigma}$. Then,

$$\langle v_{\sigma}^2 \rangle_t = (\Psi_{\sigma}^2(x_2) / (M_2 \Delta_{\sigma})) \sum_{\alpha} E_{\alpha} \mathcal{B}_{\alpha\sigma} \quad (5.41)$$

with $\mathcal{B}_{\alpha\sigma}$ given by:

$$\mathcal{B}_{\alpha\sigma} = \frac{\lambda_{\alpha\sigma}}{\xi_{\alpha\sigma}^2 + 1} \frac{\Delta_\alpha \Delta_\sigma}{\Delta_\alpha + \Delta_\sigma}. \quad (5.42)$$

Eq. (4.31) gives the definition of $\lambda_{\alpha\sigma}$, and $\xi_{\alpha\sigma} = 2(\omega_\sigma - \omega_\alpha)/(\Delta_\alpha + \Delta_\sigma)$. Setting the damping of the modes of system 1 to $\Delta_\alpha = \Delta_1 = \text{const}$ leads to:

$$\langle \mathcal{B}_{\alpha\sigma} \rangle_{\omega_\alpha} = \langle \lambda_{\alpha\sigma} \rangle_{\omega_\alpha} \frac{\Delta_1 \Delta_\sigma}{\Delta_1 + \Delta_\sigma} \frac{\pi(\Delta_1 + \Delta_\sigma)}{2\Delta\omega} \quad (5.43)$$

and Eq. (4.30) is reproduced. Assuming that $\Delta_\sigma = \Delta_1$ means that $(\xi_{\alpha\sigma}^2 + 1)^{-1}$ has always the same shape depending on the frequency values and therefore Eq. (5.41) can be plotted (see Fig. (5.2)).

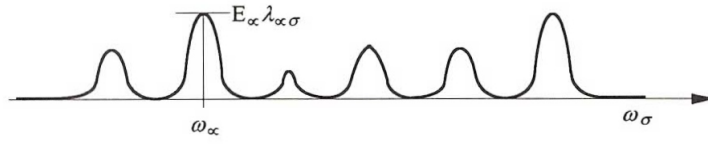


Figure 5.2: Sum of Eq. (5.41)[Lyon and DeJong 1995], p. 95

It is a sum of pulses, where the strength of the pulse is:

$$C_{\alpha\sigma} = \frac{(\Psi_\sigma^2/M_2)\Delta_1\Delta_\sigma}{\Delta_1 + \Delta_\sigma} E_\alpha \lambda_{\alpha\sigma}. \quad (5.44)$$

In chapter 4 the assumption was made that resonance frequencies of modes of the population model are independent of each other and are randomly distributed over a frequency interval $\Delta\omega$. Accordingly the occurrence of the resonance frequencies can be described by a Poisson Process. The spacings between the resonance frequencies obey the following probability density function:

$$pdf(\delta\omega) = \exp(-\delta\omega/\bar{\delta\omega})/\bar{\delta\omega}. \quad (5.45)$$

The standard deviation of Eq. (5.41) in the case of a Poisson distribution of the resonance frequencies, as derived in the literature [Lyon and Eichler 1964], becomes:

$$\sigma_{v_\sigma^2}^2 = \frac{\pi}{2} n_1(\omega) (\Delta_1 + \Delta_\sigma) \left[\frac{(\Psi_\sigma^2/M_2)\Delta_1\Delta_\sigma}{\Delta_1 + \Delta_\sigma} \right] \langle E_\alpha^2 \rangle_\alpha \langle \lambda_{\alpha\sigma}^2 \rangle_\alpha. \quad (5.46)$$

The ratio of the variance to the squared mean (termed as $m_{v_\sigma^2}^2$) is given by:

$$\frac{\sigma_{v_\sigma^2}^2}{m_{v_\sigma^2}^2} = \left[n_1 \frac{\pi}{2} (\Delta_1 \Delta_\sigma) \right]^{-1} \frac{\langle E_\alpha^2 \rangle_\alpha \langle \lambda_{\alpha\sigma}^2 \rangle_\alpha}{\langle E_\alpha \rangle_\alpha^2 \langle \lambda_{\alpha\sigma} \rangle_\alpha^2}. \quad (5.47)$$

The variance depends on uncertainties of the modal energy of the system that is directly excited and on uncertain values of the coupling parameters. It is shown that the ratio of variance to the squared mean is reduced by the number of overlapping modes.

In chapter 4 the relation $N_1 \langle \mathcal{B}_{\alpha\sigma} \rangle_\alpha \equiv \omega \eta_{21}$ was derived. The mean of the coupling loss factor is termed as m_η , then the variance and the ratio of variance to squared mean of the coupling loss

factor are given by:

$$\sigma_\eta^2 = \frac{1}{\omega^2} \langle \lambda_{\alpha\sigma}^2 \rangle \left(\frac{\Delta_1 \Delta_\sigma}{\Delta_1 + \Delta_\sigma} \right)^2 \frac{\pi}{2} n_1 (\Delta_1 + \Delta_\sigma) \quad (5.48)$$

$$\frac{\sigma_\eta^2}{m_\eta^2} = \frac{1}{\frac{\pi}{2} n_1 (\Delta_1 + \Delta_\sigma)} \frac{\langle \lambda_{\alpha\beta}^2 \rangle}{\langle \lambda_{\alpha\beta} \rangle^2}. \quad (5.49)$$

If the observation point in Eq. (5.41) is chosen randomly in space, then the factor $\langle \Psi_\sigma^4 \rangle / \langle \Psi_\sigma^2 \rangle^2$ must be added in Eq. (5.47). This factor arises because Ψ_σ^2 has to be treated as a random variable, if the observation point is located randomly. If the point force that excites system 1 is located randomly at x_1 , the mode energy due to this force will vary too. The value of $\lambda_{\alpha\sigma}$ will also fluctuate if the assumption is made that the systems are joined at a random point. Therefore the greatest value of the ratio of the variance to the squared mean of a single mode of system 2 can be expressed as:

$$\frac{\sigma_{v_\sigma^2}^2}{m_{v_\sigma^2}^2} = \left\{ n_1 \frac{\pi}{2} (\Delta_1 + \Delta_2) \right\}^{-1} \left[\frac{\langle \Psi_1^4 \rangle}{\langle \Psi_1^2 \rangle^2} \right]^2 \left[\frac{\langle \Psi_2^4 \rangle}{\langle \Psi_2^2 \rangle^2} \right]^2, \quad (5.50)$$

with Ψ_1 and Ψ_2 defining the mode shapes of the systems 1 and 2. Assuming that system 2 contains a group of modes, it has $n_2 \Delta \omega$ independent response functions, with the modal density n_2 . The ratio $\sigma_{v_\sigma^2}^2 / m_{v_\sigma^2}^2$ for the multimodal response of system 2, for each independent response function is:

$$\frac{\sigma_{v_\sigma^2}^2}{m_{v_\sigma^2}^2} = \left\{ n_1 n_2 \frac{\pi}{2} (\Delta_1 + \Delta_2) \Delta \omega \right\}^{-1} \left[\frac{\langle \Psi_1^4 \rangle}{\langle \Psi_1^2 \rangle^2} \right]^2 \left[\frac{\langle \Psi_2^4 \rangle}{\langle \Psi_2^2 \rangle^2} \right]^2. \quad (5.51)$$

The variance in this relation is symmetric in system 1 and 2. This means that the value of the variance is the same for the cases of exciting system 1 and observing the response of system 2 or vice versa. Some assumptions were made to calculate the variance. These assumptions increased the variance (except the one that $\Delta_\alpha = \Delta_1$ and $\Delta_\sigma = \Delta_2$) of the response and therefore more variance is estimated than may occur in real world problems.

5.3 Calculation of Confidence Interval

Based on the predicted mean, an interval of values is derived with the help of the estimated variance, in which a fraction of measurements lies. To calculate the probability that the observed response $\langle v^2 \rangle_t = \Theta$ lies between two defined values, a probability function, termed as $\phi(\Theta)$ is needed. By knowing the probability function, the probability that Θ lies in the ‘‘confidence interval’’ $\Theta_1 < \Theta < \Theta_2$ is given by:

$$CC = \int_{\Theta_1}^{\Theta_2} \phi(\Theta) d\Theta. \quad (5.52)$$

The variable CC defines the confidence coefficient. From basic probability theory it is known that Θ can take only positive values, the mean and the standard deviation were derived in Sec. (5.2). A well known probability function that fulfills the requirements stated here is the

gamma density:

$$\varphi(\Theta) = \Theta^{\mu-1} \exp(-\Theta/\lambda) / \lambda^\mu \Gamma(\mu). \quad (5.53)$$

The parameters are defined as $\mu = m_\Theta^2 / \sigma_\Theta^2$, $\lambda = \sigma_\Theta^2 / m_\Theta$ and $\Gamma(\mu)$ is the gamma function. Introducing that $y = \Theta m_\Theta / \sigma_\Theta^2$ means a variable change and Eq. (5.53) can be rewritten:

$$CC = \frac{1}{\Gamma(\mu)} \int_{\Theta_1 m_\Theta / \sigma_\Theta^2}^{\Theta_2 m_\Theta / \sigma_\Theta^2} y^{\mu-1} e^{-y} dy = \Gamma^{-1}(\mu) \left[\lambda \left(\mu, \frac{\Theta_2 m_\Theta}{\sigma_\Theta^2} \right) - \lambda \left(\mu, \frac{\Theta_1 m_\Theta}{\sigma_\Theta^2} \right) \right]. \quad (5.54)$$

$\lambda(\mu, B)$ states the incomplete gamma function, which is defined as:

$$\lambda(\mu, B) \equiv \int_0^B y^{\mu-1} e^{-y} dy. \quad (5.55)$$

The incomplete gamma function is well known and its values can be found in mathematical standard literature.

Eq. (5.54) can be also used in another way. It is possible to define a fixed probability and calculate the value $\Theta_{\max} \equiv r m_\Theta$, which is the upper bound of the integral in Eq. (5.54) to reach the defined probability. The equation to be solved to get this value is:

$$CC = \Gamma^{-1}(\mu) \lambda(\mu, r\mu). \quad (5.56)$$

Solving this equation results in a line of constant probability that depends on r and μ as shown in Fig. (5.3) for different CC values.

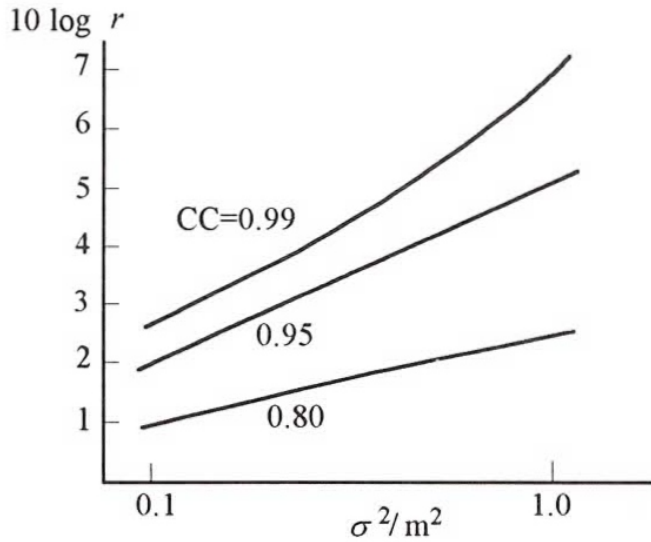


Figure 5.3: Upper bound of estimation intervals as a function of normalised variance [Lyon and DeJong 1995], p. 99

If the diagram presented in Fig. (5.3) is analysed at the point where $\sigma^2/m^2 = 1$, the following statements can be made: in 80% of the cases the measured response has a value that equals the mean plus less than 2.5 dB, in 95% of the cases this value is the mean plus less than 5 dB, and the last line means that in 99% of the cases the value of the measured response equals the mean plus less than 7 dB. It is also possible to define a symmetric interval that is bounded by the values $\Theta_1 = m_\Theta / r$ and $\Theta_2 = r m_\Theta$ to reach a defined probability. This interval implies that

the mean plus/minus some value is reached in, e.g. 80% of the cases. The equation that has to be solved to get the upper and the lower bound is:

$$CC = \Gamma^{-1}(\mu)\{\lambda(\mu, mur) - \lambda(\mu, \mu/r)\}. \quad (5.57)$$

6

Procedures of SEA

6.1 General Approach of SEA

The SEA procedure is divided into three steps that have to be fulfilled to analyse a given system.

- (1) The system model has to be defined.
- (2) The parameters that describe the given model have to be evaluated.
- (3) The response variables have to be determined and analysed.

It should be noted here that SEA is a statistical method. It evaluates the energy levels in resonant modes of dynamical systems from a statistical point of view. Therefore the number of degrees of freedom is less than in a deterministic analysis. The response quantities that SEA is mainly interested in, are the energy levels of resonant modes. Based on the energy levels the vibration and sound variables can be determined. It should be kept in mind that the response quantities are also statistical, this means that the results of SEA are averaged over frequency bands and spatial regions of the system.

6.2 Defining the System Model

The basis of SEA is the balance of dynamical energy and power flow between subsystems of a complex structure. Complex systems are divided into subsystems that are coupled mode groups belonging to the physical components of the system. The following procedure is applied to define a system model:

- (1) The whole and complex system is divided into physical components of an appropriate size. The natural modes of each physical component are concentrated into groups (subsystems) with similar features.
- (2) The physical coupling between the subsystems that are defined in step 1 must be determined.
- (3) The external excitation to the whole system must be defined.

In SEA the modes of the subsystems and the coupling between subsystems are evaluated statistically and not deterministically. This means that each subsystem has its own energy value and leads to the fact that the number of degrees of freedom in a SEA model equals the number of subsystems.

6.3 Evaluating the Subsystem Parameters

After the complex system is divided into subsystems the next step is to evaluate the subsystem' parameters. The parameters that are necessary for SEA calculations are listed below:

- (1) mode count
- (2) damping loss factor
- (3) coupling loss factor of connected subsystems
- (4) input power due to external sources.

Three different expressions of the mode count exist: first, the modal density; in a second version the mode count can be expressed by the number of resonant modes N or ΔN in a frequency band and in a third form the average frequency spacing between modal resonances can be used to describe the mode count. The mode count can be evaluated based on theoretical and numerical methods for many types of subsystems, if the geometry and the material characteristics of the subsystems are known. Sometimes the mode count can also be determined by experimental methods or empirical formulas.

Theoretical and numerical methods for evaluating the damping loss factor are in general not available because the damping depends on the details of the systems that are usually not known. Therefore experiments and empirical calculations are used to obtain the damping loss factor. But also in measurements it can be sometimes difficult to determine the damping loss factor because the separation between coupling loss and damping loss is not that easy.

Theoretical and empirical calculations can be used to evaluate the coupling loss factor of connected subsystems. In many cases it is possible to determine the coupling loss factor based on the transmission loss or the radiation efficiency. These values are well known in the literature. It is also possible to obtain the values of coupling loss factors from experimental and numerical methods, but these methods are sensitive to errors, due to the fact that at first the response of the subsystem must be calculated followed by a back calculation of the coupling loss factor. This method gives only acceptable results if the damping in the subsystems is quite high.

The power fed into a subsystem due to an external excitation source can be evaluated by the parameters of the subsystem. This procedure is possible if the amplitude of the force, pressure or imposed motion is known. In some cases it can be advantageous to use a unit excitation for the evaluation of the relative response amplitudes.

6.4 Evaluating the Response Variables

If the parameters of the subsystem are known, a power flow equation can be introduced for each subsystem (here, it is assumed that the structure contains of two subsystems):

$$\Pi_{1,\text{in}} = \Pi_{1,\text{diss}} + \Pi_{12} = 2\pi f(\eta_1 + \eta_{12})E_1 - 2\pi f\eta_{21}E_2 \quad (6.1)$$

$$\Pi_{2,\text{in}} = \Pi_{2,\text{diss}} + \Pi_{21} = -2\pi f\eta_{12}E_1 + 2\pi f(\eta_2 + \eta_{21})E_2. \quad (6.2)$$

The energies can be calculated because the number of equations is equal to the number of unknown system energies. In the case in which the analysed system is divided into a large

number of subsystems, the power flow equations are written in matrix form:

$$[A]\{\mathcal{E}\} = \{\Pi_{\text{in}}\}. \quad (6.3)$$

Matrix $[A]$ contains the damping and coupling loss factors and inverting this matrix leads to the result for the modal energy vector:

$$\{\mathcal{E}\} = [A]^{-1}\{\Pi_{\text{in}}\}. \quad (6.4)$$

Typical SEA models consist of 20 to 200 subsystems. The computation time needed for obtaining the results is modest compared to deterministic calculations for the same frequency range. Based on the results for the energies of the subsystems, other variables such as acceleration and sound pressure can be determined. Again it has to be kept in mind that these results are averaged over frequency and space.

7

Calculation of Reverberation Time with SEA

In this chapter the methods of how SEA can be used to predict the reverberation time of a single room are presented. Therefore the room is divided into several subsystems and the coupling loss factors and the damping loss factors are calculated for each of these subsystems. Furthermore the energy of every subsystem at time $t = 0$ must be known, which can be calculated over the ratio of the modes of one subsystem to the whole number of modes. By knowing these values a differential equation of the first order can be solved. The solution of this equation gives the energy decay curve. Based on the energy decay curve of the room it is also possible to calculate the reverberation time of the room, which is also shown in the following chapter. Room modes can only be calculated analytically in rectangular rooms, therefore this procedure can only be used in rectangular rooms. But the advantage of the described way is that it is also valid in rooms, where the walls have different absorption coefficients. The content of this chapter is mainly based on [Pfreundtner et al. 2015] and on [Pfreundtner 2014].

7.1 Division of Room into Subsystems

As mentioned above, the room is divided into seven subsystems, where every subsystem stands for specific modes, as can be seen in Tab. (7.1). This mentioned division of a room into subsystems was first proposed by Wilmshurst [Wilmshurst and Thompson 2012].

i	Subsystem	Reflected walls
1	x-axial modes	$x = 0, x = L_x$
2	y-axial modes	$y = 0, y = L_y$
3	z-axial modes	$z = 0, z = L_z$
4	xy-tangential modes	$x = 0, x = L_x, y = 0, y = L_y$
5	xz-tangential modes	$x = 0, x = L_x, z = 0, z = L_z$
6	yz-tangential modes	$y = 0, y = L_y, z = 0, z = L_z$
7	oblique modes	$x = 0, x = L_x, y = 0, y = L_y, z = 0, z = L_z$

Table 7.1: Subsystems of the SEA model

The energy in every subsystem decays because of the damping loss factor of the subsystem η_i and the coupling loss factor from the subsystem to the other subsystems η_{ij} . The sound energy in the room consists of the energy of the seven subsystems and decreases with time. It has to be mentioned that the dissipation of air influences the decay of the sound energy, too. The temporal development of the sound energy can be expressed in terms of a first order linear differential equation:

$$\frac{d}{dt}\mathbf{E}(t) + (\mathbf{D} + \mathbf{K})\mathbf{E}(t) = 0. \quad (7.1)$$

The vector $\mathbf{E}(t)$ consists of the energy of the seven subsystems and depends on time:

$$\mathbf{E}(t) = \begin{bmatrix} E_1(t) \\ E_2(t) \\ \vdots \\ E_7(t) \end{bmatrix} \quad (7.2)$$

The whole sound energy in the room can be written as:

$$E_{\text{room}}(t) = 10 \cdot \log \sum_{i=1}^7 E_i(t) e^{-m \cdot c \cdot t}, \quad (7.3)$$

where m is the dissipation factor of the air. The matrix of the damping loss factors is defined as:

$$\mathbf{D} = \begin{bmatrix} \eta_1 & 0 & \dots & 0 \\ 0 & \eta_2 & \dots & 0 \\ \vdots & \vdots & \ddots & \vdots \\ 0 & 0 & \dots & \eta_7 \end{bmatrix}. \quad (7.4)$$

The matrix of the coupling loss factors can be written as:

$$\mathbf{K} = \begin{bmatrix} \sum_{j \neq 1}^7 \eta_{1,j} & -\eta_{2,1} & \dots & -\eta_{7,1} \\ -\eta_{1,2} & \sum_{j \neq 2}^7 \eta_{2,j} & \dots & \eta_{7,2} \\ \vdots & \vdots & \ddots & \vdots \\ -\eta_{1,7} & -\eta_{2,7} & \dots & \sum_{j \neq 7}^7 \eta_{7,j} \end{bmatrix}. \quad (7.5)$$

In the following the damping loss factors, the coupling loss factors and the initial conditions of the differential equation have to be determined to solve the problem.

7.2 Determination of Initial Conditions

The initial condition for every subsystem of the differential equation system describes the amount of sound energy of the subsystem related to the whole stationary sound energy. The initial energy is calculated in the octave band around the analysed frequency. The initial energy of the subsystems can be calculated as the number of modes of the subsystem divided by the sum of the modes of all subsystems. In the case of subsystems 1, 2 and 3, where the modes are axial, the number of modes can be calculated with the following equation:

$$N_{1,2,3}(f) = \frac{2}{c} L_{x,y,z} (f_u - f_l), \quad (7.6)$$

where c stands for the speed of sound and $L_{x,y,z}$ describes the length of the x-, y- and z-dimension of the room. The upper frequency of the octave band f_u and the lower frequency of the octave band f_l are calculated with the following formulas:

$$f_u = f\sqrt{2}, \quad f_l = \frac{f}{\sqrt{2}}. \quad (7.7)$$

For subsystems 4, 5 and 6 the modes are tangential and the number of modes can be determined as:

$$N_{4,5,6}(f) = \frac{\pi}{c^2} L_{x,x,y} L_{y,z,z} (f_u^2 - f_l^2) - \frac{1}{c} (L_{x,x,y} + L_{y,z,z}) (f_u - f_l). \quad (7.8)$$

For subsystem 7, where the modes are oblique, the frequency dependent number of modes is defined as follows:

$$N_7(f) = \frac{4\pi V}{3c^3} (f_u^3 - f_l^3) - \frac{\pi S}{4c^2} (f_u^2 - f_l^2) + \frac{Sc}{8c} (f_u - f_l). \quad (7.9)$$

In the last equation V describes the volume of the cuboid, S the surface area of the cuboid and Sc stands for the perimeter of the edges of the cuboid:

$$V = L_x L_y L_z, \quad S = 2L_x L_y + 2L_x L_z + 2L_y L_z, \quad Sc = 4(L_x + L_y + L_z). \quad (7.10)$$

With these definitions it is possible to calculate the initial energies of all the subsystems:

$$\begin{bmatrix} E_1(0) \\ E_2(0) \\ \vdots \\ E_7(0) \end{bmatrix} = \begin{bmatrix} \frac{N_1(f)}{N_{\text{sum}}(f)} \\ \frac{N_2(f)}{N_{\text{sum}}(f)} \\ \vdots \\ \frac{N_7(f)}{N_{\text{sum}}(f)} \end{bmatrix}, \quad (7.11)$$

where $N_{\text{sum}}(f)$ is defined as:

$$N_{\text{sum}}(f) = \sum_{i=1}^7 N_i(f). \quad (7.12)$$

7.3 Calculation of Damping Loss Factors

This section deals with the calculation of the damping loss factors. To determine the damping and coupling loss factors, the idea of modes is simplified. In this simplified version modes are considered to be particles. One particle of the subsystem i propagates in the direction of the mode of this subsystem with the speed of sound. This particle is reflected exclusively at the walls that are listed in Tab. (7.1). The time after which the particle is reflected depends on the length of the mean free path:

$$\Delta t_i = \frac{\bar{l}_i}{c}. \quad (7.13)$$

The time in which n particles are reflected becomes:

$$t_i = \frac{\bar{l}_i}{c} n. \quad (7.14)$$

The mean free path length of the axial particles is equal to the room dimensions, i.e. $\bar{l}_1 = L_x$, $\bar{l}_2 = L_y$ and $\bar{l}_3 = L_z$. The mean free path length of the tangential particles can be calculated as the ratio of the surface of the treated area to the perimeter of the same area, i.e.:

$$\bar{l}_{4,5,6} = \frac{\pi S_{xy,xz,yz}}{Sc_{xy,xz,yz}}, \quad (7.15)$$

where S stands for the surface of the area and Sc stands for the perimeter of the area. The mean free path length of the oblique particles equals the mean free path length of a cuboid:

$$\bar{l}_7 = \frac{4V}{S}, \quad (7.16)$$

where again V is the volume of the cuboid and S is the surface of the cuboid. The sound energy of all the particles of a subsystem is attenuated by the mean absorption coefficient of the walls w by which the particles of the subsystem are reflected. The mean absorption coefficient is defined as:

$$\bar{\alpha}_i = \frac{\sum_w S_{i,w} \alpha_{i,w}}{S_i}, \quad (7.17)$$

with

$$S_i = \sum_w S_{i,w}. \quad (7.18)$$

To understand this equation better, a short example is given. In the case of subsystem 1, the particles can only be reflected at the wall $x = 0$ or the wall $x = L_x$. Therefore $S_i = 2L_y L_z$, and if the absorption coefficient of wall $x = 0$ is called $\alpha_{x=0}$ and the absorption coefficient of wall $x = L_x$ is called $\alpha_{x=L_x}$ then the mean absorption coefficient becomes:

$$\bar{\alpha}_1 = \frac{\alpha_{x=0} L_y L_z + \alpha_{x=L_x} L_y L_z}{S_i}. \quad (7.19)$$

After n reflections the decay of the sound energy of subsystem i can be calculated with the following equation:

$$E_i(t) = E_i(0) \cdot (1 - \bar{\alpha}_i)^n. \quad (7.20)$$

Reformulating this equation leads to the following expression for the sound energy:

$$E_i(t) = E_i(0) \cdot e^{\ln(1-\bar{\alpha}_i) \frac{c}{l_i} t}, \quad (7.21)$$

where n is substituted by Eq. (7.14). In a room without scattering objects the decay of the sound energy of a single subsystem can be generally written as:

$$E_i(t) = E_i(0) \cdot e^{-\eta_i t}. \quad (7.22)$$

The assumption that Eq. (7.21) equals Eq. (7.22) leads to the formula:

$$E_i(0) \cdot e^{-\eta_i t} = E_i(0) \cdot e^{\ln(1-\bar{\alpha}_i) \frac{c}{l_i} t}. \quad (7.23)$$

By analysing Eq. (7.23), it is clear that the equation is only valid if:

$$\eta_i = -\frac{c}{l_i} \ln(1 - \bar{\alpha}_i). \quad (7.24)$$

With Eq. (7.24) the damping loss value of every subsystem can be calculated and the matrix D can be established:

$$D = \begin{bmatrix} -\frac{c}{l_1} \ln(1 - \bar{\alpha}_1) & 0 & \dots & 0 \\ 0 & -\frac{c}{l_2} \ln(1 - \bar{\alpha}_2) & \dots & 0 \\ \vdots & \vdots & \ddots & \vdots \\ 0 & 0 & \dots & -\frac{c}{l_7} \ln(1 - \bar{\alpha}_7) \end{bmatrix}. \quad (7.25)$$

7.4 Calculation of Coupling Loss Factors

The coupling loss factors express the occurrence that energy flows from subsystem i to subsystem j because of the scattering of the walls. In the case of seven subsystems 49 coupling loss factors exist, they are determined in two steps. In the first step it has to be respected that the particles of one subsystem cannot be scattered into every other subsystem. For example it is not possible that a particle that is scattered on the wall $x = 0$ takes the direction of propagation of a z-axial mode. In the following table the possible changes of direction of particles that are reflected at the wall $x = 0$ are listed. If the entry is 1 this change of direction is allowed, if the entry is 0 the particle cannot be reflected into this subsystem.

From:	To:						
	1	2	3	4	5	6	7
1	1	0	0	1	1	0	1
2	0	0	0	0	0	0	0
3	0	0	0	0	0	0	0
4	1	0	0	1	1	0	1
5	1	0	0	1	1	0	1
6	0	0	0	0	0	0	0
7	1	0	0	1	1	0	1

Table 7.2: Possible directions of propagation for wall $x = 0$ and $x = L_x$

For example in line 1 of Tab. (7.2) this means that the particle can be reflected from subsystem 1 into subsystems 1, 4, 5 and 7. The reflection from subsystem 1 into subsystems 2, 3 and 6 is not allowed.

Knowing which changes of directions are allowed, a matrix can be defined for each wall that contains the probability of the allowed changes. The scattering is assumed to be uniform. This means that the probability of the changes of directions for one particle is the same for every direction of propagation. The probability of the change of direction of propagation from one subsystem to another subsystem depends therefore on the number of particles of the subsystems. If a subsystem contains many particles, the probability that the scattering of particles happens in a direction of propagation of the particles of the subsystem is higher than other directions of propagation. The probability of sound energy transition of subsystem i into subsystem j at wall w can be calculated by the ratio of particles of subsystem j to the sum of all particles of all possible directions of propagation at wall w . In the case of a scattering at wall $x = 0$ this

can be written mathematically as:

$$\mathbf{W}_1 = \begin{bmatrix} \frac{N_1(f)}{N_{\text{poss}}(f)} & 0 & 0 & \frac{N_1(f)}{N_{\text{poss}}(f)} & \frac{N_1(f)}{N_{\text{poss}}(f)} & 0 & \frac{N_1(f)}{N_{\text{poss}}(f)} \\ 0 & 0 & 0 & 0 & 0 & 0 & 0 \\ 0 & 0 & 0 & 0 & 0 & 0 & 0 \\ \frac{N_4(f)}{N_{\text{poss}}(f)} & 0 & 0 & \frac{N_4(f)}{N_{\text{poss}}(f)} & \frac{N_4(f)}{N_{\text{poss}}(f)} & 0 & \frac{N_4(f)}{N_{\text{poss}}(f)} \\ \frac{N_5(f)}{N_{\text{poss}}(f)} & 0 & 0 & \frac{N_5(f)}{N_{\text{poss}}(f)} & \frac{N_5(f)}{N_{\text{poss}}(f)} & 0 & \frac{N_5(f)}{N_{\text{poss}}(f)} \\ 0 & 0 & 0 & 0 & 0 & 0 & 0 \\ \frac{N_7(f)}{N_{\text{poss}}(f)} & 0 & 0 & \frac{N_7(f)}{N_{\text{poss}}(f)} & \frac{N_7(f)}{N_{\text{poss}}(f)} & 0 & \frac{N_7(f)}{N_{\text{poss}}(f)} \end{bmatrix}, \quad (7.26)$$

with

$$N_{\text{poss}}(f) = \sum_{i=1,4,5,7} N_i(f). \quad (7.27)$$

For wall $x = L_x$ the result for matrix \mathbf{W}_2 is exactly the same as \mathbf{W}_1 . For wall $y = 0$ the possible changes of direction of propagation are listed in Tab. (7.3): The matrix \mathbf{W}_3 for a scattering at

From:	To:						
	1	2	3	4	5	6	7
1	0	0	0	0	0	0	0
2	0	1	0	1	0	1	1
3	0	0	0	0	0	0	0
4	0	1	0	1	0	1	1
5	0	0	0	0	0	0	0
6	0	1	0	1	0	1	1
7	0	1	0	1	0	1	1

Table 7.3: Possible directions of propagation for wall $y = 0$ and $y = L_y$

wall $y = 0$ is the same as the matrix \mathbf{W}_4 for a scattering at wall $y = L_y$ and can be written as:

$$\mathbf{W}_3 = \begin{bmatrix} 0 & 0 & 0 & 0 & 0 & 0 & 0 \\ 0 & \frac{N_2(f)}{N_{\text{poss}}(f)} & 0 & \frac{N_2(f)}{N_{\text{poss}}(f)} & 0 & \frac{N_2(f)}{N_{\text{poss}}(f)} & \frac{N_2(f)}{N_{\text{poss}}(f)} \\ 0 & 0 & 0 & 0 & 0 & 0 & 0 \\ 0 & \frac{N_4(f)}{N_{\text{poss}}(f)} & 0 & \frac{N_4(f)}{N_{\text{poss}}(f)} & 0 & \frac{N_4(f)}{N_{\text{poss}}(f)} & \frac{N_4(f)}{N_{\text{poss}}(f)} \\ 0 & 0 & 0 & 0 & 0 & 0 & 0 \\ 0 & \frac{N_6(f)}{N_{\text{poss}}(f)} & 0 & \frac{N_6(f)}{N_{\text{poss}}(f)} & 0 & \frac{N_6(f)}{N_{\text{poss}}(f)} & \frac{N_6(f)}{N_{\text{poss}}(f)} \\ 0 & \frac{N_7(f)}{N_{\text{poss}}(f)} & 0 & \frac{N_7(f)}{N_{\text{poss}}(f)} & 0 & \frac{N_7(f)}{N_{\text{poss}}(f)} & \frac{N_7(f)}{N_{\text{poss}}(f)} \end{bmatrix}, \quad (7.28)$$

with

$$N_{\text{poss}}(f) = \sum_{i=2,4,6,7} N_i(f). \quad (7.29)$$

The possible changes of direction of propagation for the walls $z = 0$ and $z = L_z$ are given in Tab. (7.4): The matrix \mathbf{W}_5 and \mathbf{W}_6 are equal again and have to be used for scattering at walls

From:	To:						
	1	2	3	4	5	6	7
1	0	0	0	0	0	0	0
2	0	0	0	0	0	0	0
3	0	0	1	0	1	1	1
4	0	0	0	0	0	0	0
5	0	0	1	0	1	1	1
6	0	0	1	0	1	1	1
7	0	0	1	0	1	1	1

Table 7.4: Possible directions of propagation for wall $z = 0$ and $z = L_z$

$z = 0$ or $z = L_z$:

$$\mathbf{W}_5 = \begin{bmatrix} 0 & 0 & 0 & 0 & 0 & 0 & 0 \\ 0 & 0 & 0 & 0 & 0 & 0 & 0 \\ 0 & 0 & \frac{N_3(f)}{N_{\text{poss}}(f)} & 0 & \frac{N_3(f)}{N_{\text{poss}}(f)} & \frac{N_3(f)}{N_{\text{poss}}(f)} & \frac{N_3(f)}{N_{\text{poss}}(f)} \\ 0 & 0 & 0 & 0 & 0 & 0 & 0 \\ 0 & 0 & \frac{N_5(f)}{N_{\text{poss}}(f)} & 0 & \frac{N_5(f)}{N_{\text{poss}}(f)} & \frac{N_5(f)}{N_{\text{poss}}(f)} & \frac{N_5(f)}{N_{\text{poss}}(f)} \\ 0 & 0 & \frac{N_6(f)}{N_{\text{poss}}(f)} & 0 & \frac{N_6(f)}{N_{\text{poss}}(f)} & \frac{N_6(f)}{N_{\text{poss}}(f)} & \frac{N_6(f)}{N_{\text{poss}}(f)} \\ 0 & 0 & \frac{N_7(f)}{N_{\text{poss}}(f)} & 0 & \frac{N_7(f)}{N_{\text{poss}}(f)} & \frac{N_7(f)}{N_{\text{poss}}(f)} & \frac{N_7(f)}{N_{\text{poss}}(f)} \end{bmatrix}, \quad (7.30)$$

with

$$N_{\text{poss}}(f) = \sum_{i=3,5,6,7} N_i(f). \quad (7.31)$$

In the second step the amount of scattering for every subsystem at every wall has to be taken into account. The scattering factor describes the amount of sound energy for which the angle of incidence is not equal to the angle of reflection. If the particles of the wave are considered again, this means that the scattering factor s_w of wall w describes the probability that the angle of incidence is not equal to the angle of reflection for a single particle. Therefore the particles are coupled into a new subsystem based on the probability matrices \mathbf{W}_w . It can be assumed again that the particles of a subsystem are reflected after the mean free path length of the subsystem. The probability that the particles are reflected at wall w can be defined by the ratio of the surface of the wall S_w compared to the sum of all the surfaces S_i at which particles of the subsystem can be reflected. The 49 coupling factors can be determined based on the matrices \mathbf{W}_w as follows:

$$\mathbf{CF} = \sum_{w=1}^6 \mathbf{W}_w * \mathbf{H} \cdot S_w \cdot s_w \quad (7.32)$$

with

$$\mathbf{H} = \begin{bmatrix} \frac{c}{l_1 S_1} & \frac{c}{l_2 S_2} & \cdots & \frac{c}{l_7 S_7} \\ \frac{c}{l_1 S_1} & \frac{c}{l_2 S_2} & \cdots & \frac{c}{l_7 S_7} \\ \vdots & \vdots & \ddots & \dots \\ \frac{c}{l_1 S_1} & \frac{c}{l_2 S_2} & \cdots & \frac{c}{l_7 S_7} \end{bmatrix}, \quad (7.33)$$

where \mathbf{CF} has the structure:

$$\mathbf{CF} = \begin{bmatrix} \eta_{11} & \dots & \eta_{71} \\ \vdots & \ddots & \vdots \\ \eta_{17} & \dots & \eta_{77} \end{bmatrix}. \quad (7.34)$$

By knowing the matrix \mathbf{CF} it is possible to calculate the matrix \mathbf{K} . This can be done with the following equation:

$$\mathbf{K} = -\mathbf{CF} + \begin{bmatrix} \sum_{j \neq 1}^7 \eta_{ij} & 0 & \dots & 0 \\ 0 & \sum_{j \neq 2}^7 \eta_{2j} & \dots & 0 \\ \vdots & \vdots & \ddots & \vdots \\ 0 & 0 & \dots & \sum_{j \neq 7}^7 \eta_{7j} \end{bmatrix}. \quad (7.35)$$

7.5 Calculation of Damping Factor of Air

This section describes how the sound power damping factor of air, termed as m can be calculated. The method that is used for calculating m is described in [Bass et al. 1994]. Before starting with the calculations, some definitions have to be made: p_{s0} is the reference value of the atmospheric pressure, T stands for the atmospheric temperature in K , the reference atmospheric temperature T_0 is defined as $293.15K$ and the triple-point isotherm temperature is given as $T_{01} = 273.16K$. With these definitions the saturation vapor pressure can be calculated:

$$\frac{p_{\text{sat}}}{p_{s0}} = 10.79586 \left[1 - \frac{T_{01}}{T} \right] - 5.02808 \log \frac{T}{T_{01}} + 1.50474 \cdot 10^{-4} \left(1 - 10^{-8.29692 \left[\frac{T}{T_{01}} - 1 \right]} \right) - 2.2195983. \quad (7.36)$$

The relation between the absolute and relative humidity is given by the formula:

$$h = h_r \frac{p_{\text{sat}}}{p_{s0}} \%. \quad (7.37)$$

Assuming that the relative humidity of air is 50% then h_r in the previous equation must be set to 50.

Moreover the relaxation frequency for oxygen and nitrogen are needed for the calculation of the absorption factor. The relaxation frequency of oxygen is given as:

$$F_{r,O} = \frac{1}{p_{s0}} \left(24 + 4.04 \cdot 10^4 h \frac{0.02 + h}{0.391 + h} \right) \quad (7.38)$$

and the relaxation frequency of nitrogen can be calculated with:

$$F_{r,N} = \frac{1}{p_{s0}} \left(\frac{T_0}{T} \right)^{\frac{1}{2}} \left(9 + 280h \cdot e^{\left(-4.17 \left[\frac{T_0}{T} \right]^{1/3} - 1 \right)} \right). \quad (7.39)$$

Using all the described equations, finally the damping factor of air can be determined:

$$m = f^2 \left(1.84 \cdot 10^{-11} \left(\frac{T}{T_0} \right)^{1/2} + \left(\frac{T}{T_0} \right)^{-5/2} \left[0.01278 \frac{e^{-2239.1/T}}{F_{r,O} + f^2/F_{r,O}} + 0.1068 \frac{e^{-3352/t}}{F_{r,N} + f^2/F_{t \text{ extr}, N}} \right] \right) \frac{\text{Neper}}{m}, \quad (7.40)$$

where f stands for the analysed frequency.

7.6 Solving the System of Differential Equations

All the values that are needed for solving Eq. (7.1) have been derived. In this section the way to solve the system of first order linear differential equations that was defined in Eq. (7.1) is presented. Therefore Eq. (7.1) is rewritten:

$$\begin{bmatrix} \frac{dE_1(t)}{dt} \\ \frac{dE_2(t)}{dt} \\ \vdots \\ \frac{dE_7(t)}{dt} \end{bmatrix} = -\mathbf{A} \begin{bmatrix} E_1(t) \\ E_2(t) \\ \vdots \\ E_7(t) \end{bmatrix}, \quad (7.41)$$

where

$$\mathbf{A} = \mathbf{D} + \mathbf{K}. \quad (7.42)$$

The eigenvalues $\lambda_1 \dots \lambda_7$ of the matrix \mathbf{A} have to be calculated. Based on these (here: seven) eigenvalues, the eigenvectors $\mathbf{c}_1 \dots \mathbf{c}_7$ that belong to these eigenvalues can be determined. By knowing the eigenvalues and eigenvectors of the matrix \mathbf{A} the system of differential equations can be solved using the following formula:

$$\begin{bmatrix} E_1(t) \\ E_2(t) \\ \vdots \\ E_7(t) \end{bmatrix} = [\mathbf{c}_1 \quad \mathbf{c}_2 \quad \dots \quad \mathbf{c}_7] \begin{bmatrix} c_1 e^{\lambda_1 t} \\ c_2 e^{\lambda_2 t} \\ \vdots \\ c_7 e^{\lambda_7 t} \end{bmatrix}. \quad (7.43)$$

In Eq. (7.38) the values for $c_1 \dots c_7$ can be calculated with the help of the initial energies:

$$\begin{bmatrix} c_1 \\ c_2 \\ \vdots \\ c_7 \end{bmatrix} = [\mathbf{c}_1 \quad \mathbf{c}_2 \quad \dots \quad \mathbf{c}_7]^{-1} \begin{bmatrix} E_1(0) \\ E_2(0) \\ \vdots \\ E_7(0) \end{bmatrix}. \quad (7.44)$$

The energy of all the subsystems can be determined and finally the energy states of the room which are time-dependent can be calculated by inserting the energy of the subsystems in Eq. (7.3). Using this result a decay curve can be calculated. In Fig. (7.1) a decay curve for a rectangular room with the dimensions of 5 m x 3 m x 2.5 m can be seen. The absorption coefficient of the walls was $\alpha = 0.05$, only for the ceiling it was set to $\alpha = 0.57$. The frequency band with the center frequency 500 Hz was analysed and the damping factor of the air was set to $m = 0.000628$. The scattering factor of the six walls was set to 0.03. In Fig. (7.1) the energy decay curve has a double slope. This means that the energy decay curve is not a straight line but has a break. In [Nilsson 2004] this break is explained by a sound field that consists of grazing and non-grazing parts. The grazing part contains waves that propagate in a direction that is parallel to the highly absorbent wall and the non-grazing part consists of waves that propagate with oblique incidence towards the absorbent wall. The whole energy in the room can be calculated as the sum of the grazing and non-grazing parts. [Nilsson 2004] described this phenomenon based on a model that consists of two subsystems. In this chapter the SEA model to calculate the energy decay curve of the room consisted of seven subsystems. Each of the

subsystems has an influence on the decay curve and the sound field contains of seven different parts. The whole energy decay curve is a sum over these seven parts and this sum explains the break in the decay curve.

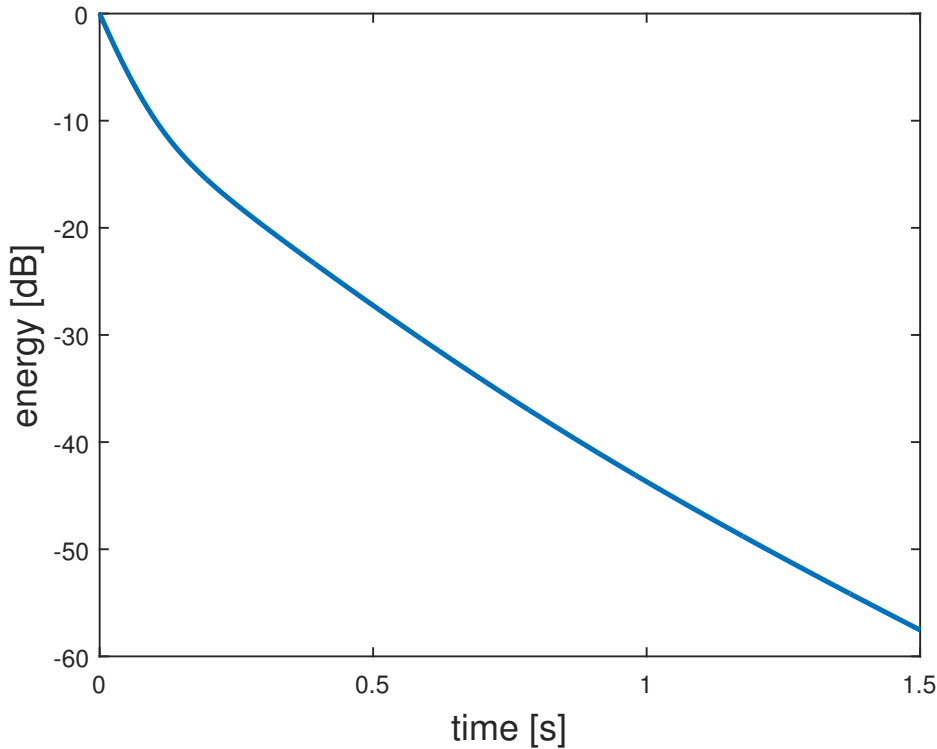


Figure 7.1: Example: Decay curve rectangular room 5 m x 3 m x 2.5 m, ceiling absorbent

7.7 Calculation of T_{60} , T_{30} and T_{20}

The next step is to calculate the reverberation time of the room based on the energy decay curve. When the decay curve was calculated as described in the previous section, it is not difficult to calculate the reverberation time. At first the point of intersection between the decay curve and a linear slope that is constantly -5dB has to be found (see Fig. (7.2), same room configuration as in the example shown before). If the reverberation time T_{60} should be calculated, also the point of intersection of the decay curve and a linear slope that is constantly -65 dB has to be determined. This can be seen in Fig. (7.3). In the next step a polynomial of degree 1 is fit to the two points of the decay curve with the help of the build-in MATLAB function “polyfit”. The polynomial has the form (see [MATHEMATICS]):

$$p(x) = p_1x^1 + p_2x^0. \quad (7.45)$$

The output of the function “polyfit” are the values for p_1 and p_2 . Knowing these values, replacing $p(x)$ of the previous equation with -60 and reformulating the equations gives the following formula for the reverberation time:

$$\frac{-60 - p_2}{p_1} = x, \quad (7.46)$$

where x is the reverberation time.

For the calculation of T_{30} and T_{20} the procedure is nearly the same but instead of the -65 dB linear slope, a -35 dB and a -25 dB linear slope have to be used. For T_{early} the polynomial was fitted between the 0 dB point of the decay curve and the -5 dB linear slope and for T_{late} the polynomial was fitted between the -45 dB point of the decay curve and the -65 dB point of the decay curve. The rest of the method is completely the same. For the presented example the values for the reverberation times are: $T_{60} = 1.5554$, $T_{30} = 1.3152$, $T_{20} = 1.1565$, $T_{\text{early}} = 0.5519$ and $T_{\text{late}} = 1.5942$.

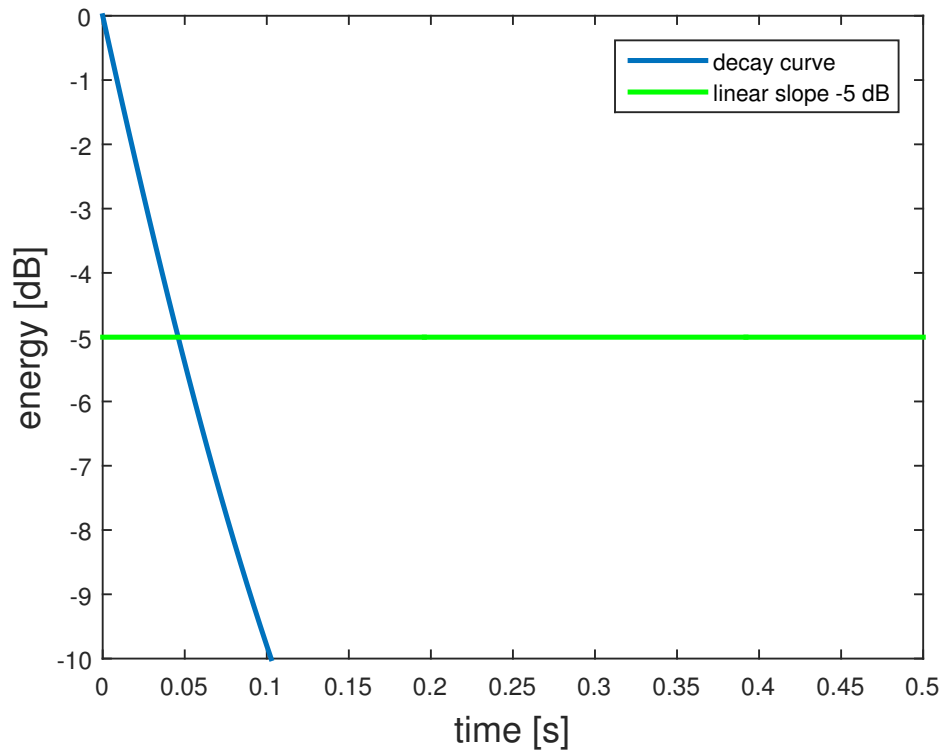


Figure 7.2: Point of intersection at -5dB

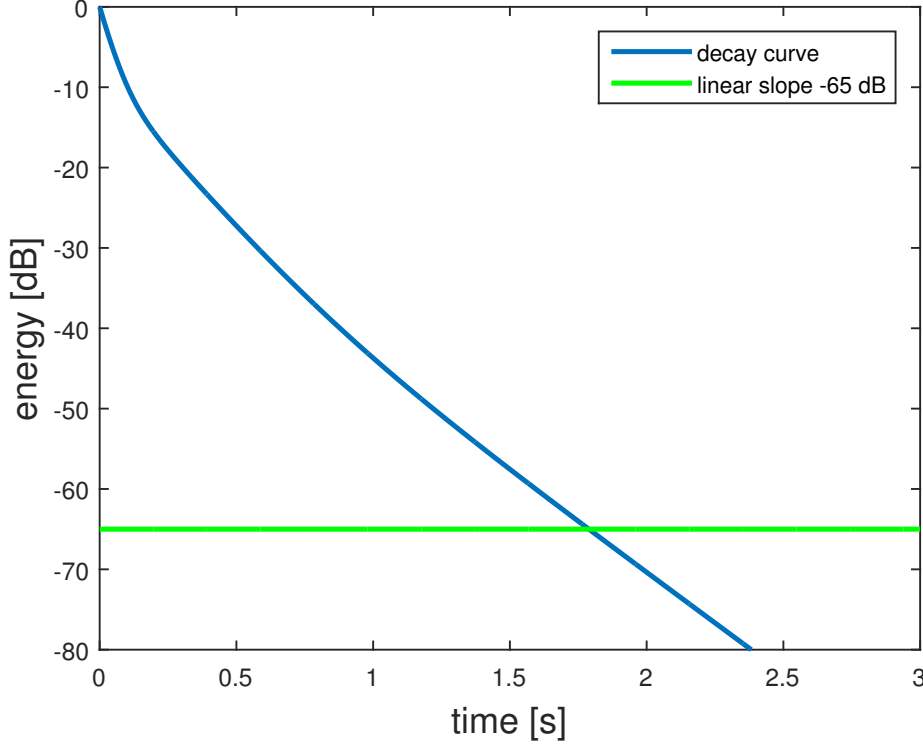


Figure 7.3: Point of intersection at -65dB

7.8 Proof of Concept Experiment

The room impulse responses were measured in a real room and the data obtained from these measurements is used to calculate the decay curve of the room with the Schroeder backward integration. Then the decay curve of the same room is predicted with SEA as described above and the two decay curves are compared. With this procedure the accuracy of predicting the decay curve with the presented SEA technique can be evaluated. In the first experiment the measurement was done in the empty room without absorbers. The dimensions of the room are $4.39\text{ m} \times 3.29\text{ m} \times 2.95\text{ m}$, a picture of the empty room is shown in Fig. (7.4). The analysis frequency was set to 1000 Hz which is definitely in the valid frequency range of SEA. In [Zeitler 2006, p. 38] it is written that three or more modes in the analysed frequency band are enough, so that the method of SEA gives results with 2-3 dB of error. In the octave band with the centre frequency of 1000 Hz this restriction is fulfilled in any case. In this case all the walls in the SEA model are defined as reverberant with an absorption coefficient of $\alpha = 0.03$ and a scattering factor of 0.03, the absorption coefficient of air was calculated with the equations presented in Sec. (7.5), where the temperature was 20°C and the relative humidity was set to 50%. As can be seen in Fig. (7.5) there is an excellent agreement between the decay curve of the measured data and the predicted decay curve. This means that in the described situation the prediction of the decay curve with SEA works very well.

In a second proof of concept experiment parts of the floor of the room are covered with an absorber. The absorber has the dimensions of $2.38\text{ m} \times 2.38\text{ m}$ and at 1000 Hz the absorption coefficient is $\alpha = 1.1353$. The mean absorption coefficient of the floor was calculated as (final value: 0.3359):

$$\alpha_m = \frac{(A_f - A_a)\alpha_f + A_a\alpha_a}{A_f}, \quad (7.47)$$



Figure 7.4: Empty room in which the measurement data was obtained

where A_f is the area of the floor, A_a is the area of the absorber, α_f is the absorption coefficient of the floor and α_a is the absorption coefficient of the absorber. The comparison of the decay curves for this second experiment is shown in Fig. (7.6). Again there is a good agreement between the decay curve of the measured data and the decay curve obtained with SEA method. To sum this proof of concept experiments up, it can be said that the prediction of the decay curve with the SEA method works excellent. In both experiments, for the empty room and the room with absorber on the floor, the SEA method provides the same result as obtained with measurements and therefore also the values for the reverberation time would be the same. In Fig. (7.6) it can be seen that starting at roughly 0.7 s the measured curve and the simulated curve differ. This can be explained by the background noise that exists in the measurement.

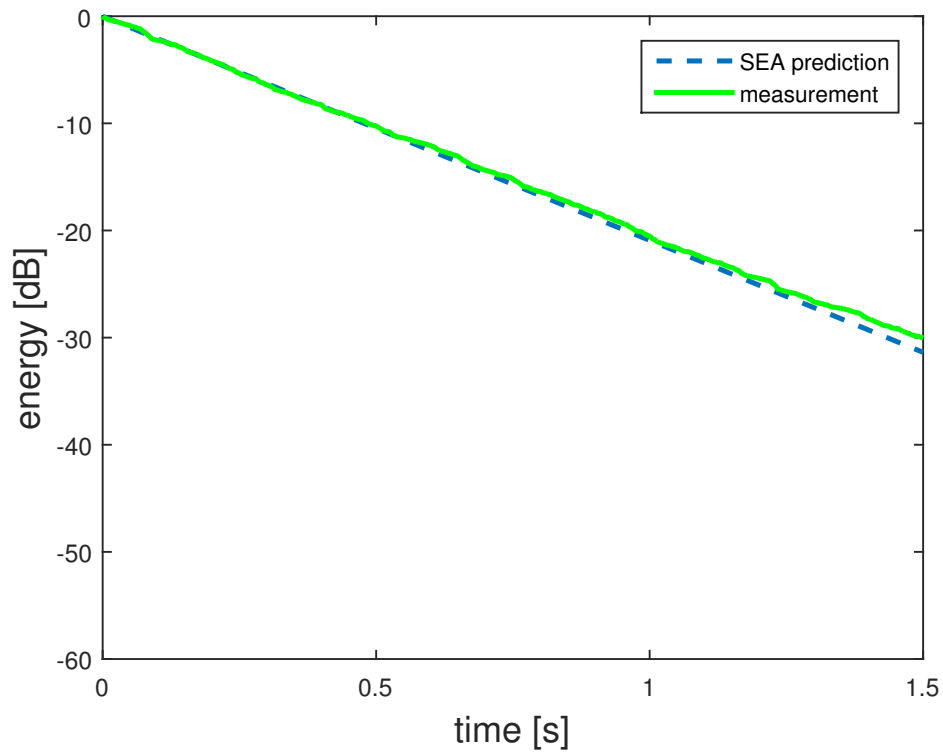


Figure 7.5: Comparison measurement and simulation, empty room, frequency band with centre frequency 1000 Hz

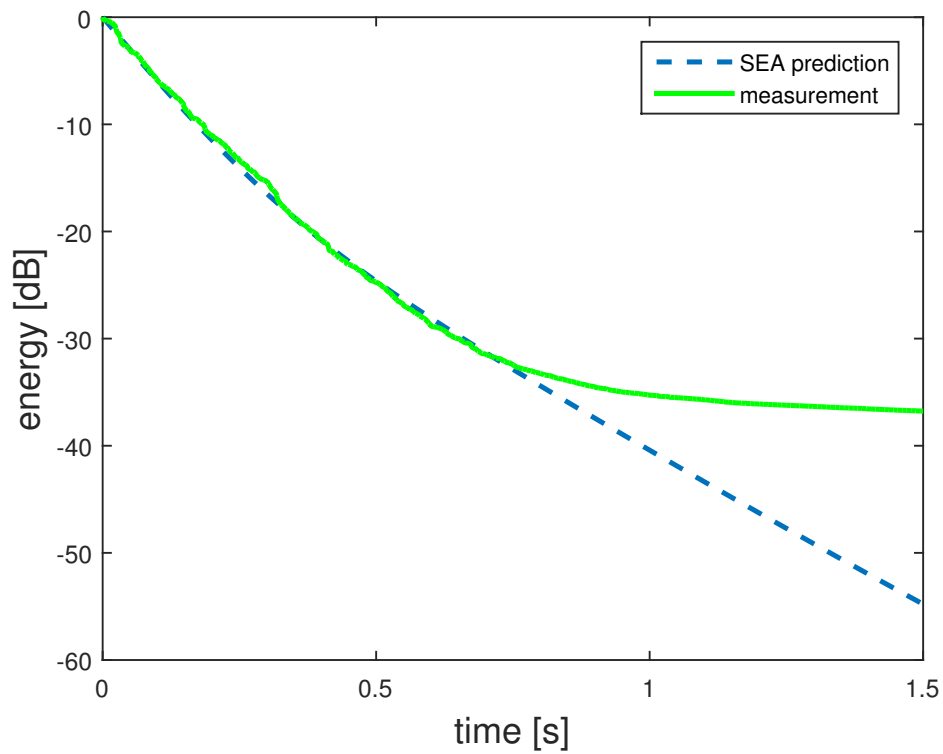


Figure 7.6: Comparison measurement and simulation, room with absorber on the floor, frequency band with centre frequency 1000 Hz

8

Calculation of Decay Curves of Coupled Rooms with SEA

In this chapter it is discussed how to determine the reverberation time in the case of two coupled rooms with SEA. In Fig. (8.1) the ground plot of two coupled rooms can be seen, where S stands for the aperture size. When two or more spaces are connected through an aperture the connected rooms are called coupled rooms. The method of coupling rooms is even used in the design of concert halls to use the acoustical efforts of coupled systems (nonexponential energy decay [Bradley and Wang 2005]). As in chapter 7, subsystems have to be defined, the damping

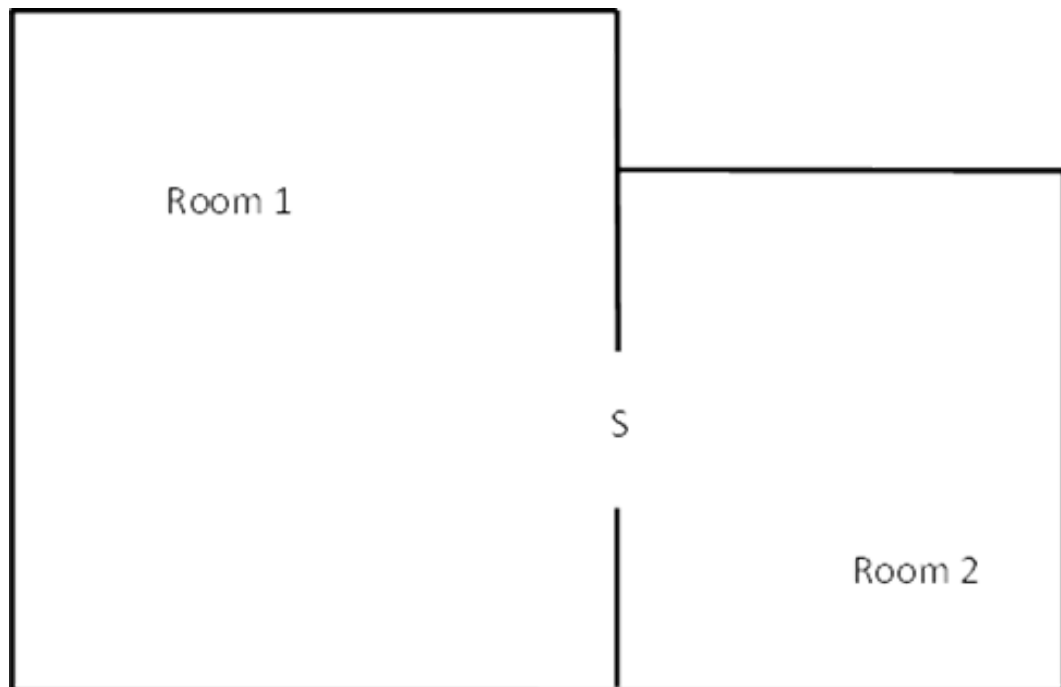


Figure 8.1: Two Coupled rooms: ground plot

and coupling loss factors have to be derived and finally a system of differential equations has to be solved. As an example two rooms that are coupled by an aperture are analysed. In this case the SEA model consists of two subsystems, therefore two damping loss factors and a 2×2 coupling loss matrix are needed. Moreover two differential equations have to be solved.

8.1 Calculation of Damping Loss Factors

The damping loss factor of a room can be calculated by the following equation [Zeitler 2006]:

$$\eta_i = \frac{2.2}{fT_i}, \quad (8.1)$$

where f is the frequency of interest and T_i is the reverberation time of the room⁶. The difficulty in this equation is the determination of the reverberation time. But with the derivations and explanations of the previous chapter the reverberation time of rooms can be accurately predicted, as proven before.

8.2 Calculation of Coupling Loss Factors

The calculation of coupling loss factors for the scenario room to room is also defined in the work of [Zeitler 2006]:

$$\eta_{ij} = \frac{c_0 S \tau_{ij}}{8\pi f V_i}, \quad (8.2)$$

where c_0 stands for the speed of sound of air, S for the area of the aperture, τ_{ij} for the transmission coefficient between the subsystems and V_i for the volume of room i . With the knowledge of the damping and coupling loss factors, a loss factor matrix can be derived and the differential equations for the two subsystems can be solved.

8.3 Solving the System of Differential Equations

For the case of two coupled rooms the matrix of coupling and damping loss values can be defined analogue to the previous chapter and this results in:

$$\mathbf{A} = \begin{bmatrix} \eta_1 + \eta_{12} & -\eta_{21} \\ -\eta_{12} & \eta_2 + \eta_{21} \end{bmatrix}. \quad (8.3)$$

The system of differential equations becomes:

$$\begin{bmatrix} \frac{dE_1(t)}{dt} \\ \frac{dE_2(t)}{dt} \end{bmatrix} = \mathbf{A} \begin{bmatrix} E_1(t) \\ E_2(t) \end{bmatrix}. \quad (8.4)$$

The same procedure as in the section before is applied, the eigenvalues and eigenvectors are calculated. Based on the initial energies the constants that are needed for solving the differential equations can be determined. In the case of coupled rooms, at time $t = 0$ the whole energy is in the room that is excited. Therefore the initial energy of *room1* is set to 1 and the initial energy of *room2* is set to 0, i.e. $E_1(0) = 1$ and $E_2(0) = 0$. Finally the solution of the system of differential equations in matrix form is:

$$\begin{bmatrix} E_1(t) \\ E_2(t) \end{bmatrix} = \begin{bmatrix} \mathbf{c}_1 & \mathbf{c}_2 \end{bmatrix} \begin{bmatrix} c_1 e^{\lambda_{s,1}t} \\ c_2 e^{\lambda_{s,2}t} \end{bmatrix}, \quad (8.5)$$

where λ_1 and λ_2 are scaled by the angular, centre frequency of the analysed octave band, i.e.:

$$\lambda_{s,i} = 2\pi f \lambda_i. \quad (8.6)$$

With the help of Eq. (7.3) the energy of the whole system depending on time can be calculated. To determine the decay curve, the total energy has to be normalised by the maximum energy

⁶ This equation was also derived in Sec. (3.1.2)

value. The last two statements can be written in a mathematical sense as:

$$E_{\text{tot}}(t) = 10 \cdot \log \frac{\sum_{i=1}^2 E_i(t) e^{-mct}}{\sum_{i=1}^2 E_i(0)}. \quad (8.7)$$

Knowing the decay curve, the values for T_{20} , T_{30} and T_{60} can be found by the same method as in chapter 7.

8.4 Proof of Concept Experiment

In this section the results obtained with the presented SEA method for coupled rooms are compared with a method presented by David Bradley and Lily Wang in the paper “The effects of simple coupled volume geometry on the objective and subjective results from nonexponential decay” [Bradley and Wang 2005]. In this paper a method for calculating the decay curve of two coupled rooms is defined. A power balance equation is derived for *room1*:

$$P - \frac{A_1 \alpha_1 c_0 E_1}{4} - \frac{S c_0 E_1}{4} + \frac{S c_0 E_2}{4} = 0 \quad (8.8)$$

and for *room2*:

$$-\frac{A_2 \alpha_2 c_0 E_2}{4} - \frac{S c_0 E_2}{4} + \frac{S c_0 E_1}{4} = 0, \quad (8.9)$$

where A_i stands for the surface of the i^{th} room, α_i is the average absorption coefficient of the i^{th} room, E_i describes the energy of the i^{th} room and P stands for the power of the sound source. These two equations define the steady state response of the rooms. Setting P to zero two differential equations can be derived, which describe the decay curve of the rooms:

$$\frac{c_0}{4} (A_{1S} E_1 - S E_2) = -V_1 \frac{dE_1}{dt} \quad (8.10)$$

and

$$\frac{c_0}{4} (-S E_1 + A_{2S} E_2) = -V_2 \frac{dE_2}{dt}. \quad (8.11)$$

In Eq. (8.10) and Eq. (8.11) $A_{iS} = A_i \alpha_i + S$ and for E_i the form

$$E_i = E_{i0} e^{-2\delta t} \quad (8.12)$$

is assumed, where E_{i0} stands for the initial energy of the i^{th} room and δ is the decay constant of the room. Using Eq. (8.12) in Eq. (8.10) and (8.11) leads to the following equations:

$$\frac{c_0}{4} (A_{1S} E_{10} e^{-2\delta t} - S E_{20} e^{-2\delta t}) = 2V_1 \delta E_{10} e^{-2\delta t} \quad (8.13)$$

and

$$\frac{c_0}{4} (-S E_{10} e^{-2\delta t} + A_{2S} E_{20} e^{-2\delta t}) = 2V_2 \delta E_{20} e^{-2\delta t}. \quad (8.14)$$

The terms $e^{-2\delta t}$ in Eq. (8.13) and Eq. (8.14) can be cut and the two equations can be rewritten in matrix form as:

$$\begin{bmatrix} \frac{c_0}{4} [A_{1S} - 2V_1 \delta] & -\frac{c_0}{4} S \\ -\frac{c_0}{4} S & \frac{c_0}{4} [A_{2S} - 2V_2 \delta] \end{bmatrix} \begin{bmatrix} E_{10} \\ E_{20} \end{bmatrix} = \begin{bmatrix} 0 \\ 0 \end{bmatrix}. \quad (8.15)$$

Setting up the determinant of this matrix system results in:

$$4V_1V_2\delta^2 - \frac{c_0}{2}(A_{1S}V_2 + A_{2S}V_1) + \frac{c_0^2}{16}(A_{1S}A_{2S} - S) = 0. \quad (8.16)$$

This equation can be solved, if the volume of the rooms, the absorption coefficients of the walls of the rooms and the size of the aperture are known. Solving this quadratic equation leads to two values for δ , i.e. δ_1 and δ_2 :

$$\delta_{1,2} = \frac{c_0}{16V_1V_2}(A_{1S}V_2 + A_{2S}V_1) \pm \sqrt{\left[\frac{c_0}{16V_1V_2}(A_{1S}V_2 + A_{1S}V_1)\right]^2 - \frac{c_0^2(A_{1S}A_{2S} - S)}{64V_1V_2}}. \quad (8.17)$$

With the help of these two values, the reverberation time of the two rooms can be calculated with the equation:

$$T_i = \frac{6.9}{\delta_i}. \quad (8.18)$$

In [Bradley and Wang 2005] an equation found by [Cremer et al. 1982] is used to calculate the decay curve of *room1*:

$$L_i(t) = -\left(\frac{60}{T_i}\right)t + 10\log\left(\frac{E_{i0}}{E_{\text{ref}}}\right), \quad (8.19)$$

where L_i stands for the sound pressure level in the i^{th} space. For the case that δ_1 is bigger than δ_2 the early portion of the sound energy in *room1* is dominated by the characteristics of *room1* and the late portion of the sound energy in *room1* is dominated by the characteristics of *room2* on *room1*. Therefore a break results in the decay curve of *room1* and the equation for the early and the late parts of the energy decay are:

$$L_{1\text{early}}(t) = -\left(\frac{60}{T_1}\right)t + 10\log\left(\frac{E_{10}}{E_{\text{ref}}}\right), \quad (8.20)$$

and

$$L_{1\text{late}}(t) = -\left(\frac{60}{T_2}\right)t + 10\log\left(\frac{E_{21}}{E_{\text{ref}}}\right), \quad (8.21)$$

where E_{21} is given by:

$$E_{21} = k_1k_2E_{10}. \quad (8.22)$$

The energy that is transported from *room2* into *room1*, i.e. E_{21} , is defined by the initial energy in *room1* and the coupling factors k_1 and k_2 that are defined by the geometry and the absorption of the rooms:

$$k_1 = \frac{S}{A_{1S}}, \quad k_2 = \frac{S}{A_{2S}}. \quad (8.23)$$

Assuming that E_{ref} in Eq. (8.20) and Eq. (8.21) is equal E_{10} and inserting Eq. (8.22) in Eq. (8.21) the equations for the early and late decay parts become:

$$L_{1\text{early}}(t) = -\left(\frac{60}{T_1}\right)t, \quad (8.24)$$

and

$$L_{1\text{late}}(t) = - \left(\frac{60}{T_2} \right) t - 10 \log \left(\frac{A_{1S} A_{2S}}{S^2} \right). \quad (8.25)$$

In the following table values for the room dimensions, the absorption coefficients of the walls and the aperture are given. The SEA method presented in Sec. (8.1-8.3) is compared with the method explained in Sec. (8.4) by using the values of Tab. (8.1) and Tab. (8.2). The aperture

x-dimension	$L_x = 15m$
y-dimension	$L_y = 10m$
z-dimension	$L_z = 2.5m$
absorption coefficient ceiling	$\alpha_c = 0.9$
absorption coefficient floor	$\alpha_f = 0.9$
absorption coefficient front	$\alpha_{fr} = 0.9$
absorption coefficient back	$\alpha_b = 0.1$
absorption coefficient left	$\alpha_l = 0.1$
absorption coefficient right	$\alpha_r = 0.1$

Table 8.1: Dimensions and absorption coefficients of room1

x-dimension	$L_x = 15m$
y-dimension	$L_y = 10m$
z-dimension	$L_z = 2.5m$
absorption coefficient ceiling	$\alpha_c = 0.03$
absorption coefficient floor	$\alpha_f = 0.03$
absorption coefficient front	$\alpha_{fr} = 0.03$
absorption coefficient back	$\alpha_b = 0.03$
absorption coefficient left	$\alpha_l = 0.03$
absorption coefficient right	$\alpha_r = 0.03$

Table 8.2: Dimensions and absorption coefficients of room2

size was set to $S = 7 \text{ m}^2$ and the analysed frequency band had a centre frequency of $f = 1000$ Hz. Before comparing the results of the two methods, in Fig. (8.2) the early and late decay curves of the Bradley&Wang (B&W) method can be seen: The point of intersection between the early and the late decay curve is calculated. In the first part, till the point of intersection is reached, the early decay curve is used and for the late decay the influence of the second room dominates the decay curve of the first room. Therefore the decay curve of the coupled rooms has a double slope and its typical characteristics can be seen in Fig. (8.3). In Fig. (8.4) the decay curve obtained with the Bradley&Wang method is compared with the SEA method for calculating the decay curve of coupled rooms. It can be seen that the general characteristics of the decay curve in both models is the same. Both curves have the typical double slope in the case that the walls of *room1* are quite absorbent and the walls of *room2* have small absorption coefficients. With this setup the early decay is dominated by the effects of *room1* and the late decay is given by the decay of *room2* because the energy decays slower in *room2* than in *room1*. The descent in the late decay is also equal, the only difference between the methods is that the “point of intersection” is reached earlier in the case of the SEA method. In the Bradley&Wang method the early part only consists of the effects of *room1*. In the SEA method an overall result is obtained that is influenced by the effects of both rooms. So in the SEA method the early part is dominated by the effects of *room1* but also effects of *room2* are present and therefore there

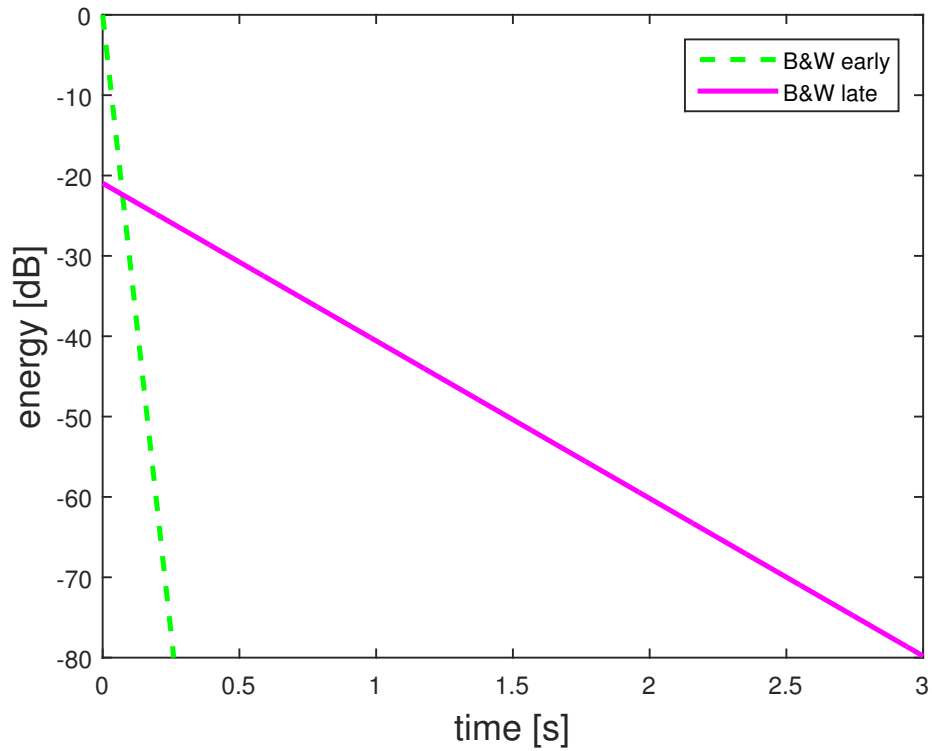


Figure 8.2: Early and late decay curves of two coupled rooms using Bradley & Wang method

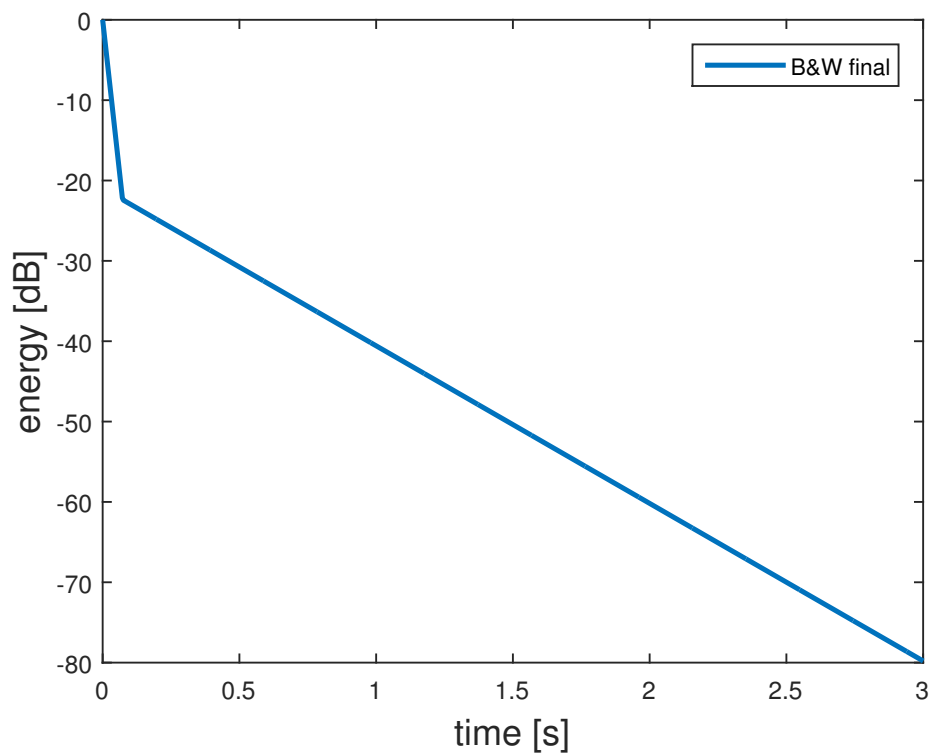


Figure 8.3: Final decay curve of two coupled rooms using Bradley & Wang method

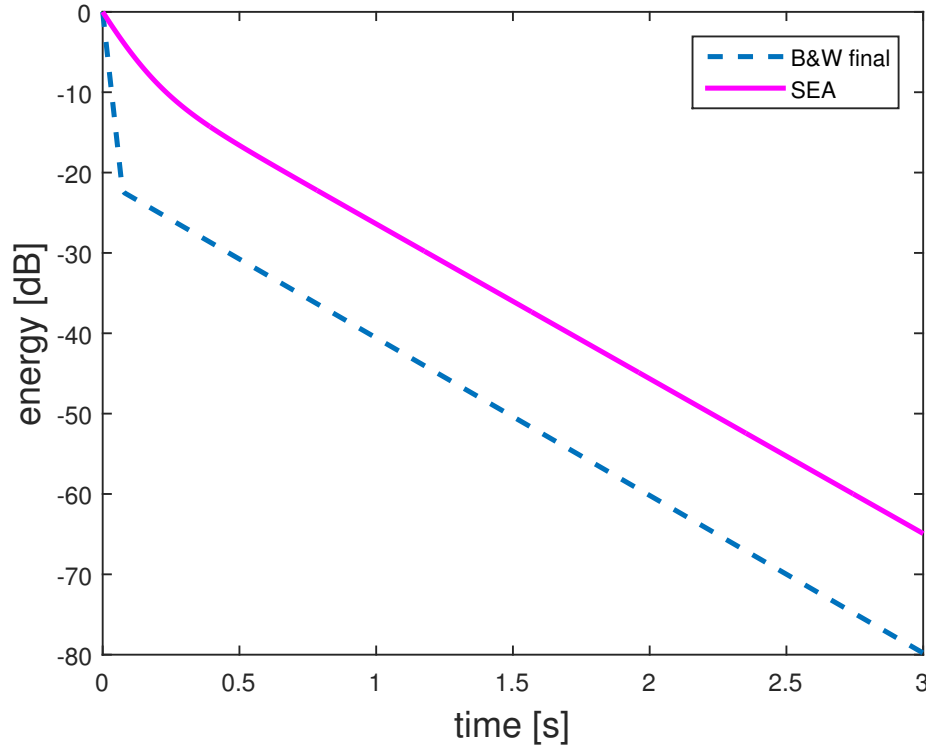


Figure 8.4: Decay curve of two coupled rooms: SEA method compared with Bradley & Wang method, room1 absorbent

is a difference in the steepness of the early decay.

Based on this comparison and explanations it can be said that the presented, new SEA method for calculating the decay curves of coupled rooms seems to give right results. The main advantage of the SEA method compared to the Bradley&Wang method is that there are no restrictions. The Bradley&Wang method can only be used if the condition that $\delta_1 > \delta_2$ (see paragraph below Eq. (8.17)) is fulfilled. This means that the walls of *room1* have to be more absorbent than the walls of *room2*. The method cannot give right results if the absorption coefficients are chosen the other way round, i.e. the walls of *room2* are more absorbent than the walls of *room1*, but the SEA method can handle this case. Another disadvantage of the Bradley&Wang method is that the results are not frequency dependent. For every frequency the same result is obtained, in the new SEA method decay curves for different frequencies give different results due to the frequency dependency of the presented equations.

In Fig. (8.5) the results for the SEA method and the Bradley&Wang method are shown, if the absorption values for the rooms are chosen as presented in Tab. (8.3) and Tab. (8.4) (the absorption values for the two rooms from the experiment before were just swapped). It can be seen that the Bradley&Wang method gives wrong results if $\delta_1 < \delta_2$ which is not surprising because it was mentioned in the derivation of the method that it does not work in cases, where $\delta_1 < \delta_2$. However, the results obtained with the SEA method seem to be right in this case too. The double slope of the decay curve vanished, because the effects of *room2* have no influence on the decay curve of *room1*. In the beginning there is only a slight energy exchange between the two rooms, therefore the early decay of *room1* is always dominated by the effects of *room1*. In the example that was discussed before the late decay was dominated by the effects of *room2*, which is not the case here because the energy in *room2* dissipates much faster than the energy in *room1*. Therefore also the late decay is only dependent on the decay of *room1* and the resulting decay curve becomes a linear slope.

x-dimension	$L_x = 15m$
y-dimension	$L_y = 10m$
z-dimension	$L_z = 2.5m$
absorption coefficient ceiling	$\alpha_c = 0.03$
absorption coefficient floor	$\alpha_f = 0.03$
absorption coefficient front	$\alpha_{fr} = 0.03$
absorption coefficient back	$\alpha_b = 0.03$
absorption coefficient left	$\alpha_l = 0.03$
absorption coefficient right	$\alpha_r = 0.03$

Table 8.3: Dimensions and absorption coefficients of room1

x-dimension	$L_x = 15m$
y-dimension	$L_y = 10m$
z-dimension	$L_z = 2.5m$
absorption coefficient ceiling	$\alpha_c = 0.9$
absorption coefficient floor	$\alpha_f = 0.9$
absorption coefficient front	$\alpha_{fr} = 0.9$
absorption coefficient back	$\alpha_b = 0.1$
absorption coefficient left	$\alpha_l = 0.1$
absorption coefficient right	$\alpha_r = 0.1$

Table 8.4: Dimensions and absorption coefficients of room2

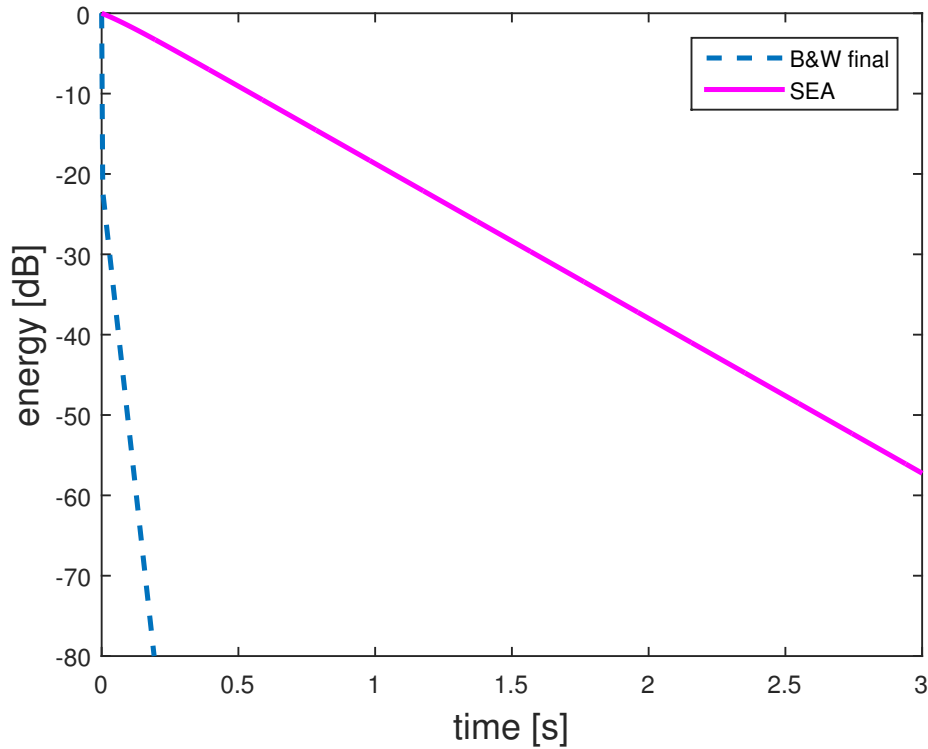


Figure 8.5: Decay curve of two coupled rooms: SEA method compared with Bradley & Wang method, room2 absorbent

8.5 Decay Curves of Different Room Configurations

In this section it is analysed how the geometry of the coupled rooms, the aperture and the absorption coefficients influence the decay curve of the coupled rooms. In Fig. (8.6) three decay curves are compared, the analysed frequency was set to 1000 Hz and the aperture was 5 m^2 . The solid line (named SEA1) stands for the same case as presented before, obtained with the values of Tab. (8.1) and Tab. (8.2). The dashed line presents the results in the case that *room1* has the same dimensions and absorption coefficients as before but the coupled room is smaller than in SEA1. In Tab. (8.5) the parameters for *room2* are given. In SEA3 both rooms are

x-dimension	$L_x = 5m$
y-dimension	$L_y = 3m$
z-dimension	$L_z = 2.5m$
absorption coefficient ceiling	$\alpha_c = 0.03$
absorption coefficient floor	$\alpha_f = 0.03$
absorption coefficient front	$\alpha_{fr} = 0.03$
absorption coefficient back	$\alpha_b = 0.03$
absorption coefficient left	$\alpha_l = 0.03$
absorption coefficient right	$\alpha_r = 0.03$

Table 8.5: Dimensions and absorption coefficients of *room2*, SEA2

x-dimension	$L_x = 5m$
y-dimension	$L_y = 3m$
z-dimension	$L_z = 2.5m$
absorption coefficient ceiling	$\alpha_c = 0.9$
absorption coefficient floor	$\alpha_f = 0.9$
absorption coefficient front	$\alpha_{fr} = 0.9$
absorption coefficient back	$\alpha_b = 0.1$
absorption coefficient left	$\alpha_l = 0.1$
absorption coefficient right	$\alpha_r = 0.1$

Table 8.6: Dimensions and absorption coefficients of *room1*, SEA3

quite small and *room1* is absorbent and *room2* reverberant. The used values for SEA3 for *room1* are given in Tab. (8.6) and for *room2* the same values as before were used and can be looked up in Tab. (8.5). For the case SEA1, in which *room1* was large and absorbent and *room2* was large and reverberant, the decay curve shows the typical double slope. Comparing the decay curve of SEA2 with SEA1, the only thing that changed is the size of *room2*, it can be seen that the curve obtained with SEA2 is steeper than the curve of SEA1. This means that the energy dissipates faster because of the fact that *room2* is smaller. This effect can be seen even stronger in case of SEA3, were both rooms are small. To sum this example up it was found out that the room dimensions have an influence on the steepness of the decay curves: the smaller the rooms, the steeper the decay curves and the shorter the reverberation times. Comparing these results with Sabine's equation for calculating the reverberation time of rooms, it can be seen that also in Sabine's equation bigger volumes lead to larger values for the reverberation times. Moreover it can be seen that the breakpoint appears earlier in time if the energy decay curve is steeper. In large rooms the breakpoint appears later.

The same room configurations as for Fig. (8.6) are used in Fig. (8.7) but the aperture was reduced from 5 m^2 to 1 m^2 . Changing the aperture size leads to the situation that the influence of *room2* arises later, i.e. that the breakpoint in the decay curves appears later in both directions

(smaller dB values but greater time values). The explanation for this phenomenon is that the smaller aperture decreases the energy exchange between the two rooms and therefore *room1* has more influence on the decay curve as compared to Fig. (8.6) where the aperture was larger. Furthermore it can be noticed that the late part of the decay curve, where the effects of the second room dominate, is not as steep as in the case where the aperture was $5 m^2$.

In the next experiment the aperture size was set to $1 m^2$ and the same results as discussed before were analysed for different frequencies. In Fig. (8.8) the comparison between the results of SEA1, SEA2 and SEA3 obtained for the octave band with centre frequency 1000 Hz are compared to the same experiments obtained at 2000 Hz. In Fig. (8.9) the frequency of the blue curves was 500 Hz. These experiments show that the higher the frequency the steeper the decay curves. This means that the reverberation time becomes shorter, if the frequency is increased. This makes sense because for higher frequencies energy dissipates faster. The breakpoint is shifted down on the vertical axis if the frequency is increased, whereas the horizontal position of the breakpoint is shifted to the left if the frequency is higher.

In the last experiment (result see Fig. (8.10)) the absorption coefficients of the walls of *room2* were set to $\alpha = 0.1$. Again the results are compared to the values presented in Fig. (8.6). It can be seen that an increase of the absorption coefficients leads to steeper decay curves and therefore shorter reverberation times. Energy is dissipated faster if the absorption coefficients are increased. The breakpoint is shifted down on the vertical axis and a little bit to the right on the horizontal axis in the case that the absorption of *room2* is increased.

In the following table the findings from these experiments are summed up, \uparrow stands for increase \downarrow for decrease (for the decay curve increase means steeper and decrease means smoother). The SEA model is therefore in good agreement with well-known phenomena.

Parameter change	Decay curve
room size \uparrow	\downarrow
frequency \uparrow	\uparrow
aperture \uparrow	early \downarrow ; late \uparrow
absorption \uparrow	\uparrow

Table 8.7: Changes of parameters and effects on decay curve

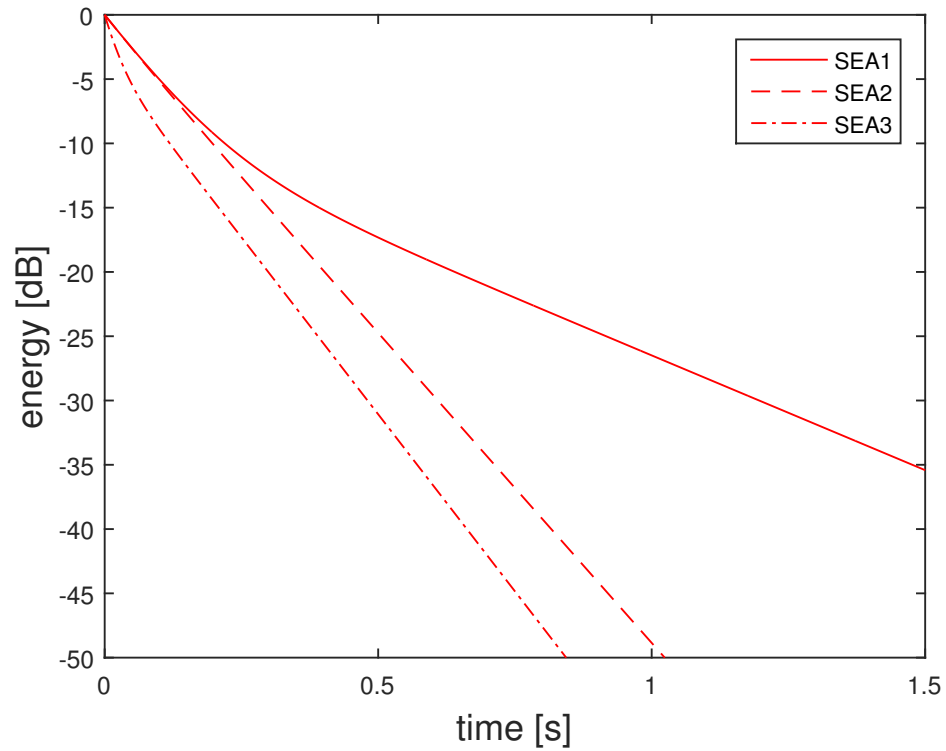


Figure 8.6: Comparison decay curves for different room setups, 1000Hz, aperture 5m^2

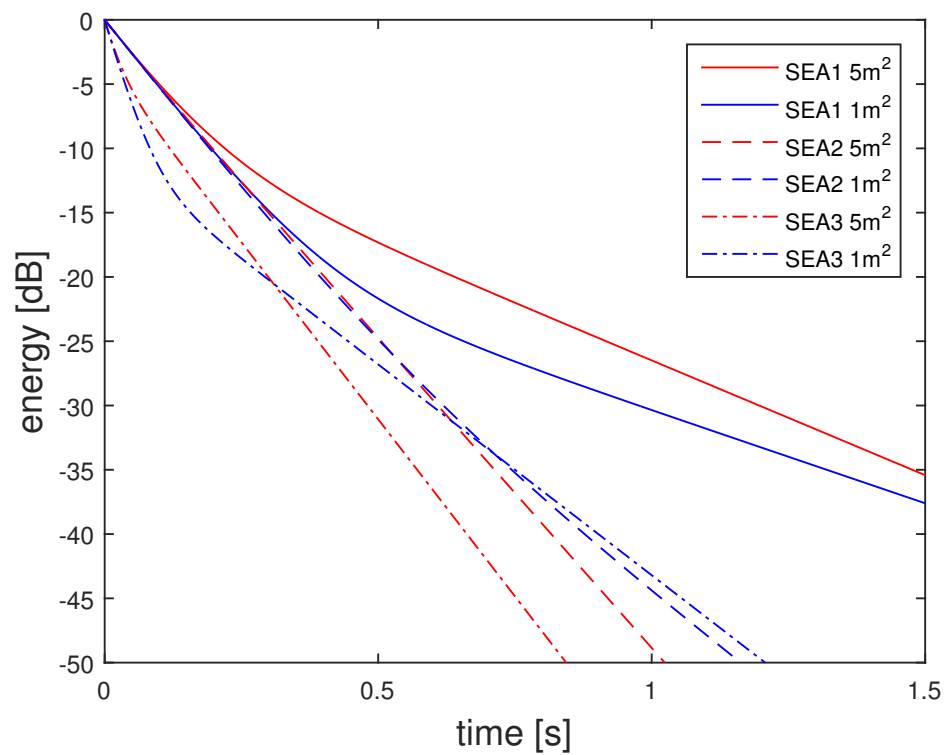


Figure 8.7: Comparison decay curves for different room setups, 1000Hz, aperture 1m^2

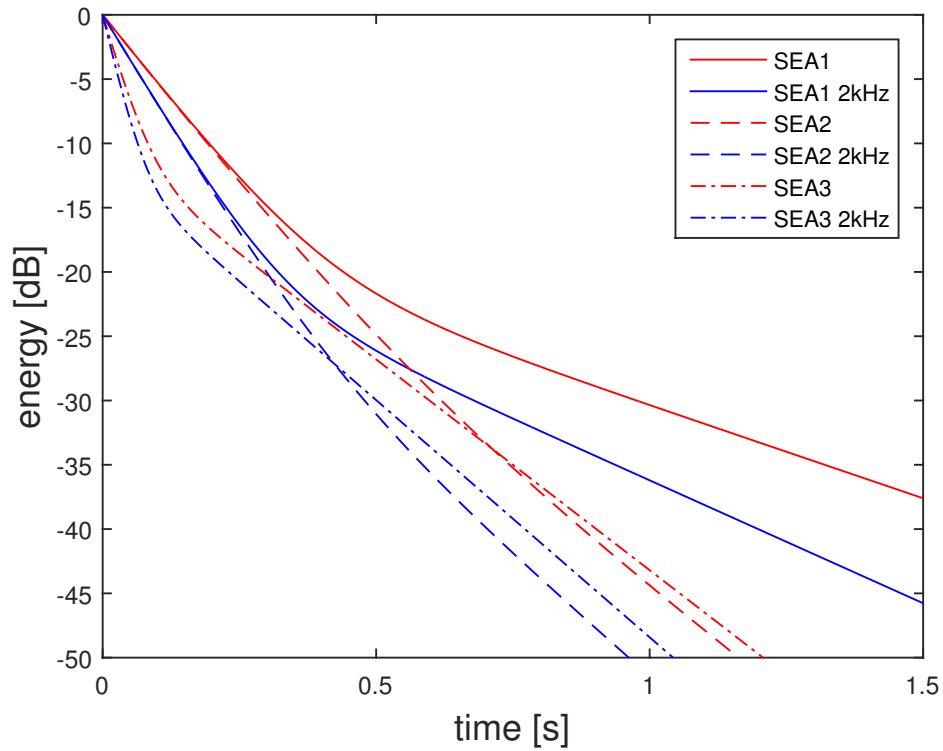


Figure 8.8: Comparison decay curves for different room setups, 2000Hz, aperture $1m^2$

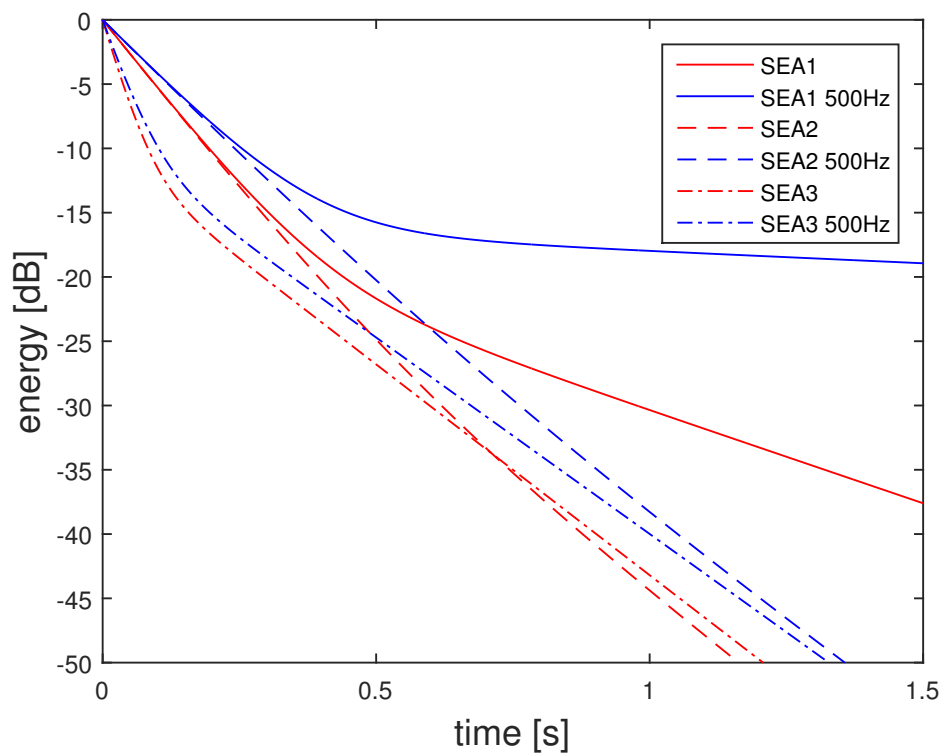


Figure 8.9: Comparison decay curves for different room setups, 500Hz, aperture $1m^2$

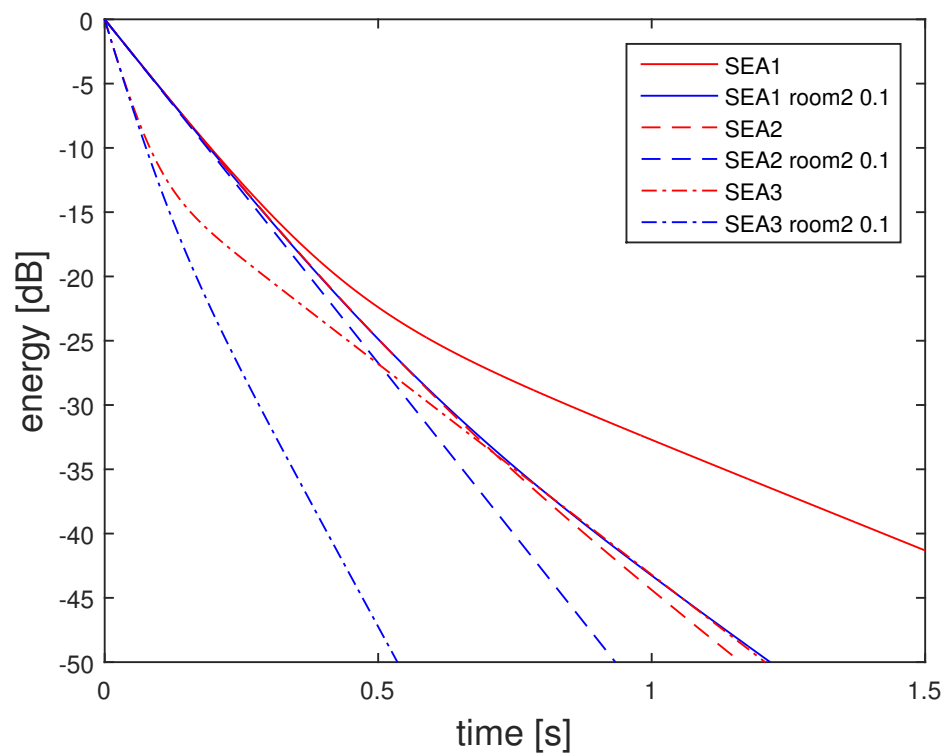


Figure 8.10: Comparison decay curves for different room setups, 1000Hz, aperture 1m², α room2 0.1

9

Calculation of Decay Curves of Rooms Containing Plates

In this chapter the whole SEA system consists of two subsystems: one is a rectangular room and the other subsystem is a plate. As described in the sections before, again the damping loss values and the coupling loss values for the two subsystems have to be determined. With the knowledge of the loss factor matrix, the solution to the system of differential equations is exactly the same as in chapter 8. The difficulty in solving the described problem lies in the determination of the damping and coupling loss factors that characterise the plate. The damping loss factor of the room can be found exactly in the same way as in chapter 8.

9.1 Radiation Factor

One very important value, when calculating the damping loss factor of a plate and later on the coupling loss factor of a plate, is the radiation factor of the analysed plate. In the next section the radiation factor of a plate termed σ is derived.

9.1.1 Meaning of the Radiation Factor

The meaning of the radiation factor in acoustics is shortly described in this subsection. All the information given here is based on [Kollmann et al. 2006].

If a structure produces structure-borne sound and if this sound has a velocity component perpendicular to the surface of the structure, then sound waves are radiated into the air. The radiation factor describes how much sound power is transported from a structure into the air. The specific impedance of air is known as:

$$Z = \rho_0 c_0, \quad (9.1)$$

where ρ_0 stands for the density of air and c_0 is the sound velocity of air. The surface of the structure is called S and \tilde{v}^2 stands for the squared sound particle velocity averaged over S . The effective, radiated sound power is termed P and by using these definitions the radiation factor can be calculated with the following equation:

$$\sigma = \frac{P}{\rho_0 c_0 S \tilde{v}^2}. \quad (9.2)$$

If a rigid surface (e.g. a bulb) is vibrating with a frequency that has a much smaller wavelength in air than the lengths of the surface, then the velocity of the particles in the air has to be equal the velocity of the rigid surface. This means that a plane wave is radiated and therefore the sound particle velocity and sound pressure are in phase. If \tilde{v} is the effective velocity of the radiating surface, then the effective sound pressure of the radiating surface can be calculated

with:

$$\tilde{p} = \rho_0 c_0 \tilde{v}. \quad (9.3)$$

Using this equation the radiated sound power becomes:

$$P = S\tilde{p}\tilde{v} = S\rho_0 c_0 \tilde{v}^2. \quad (9.4)$$

If Eq. (9.4) is inserted into Eq. (9.2) it can be easily seen that $\sigma = 1$. The radiation factor of a vibrating surface is therefore the same as the ratio of the actually radiated power of the structure to the maximum power that a bulb with the same surface as the analysed structure would radiate at the same frequency. It is noticed once again that this maximum power that the bulb radiates is only reached if the bulb's dimensions are large compared to the wavelength of the radiated sound waves. In most of the cases σ is smaller than 1 but there are also cases where $\sigma > 1$.

It is assumed that a plate is excited with a frequency higher than the first resonance frequency of the plate. Furthermore it is supposed that the plate is vibrating with more or less one eigenmode. The plate consists of different regions, where each of the regions vibrates in-phase but adjacent regions vibrate inversely phased. The radiated sound power is dependent on the ratio of the distance between the in-phase antinodes on the plate to the wavelength λ_L of the wave that is radiated into the air. This distance equals the wavelength of the bending wave λ_B . If $\lambda_B < \lambda_L$, then the inversely phased regions of the plate influence the near-field as well as the far-field of the radiated airborne sound, and a phenomenon known as acoustic short-circuit occurs. This means that the vibrations of the plate are immediately balanced by local airflows and this effect degrades the radiation power of the plate.

For the case that $\lambda_B > \lambda_L$, the radiation is termed "complete radiation". The radiation of the wave that is propagating in the air is not happening perpendicular to the surface of the plate. But as coincidence frequency is reached, i.e. $\lambda_B = \lambda_L$, the waves radiated into the air are propagating parallel to the surface of the plate. The wave-field of the bending waves and the wave-field of the waves in the air are in-phase. Therefore the airborne sound wave is fed with new power every time a antinode of the plate is passed. Because of this effect the power supply at coincidence frequency can be much higher than at frequencies higher than f_c , where the angle of radiation is smaller than 90° . At frequencies below the first resonance frequency of the plate, all points of the plate vibrate in-phase and the radiation behaviour of the plate can be described by the radiation behaviour of a bulb.

9.1.2 Determination of the Radiation Factor

The radiation factor of the plate depends on the dimensions of the plate and the plate's material. Because of the importance of the radiation factor in many acoustics problems, e.g. in machines or cars many rectangular plates are used, analytical formulas for calculating the radiation factor exist. The radiation factor is frequency dependent, rising from low frequencies to its maximum value at $f = f_c$, where f_c is known as coincidence frequency. After reaching its maximum value, the radiation factor decreases if frequency is further increased. At high frequencies the value of the radiation factor approaches asymptotically the value 1 as described in the previous subsection in more detail. In [Zeitler 2006] or [Crocker 2007] or [Kollmann et al. 2006] equations for calculating the radiation factor dependent on frequency are given (here the equations from [Zeitler 2006] are used). Some restrictions have to be made to calculate the radiation factor of plates:

- (1) The plate is excited by a concentrated force.
- (2) Only modes that have resonance frequencies in the analysed frequency interval are used.
- (3) The amplitudes of the modes are on average the same and their phases are randomly distributed.

(4) The analysed plate is build in an infinitely extended plate, because this guarantees that there is no air exchange between the upper surface and the lower surface of the analysed plate.

Before deriving the formulas for determining the radiation factor, the equation for calculating the coincidence frequency has to be presented. The coincidence frequency is [Kollmann et al. 2006], defined as:

$$f_c = \frac{c_0^2}{2\pi} \sqrt{\frac{\rho_p L_{z,p}}{B}}, \quad (9.5)$$

where B is the bending stiffness, ρ_p stands for the density of the material the plate is made of and $L_{z,p}$ is the length of the z-dimension of the plate. The bending stiffness can be calculated with [Möser 2009]:

$$B = \frac{E \cdot L_{p,z}^3}{12(1 - \mu^2)}. \quad (9.6)$$

In Eq. (9.6) E stands for the Young's modulus, and μ is known as Poisson number, both E and μ depend on the material. The frequency range for calculating the radiation factor is divided into four regions. In every region different equations for determining the radiation factor are needed. The first frequency interval is lower bounded by 20 (smallest frequency that can be heard) and upper bounded by f_{11} that is given by:

$$f_{11} = \frac{c_0^2 \beta}{2S f_c}, \quad (9.7)$$

with

$$\beta = \frac{\frac{L_{p,x}}{L_{p,y}} + \frac{L_{p,y}}{L_{p,x}}}{2} \quad (9.8)$$

and S the surface of the plate. In the frequency region $20 < f < f_{11}$ the radiation factor is defined as:

$$\sigma = \frac{4S}{c_0^2} \cdot f^2, \quad 20 < f < f_{11}. \quad (9.9)$$

In the frequency region between f_{11} and the coincidence frequency f_c the radiation factor is approximately given by:

$$\sigma \approx \frac{\lambda_c}{S} g_1(\alpha) + \frac{P \lambda_c}{S} g_2(\alpha), \quad f_{11} < f < f_c. \quad (9.10)$$

Before using this equation certain variables have to be defined. The wavelength at coincidence frequency λ_c is defined as:

$$\lambda_c = \frac{c_0}{f_c}. \quad (9.11)$$

In Eq. (9.9) c_0 can be inserted because the speed of sound at the coincidence frequency is equal to the speed of sound of air. This is known by the definition of the coincidence frequency. The variable P in the second term on the right hand side of Eq. (9.8) stands for the perimeter of the plate:

$$P = 2L_x + 2L_y. \quad (9.12)$$

The frequency dependent scaling factors in Eq. (9.8) $g_1(\alpha)$ and $g_2(\alpha)$ can be calculated with the following two equations:

$$g_1(\alpha) = \begin{cases} \frac{8}{\pi^4} \frac{(1-2\alpha^2)}{\alpha(1-\alpha^2)^{\frac{1}{2}}} & f < \frac{f_c}{2} \\ 0 & f > \frac{f_c}{2} \end{cases}, \quad (9.13)$$

and

$$g_2(\alpha) = \frac{1}{4\pi^2} \left[\frac{(1-\alpha^2) \ln\left(\frac{1+\alpha}{1-\alpha}\right) + 2\alpha}{(1-\alpha^2)^{\frac{3}{2}}} \right], \quad (9.14)$$

where α is defined as the square root of the ratio of the analysed frequency to the coincidence frequency, i.e.:

$$\alpha = \sqrt{\frac{f}{f_c}}. \quad (9.15)$$

At coincidence frequency the radiation factor is defined as:

$$\sigma \approx \sqrt{\frac{L_{p,x}}{\lambda_c}} + \sqrt{\frac{L_{p,y}}{\lambda_c}}, \quad f = f_c. \quad (9.16)$$

The radiation factor at f_c depends on the lengths of the plate and the wavelength of the plate at coincidence frequency. At f_c the radiation factor reaches its maximum value. For the case that f is greater than f_c the radiation factor can be determined with the following formula:

$$\sigma \approx \frac{1}{\sqrt{1 - \frac{f_c}{f}}}, \quad f > f_c. \quad (9.17)$$

In the calculations of the radiation factor, there is a case decision: if $\sigma(f)$ reaches a higher value than the value at coincidence frequency, the value of σ is set to the value of σ at f_c because it is not possible that σ is larger than $\sigma(f_c)$. This case decision is especially used in frequencies slightly above f_c because for those frequencies the term in the nominator of Eq. (9.17) can become very small and therefore the value for σ quite high. To avoid this problem the value of the radiation factor for these critical frequencies is set to $\sigma(f_c)$.

As an example the radiation factor of a plate made of acryl glass is analysed. In Tab. (9.1) the material properties and the dimensions of the plate are given.

Length x-dimension	$L_x = 1m$
Length y-dimension	$L_y = 1m$
Length z-dimension	$L_z = 0.008m$
Young's modulus	$E = 2700N/mm^2$
Poisson number	$\mu = 0.37$
Density	$\rho_p = 1180kg/m^3$
Coincidence frequency	$f_c = 4979.6Hz$

Table 9.1: Material values and dimension for a plate of acryl glass

Knowing all the values that are important for calculating the radiation factor, it is possible to plot the radiation factor over frequency (see Fig. (9.1)).

Fig. (9.1) shows the typical course of the radiation factor, when it is plotted over frequency.

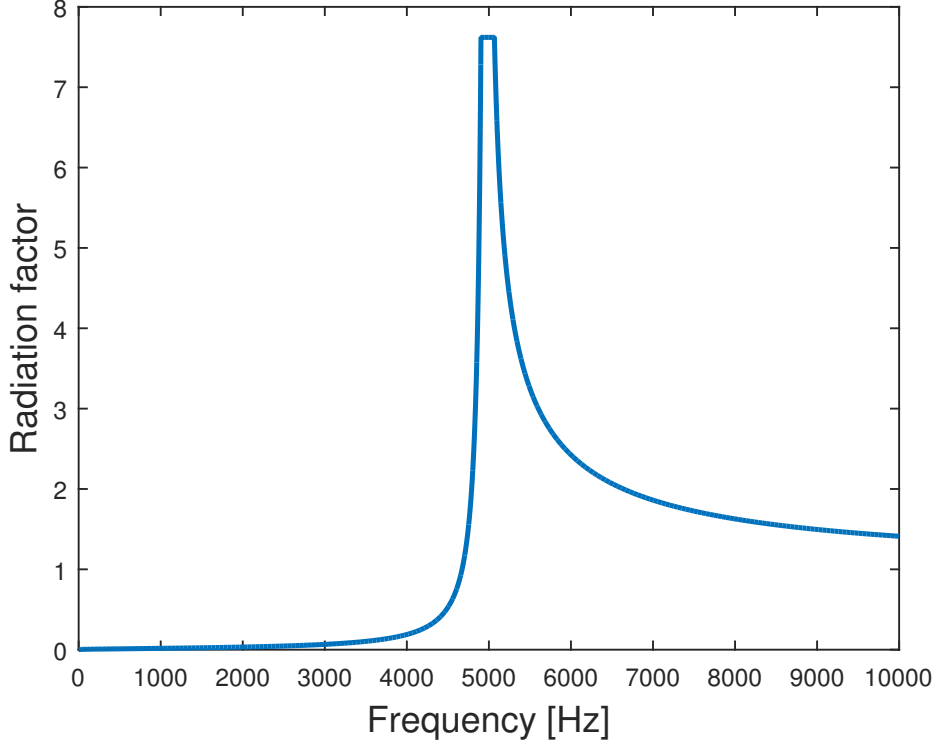


Figure 9.1: Example: Radiation factor for an acrylic glass plate

At low frequencies the radiation factor is increasing until it reaches the coincidence frequency. Then it stays constant (problem described before) and decreases asymptotically. At very high frequencies it reaches the value of 1.

9.2 Calculation of Damping Loss Factors

In [Zeitler 2006] it is mentioned that the damping loss factors of the plate are often looked up in tables but that they can also be calculated. The damping loss factor of a plate can be determined using [Zeitler 2006] or [Norton and Karczub 2003]:

$$\eta = \frac{\rho_0 c_0 \sigma}{\omega m_p}, \quad (9.18)$$

where ρ_0 is the density of air, c_0 is the speed of sound of air, σ is the radiation factor of the plate, ω is the angular frequency and m_p stands for the area specific mass. The specific mass is defined as ([Weselak 2014], [Friesecke 2014]):

$$m_p = \frac{\rho_p V_p}{L_{x,p} L_{y,p}} = \rho_p L_{z,p}, \quad (9.19)$$

with ρ_p the density of the material the plate is made of, V_p the volume of the plate and $L_{x,p}$, $L_{y,p}$ and $L_{z,p}$ stand for the x-, y- and z-dimension of the plate.

9.3 Calculation of Coupling Loss Factors

In this section the calculation of the loss factor due to coupling of the room to plate and plate to room respectively, is presented. [Zeitler 2006] shows an equation for determining the coupling loss factor in the case of the coupling of a plate to a room. By using the reciprocity principle that was presented in Sec. (5.3) in Eq. (5.11) the coupling loss factor for room to plate can be calculated based on the coupling loss factor plate to room. The coupling loss factor for the plate to room scenario is defined in [Zeitler 2006] as (the factor of 2 is introduced here because it is assumed that the plate radiates into the room from two sides, see: [Norton and Karczub 2003, p. 426]):

$$\eta_{pr} = \frac{2\rho_0 c_0 \sigma}{2\pi f m_p}, \quad (9.20)$$

where m_p is the area specific mass of the plate (see Eq. (9.19)). With the help of the reciprocity principle it can be written that:

$$\eta_{rp} n_p = \eta_{pr} n_r, \quad (9.21)$$

where n_p and n_r describe the modal density of the plate and room, respectively. To use this procedure the modal densities of the plate and the room have to be calculated at first. According to [Zeitler 2006] the modal density of a plate can be calculated as:

$$n_p(\omega) \approx \frac{L_{p,x} L_{p,y}}{4\pi} \sqrt{\frac{\rho_p}{B}}. \quad (9.22)$$

This equation for determining the modal density of plates is valid for frequencies higher than f_{11} that was derived in Eq. (9.5). The modal density of the plate is therefore only depending on the mechanical and geometric properties. Moreover the modal density for the room has to be defined. This is again done with [Zeitler 2006], where the modal density of rooms is calculated with:

$$n_r(\omega) = \left(\frac{\omega^2}{2\pi^2 c_0^3} \right) V + \left(\frac{\omega}{8\pi c_0^2} \right) S_A + \left(\frac{1}{16\pi c_0} \right) S_c. \quad (9.23)$$

In Eq. (9.20) V stands for the volume of the room, S_A describes the surface of the room and S_c the length of all the walls of the room. In the case of a rectangular room this values can be calculated as:

$$S_c = 2(L_x L_y + L_x L_z + L_y L_z) \quad (9.24)$$

and

$$S_A = 4(L_x + L_y + L_z). \quad (9.25)$$

With all these definitions the coupling loss factor from room to plate becomes:

$$\eta_{rp} = \frac{\rho_0 c_0 \sigma}{2\pi f m_p} \cdot \frac{n_p}{n_r}. \quad (9.26)$$

Knowing the coupling and damping loss factors, again a system of two differential equations must be solved to get the decay curve and therefore the reverberation time. The system of differential equations is exactly the same as in chapter 8, with the difference that the damping and coupling loss factors of Sec. (9.2) and Sec. (9.3) have to be inserted in Eq. (8.3). The way to solve the differential equations is not presented again here because it is analogue to Sec.

(8.3). But results for a system that contains of a room and a plate are shown in Sec. (9.4).

9.4 Proof of Concept Experiment

In this chapter the results obtained with the SEA method are compared to measurement results. The measurements were made in the same room as presented in Sec. (7.8). Here, the room (parameters see chapter 7.8) was coupled with three plates of acryl glass (parameters see Tab. 9.1) of dimensions $1\text{ m} \times 1\text{ m} \times 0.008\text{ m}$. The plates and the room are coupled but there is no coupling between the plates (see zeros in Eq. (9.27)). The loss factor matrix of this system becomes a 4×4 matrix and can be written as:

$$\mathbf{A} = \begin{bmatrix} \eta_1 + \eta_{12} + \eta_{13} + \eta_{14} & -\eta_{21} & -\eta_{31} & -\eta_{41} \\ -\eta_{12} & \eta_2 + \eta_{21} & 0 & 0 \\ -\eta_{13} & 0 & \eta_3 + \eta_{31} & 0 \\ -\eta_{14} & 0 & 0 & \eta_4 + \eta_{41} \end{bmatrix}. \quad (9.27)$$

The initial energy is assumed to be in the room at first, therefore the vector of the initial energies is:

$$\begin{bmatrix} E_1(0) \\ E_2(0) \\ E_3(0) \\ E_4(0) \end{bmatrix} = \begin{bmatrix} 1 \\ 0 \\ 0 \\ 0 \end{bmatrix}. \quad (9.28)$$

With these definitions it is possible to solve the system of differential equations as shown before (see Sec. (7.6) and Sec. (8.3)). In Fig. (9.2) the results obtained with the SEA method are compared to measurement results, the frequency was set to 1000 Hz. It can be seen that the results of the measurement and SEA method agree nearly perfectly. In the next figure the measurement and SEA results were compared again, this time at a frequency of 4000 Hz. Again the predicted and the measured decay curves fit together very well (the discrepancy starting at around 1 second is again because of the background noise in the measurements). The same absorber as described in Sec. (7.8) was put on the floor. For the 1000 Hz scenario the absorption coefficient was given in Sec. (7.8), in the case of 4000 Hz the absorption value of the used absorber is $\alpha = 1,07479$. In Fig. (9.4) and Fig. (9.5) the decay curves of the room containing an absorber on the floor and coupled with three plates can be seen. Also in the case where SEA is used to calculate the decay curve of a room that contains an absorber on the floor and additionally three plates, it can be said that the method works quite good. There is a discrepancy in the case where the analysis frequency was set to 1000 Hz but for the scenario, where the analysis frequency was set to 4000 Hz the measurement results and the predicted results obtained with SEA are nearly equal. For the 1000 Hz case it could be that the radiation factors of the plate are underestimated by the given equations. The presented plate has a coincidence frequency that is far above 1000 Hz and has a small radiation efficiency at 1000 Hz, which could explain the mismatch between measurement and simulation.

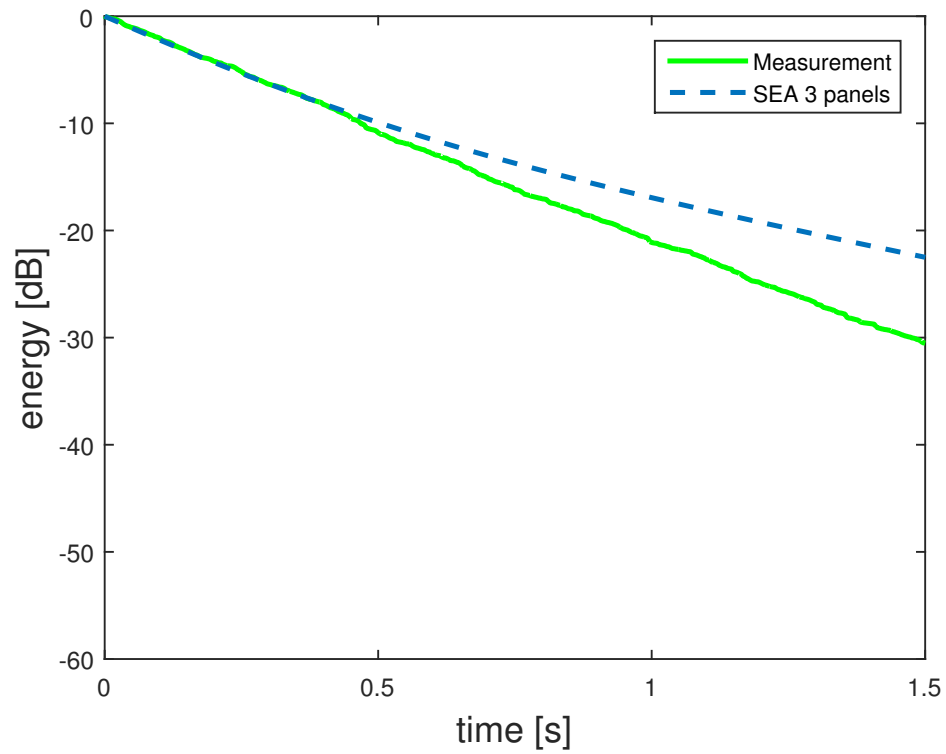


Figure 9.2: Comparison measurement and SEA method: Room coupled with three plates of acryl-glass, 1000Hz

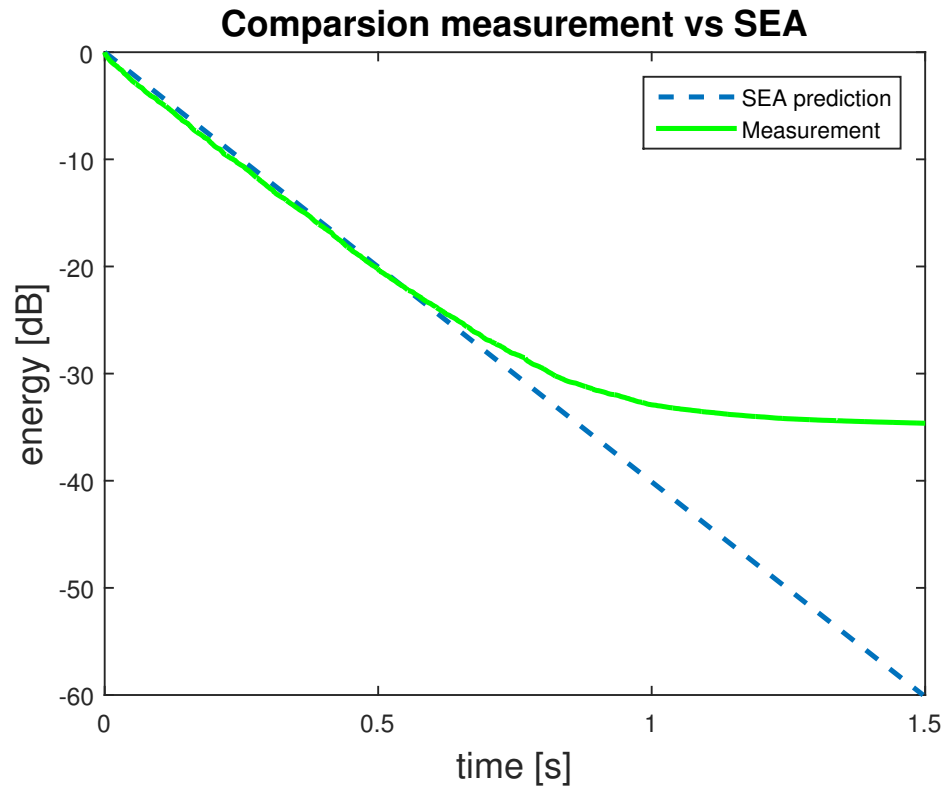


Figure 9.3: Comparison measurement and SEA method: Room coupled with three plates of acryl-glass, 4000Hz

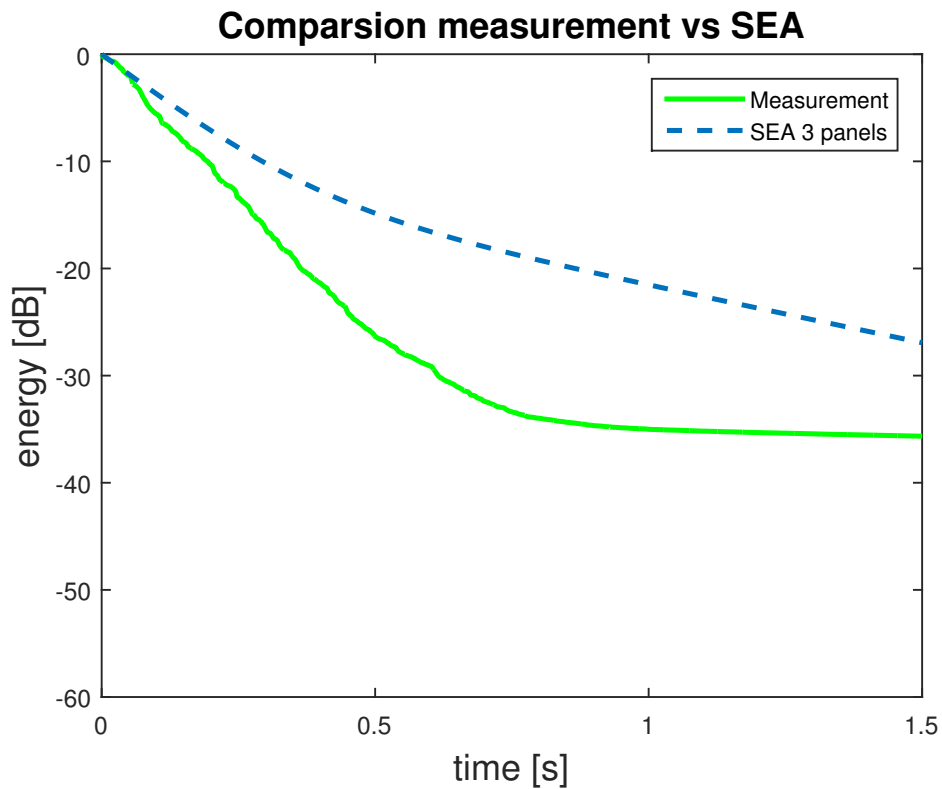


Figure 9.4: Comparison measurement and SEA method: Room coupled with three plates of acryl-glass, absorber on the floor, 1000Hz

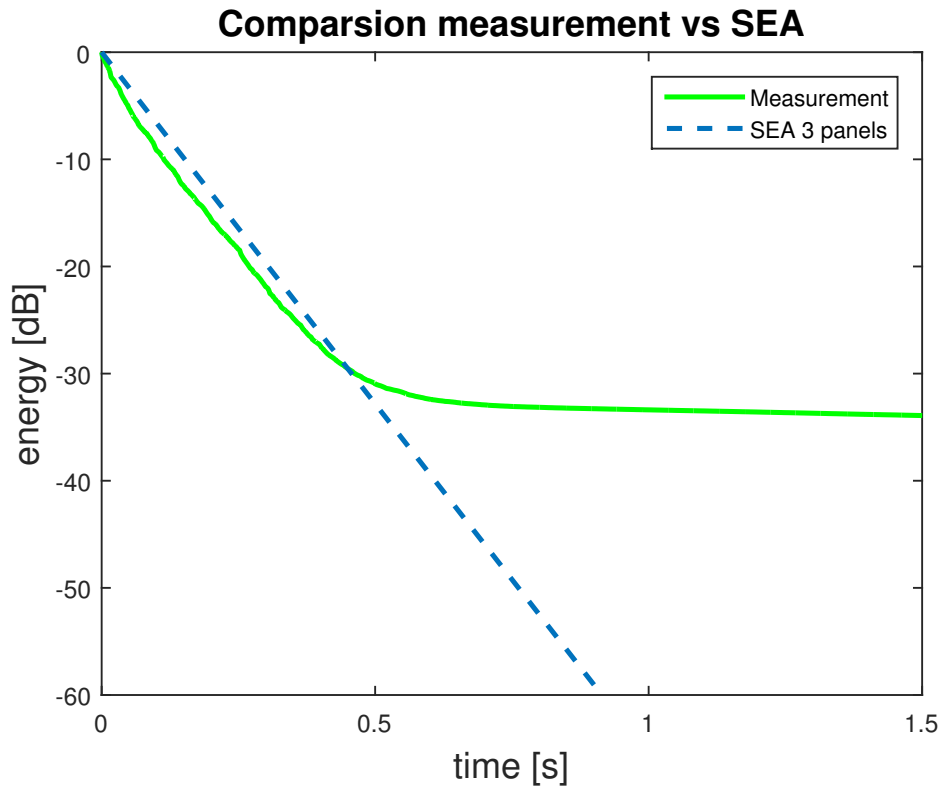


Figure 9.5: Comparison measurement and SEA method: Room coupled with three plates of acryl-glass, absorber on the floor, 4000Hz

10

Calculation of Energy Decay Curve of non-rectangular Rooms

In this chapter SEA is used to determine the energy decay curve of a non-rectangular room. The results simulated with the SEA method are compared to measurement results obtained in a reverberation chamber. It is evaluated if SEA can be used in non-rectangular rooms too, or if it is restricted to rectangular rooms. The procedure used in this chapter is exactly the same as presented before, therefore the main focus in this chapter lies in the analysis of the results.

10.1 Analysis of Energy Decay Curves of non-rectangular Rooms

The measurement results were obtained in a reverberation chamber. The dimensions of the room can be seen in the following two figures (see Fig. (10.1) and Fig. (10.2)). It is clearly visible that the reverberation chamber is non-rectangular.

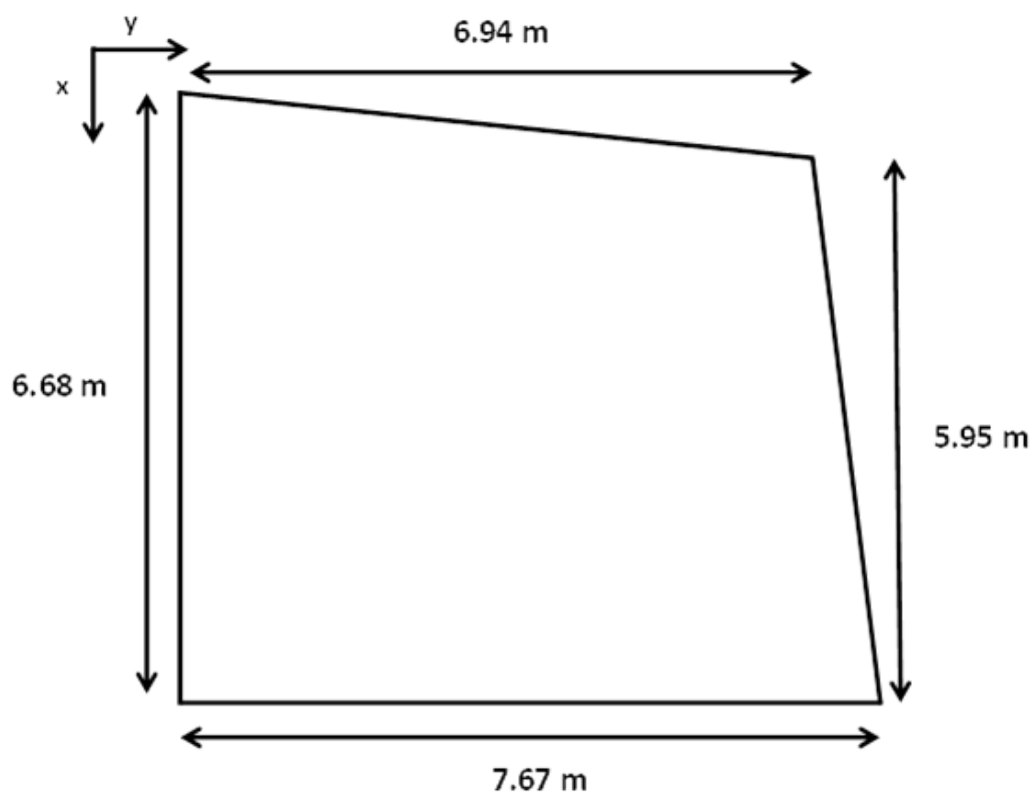


Figure 10.1: Reverberation chamber: ground plot

To use the SEA method presented before that was only valid for rectangular rooms, here, the

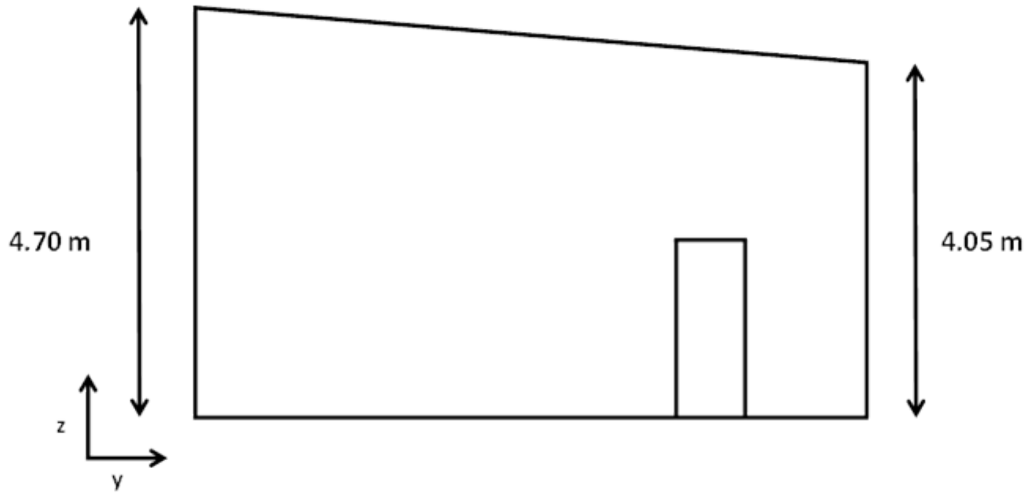


Figure 10.2: Reverberation chamber: front elevation

reverberation chamber is approximated by a cuboid that has the same volume as the actual reverberation chamber. Therefore the dimensions of the room were set to $7.36\text{ m} \times 6.25\text{ m} \times 4.375\text{ m}$. The surface of the floor of the reverberation chamber is 46 m^2 and the volume is 201.25 m^3 . The cuboid has exactly the same surface and the same volume as the reverberation chamber. In the first experiment the measurement results obtained in the empty room, in which all the walls were reverberant, were compared to the SEA results. The absorption coefficient in case of reverberant walls was set to 0.03 in the SEA method. In Fig. (10.3) the results for this scenario for an analysis frequency of 1000 Hz are shown. Notice that for all presented results in this chapter, the measurement results were averaged over 8 microphone positions and two source positions. All together this is an averaging over 16 measurement points. In Fig. (10.4) the comparison of the energy decay curve for the same experiment as before but with an analysis frequency of 4000 Hz is presented. Comparing Fig. (10.3) and Fig. (10.4) shows that if the analysis frequency is changed from 1000 Hz to 4000 Hz the agreement between the energy decay curve obtained by measurement and the one resulting from the SEA method is even increased. Although the values obtained from measurement and prediction are not exactly the same in the 1000 Hz scenario, the SEA method predicts the actual results quite well. The general course of the decay is the same for both methods.

In the next step an absorber is put on the floor. The area of the floor that was covered with the absorber was 13.5 m^2 and the absorption coefficient of the absorber was $\alpha = 1.04$ for 1000 Hz as well as for 4000 Hz. The absorption coefficient of the whole floor was calculated with Eq. (7.47). In Fig. (10.5) and Fig. (10.6) the results of the energy decay curve for the reverberation chamber with an absorber on the floor are presented for an analysis frequency of 1000 Hz and 4000 Hz respectively. Again it can be seen that the SEA method predicts the energy decay curves quite well. The general course of the two curves in Fig. (10.5) and Fig. (10.6) are equal, although there are slight differences in the exact values of the curves.

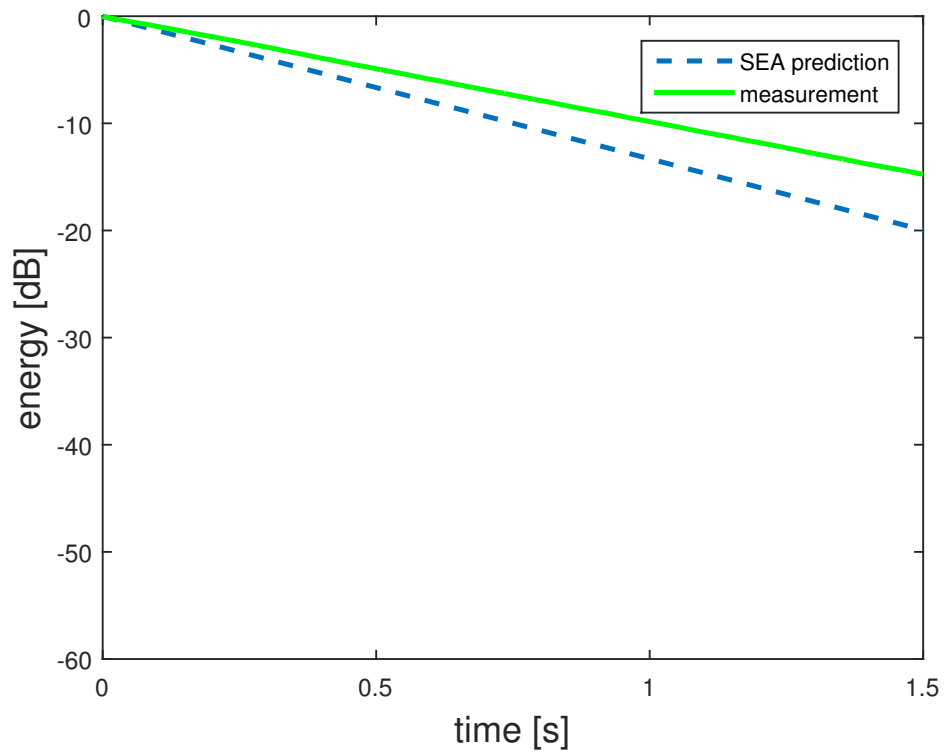


Figure 10.3: Comparison SEA vs measurement: energy decay curve non-rectangular room, all walls reverberant, 1000 Hz

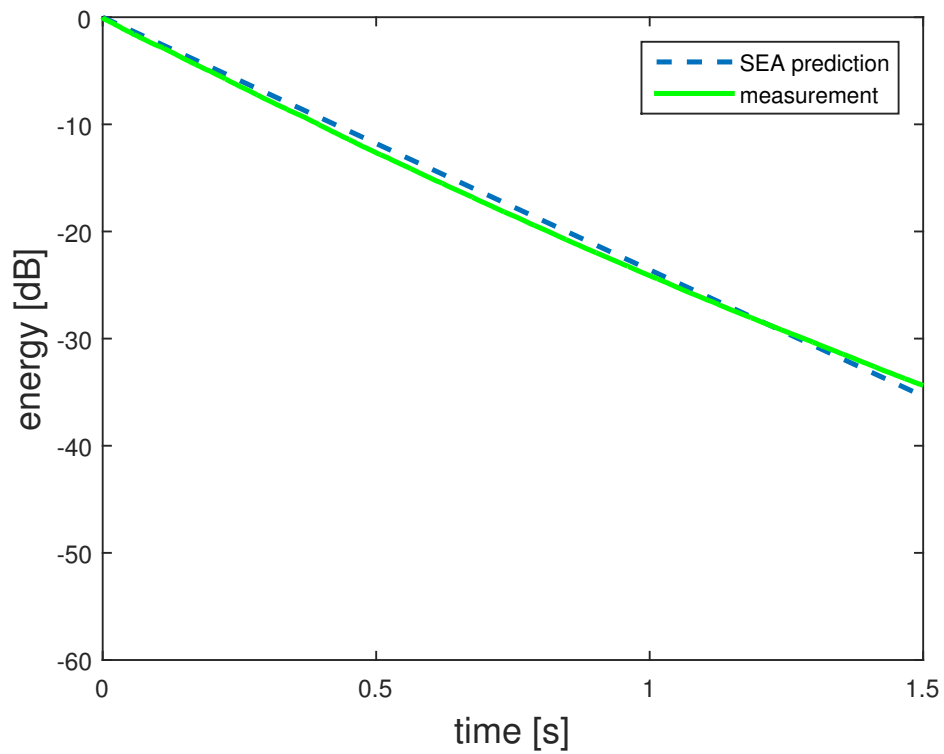


Figure 10.4: Comparison SEA vs measurement: energy decay curve non-rectangular room, all walls reverberant, 4000 Hz

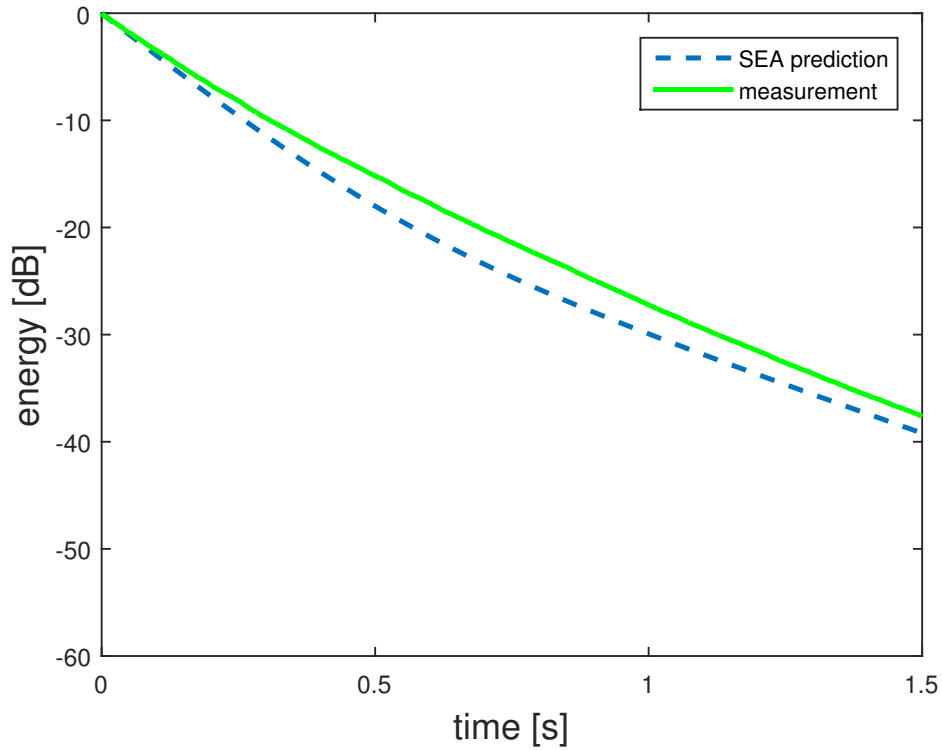


Figure 10.5: Comparison SEA vs measurement: energy decay curve non-rectangular room, absorber on the floor, 1000 Hz

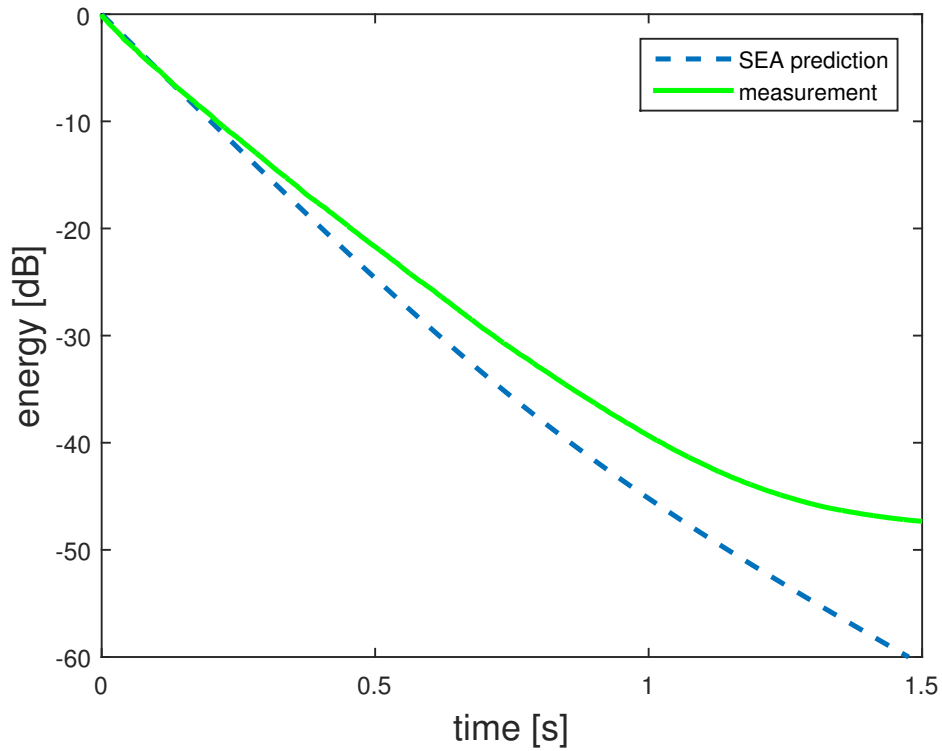


Figure 10.6: Comparison SEA vs measurement: energy decay curve non-rectangular room, absorber on the floor, 4000 Hz

10.2 Energy Decay Curve of non-rectangular Room with Diffusors

In reverberation chambers diffusors are used to obtain a diffuse sound field. In the presented reverberation chamber measurements were made for five different setups. The number of the diffusors and the size of the diffusors was different in each setup. The diffusors were made of acryl glas, the main values of acryl glas can be looked up in Tab. (9.1). In chapter 9 a method was presented to calculate the energy decay curve of rooms coupled with plates (here: plate represents the diffusor). This method can be used to compare the energy decay curves obtained by measurement and by the SEA method for these four setups. In the following table, the main values for each setup are presented, the thickness of all the diffusors was 5mm . The energy

Setup	Number of diffusors	One-sided area of diffusors	Dimensions of diffusors	Total area setup	Total area diffusors room
0	0	0 m^2		0 m^2	0 m^2
1	2	3 m^2	$2\text{ m} \times 1.5\text{ m}$	6 m^2	6 m^2
2	1	1.5 m^2	$1\text{ m} \times 1.5\text{ m}$	6 m^2	12 m^2
	2	2.25 m^2	$1.5\text{ m} \times 1.5\text{ m}$		
3	1	1.5 m^2	$1\text{ m} \times 1.5\text{ m}$	6 m^2	18 m^2
	3	1.56 m^2	$1.25\text{ m} \times 1.25\text{ m}$		
4	4	0.8 m^2	$0.8\text{ m} \times 1\text{ m}$	7 m^2	25 m^2
	1	1.5 m^2	$1\text{ m} \times 1.5\text{ m}$		
	1	2.25 m^2	$1.5\text{ m} \times 1.5\text{ m}$		

Table 10.1: Main values of different setups analysed in reverberation chamber

decay curve for these five different setups was calculated for an analysis frequency of 1000 Hz and 4000 Hz. Based on these energy decay curves the reverberation times T_{20} and T_{30} were calculated. The values for the reverberation time obtained by measurement are compared to the values of the reverberation time obtained by prediction with the SEA method. In Tab. (10.2) the values of the reverberation times are presented for the case where the room did not contain an absorber and the analysis frequency was set to 1000 Hz. The absolute value of the difference between the reverberation times is also given. The same comparison was also done for an analysis

Setup	0	1	2	3	4
Measurement (T30)	6.2021	5.8480	5.7562	5.6828	5.6053
SEA method (T30)	4.5116	8.1739	9.078	9.4915	9.8375
Difference (T30)	1.6905	2.3259	3.3218	3.8087	4.2322
Measurement (T20)	6.1530	5.7985	5.7186	5.6277	5.5743
SEA method (T20)	4.5108	6.8045	8.2981	9.0206	9.5061
Difference (T20)	1.6422	1.006	2.5795	3.3929	3.9318

Table 10.2: Comparison reverberation time, measurement vs SEA, different setups, 1000 Hz, empty room; values in s

frequency of 4000 Hz (see Tab. (10.3)). In the next experiment an absorber was put on the floor of the room and again the reverberation times for different setups obtained by measurement and SEA method were compared. In Tab. (10.4) the results for an analysis frequency of 1000 Hz for all the setups for the room containing an absorber on the floor can be seen. In Tab. (10.5) the analysis frequency was set to 4000 Hz and again the results for the room containing an absorber on the floor are presented. The same comparison was also done for an analysis frequency of

Setup	0	1	2	3	4
Measurement (T30)	2.6157	2.4534	2.3761	2.3807	2.3549
SEA method (T30)	2.5453	1.9026	1.7632	1.7877	1.8112
Difference (T30)	0.0704	0.5508	0.6129	0.593	0.5437
Measurement (T20)	2.5071	2.3460	2.2808	2.2885	2.2662
SEA method (T20)	2.5453	1.8898	1.7432	1.7627	1.7822
Difference (T20)	0.0382	0.4562	0.5376	0.5258	0.484

Table 10.3: Comparison reverberation time, measurement vs SEA, different setups, 4000 Hz, empty room; values in s

Setup	0	1	2	3	4
Measurement (T30)	2.3604	1.8218	1.7094	1.5559	1.5208
SEA method (T30)	2.1690	7.1029	7.8788	8.1643	8.3921
Difference (T30)	0.1914	5.2811	6.1694	6.6084	6.8713
Measurement (T20)	2.2256	1.7701	1.6684	1.5544	1.5121
SEA method (T20)	1.8490	4.9657	6.6816	7.4157	7.845
Difference (T20)	0.3766	3.1956	5.0132	5.8613	6.3329

Table 10.4: Comparison reverberation time, measurement vs SEA, different setups, 1000 Hz, room with absorber; values in s

4000 Hz. By analysing the results it can be seen that the SEA method predicts the course of

Setup	0	1	2	3	4
Measurement (T30)	1.4791	1.2817	1.2119	1.1305	1.1141
SEA method (T30)	1.2467	1.2644	1.2229	1.2667	1.3079
Difference (T30)	0.2324	0.0173	0.011	0.1362	0.1938
Measurement (T20)	1.4337	1.2673	1.2010	1.1157	1.1013
SEA method (T20)	1.2194	1.2318	1.1695	1.1950	1.2219
Difference (T20)	0.2143	0.0355	0.0315	0.0793	0.1206

Table 10.5: Comparison reverberation time, measurement vs SEA, different setups, 4000 Hz, room with absorber; values in s

the reverberation times right in the case of an analysis frequency of 4000 Hz. In the case where the floor of the room was covered with an absorber, the SEA method predicts the reverberation times for an analysis frequency of 4000 Hz even very good for all the different setups. There are only small differences between measurement and simulation in this scenario. In the case of an analysis frequency of 1000 Hz the SEA method gives wrong results. The more plates in the room, the higher the values of the reverberation times of the room. This wrong behaviour can be explained by the value of the radiation factor and the values of the damping and coupling loss factors of the plate. The analysis frequency of 1000 Hz lies far below the coincidence frequencies of the used plates. This means that the radiation factor for the analysis frequency is very small. Therefore the coupling and damping loss factors of the plates are very small (they are multiplied by the value of the radiation factor for the analysis frequency) and the energy decay curve is far too flat. So the 1000 Hz scenario can not be predicted right by the SEA method. Another point that should be mentioned here is that in case of very flat decay curves (this is true for reverberation chambers) slight differences in the steepness of the curve lead to

big differences in the reverberation times, because it takes comparatively long till the -65 , -35 or -25 dB points of the decay curve are reached.

11

Summary and Outlook

11.1 Summary and Outlook

In this chapter a short summary of the thesis is given and the chapter is finished by an outlook how future works could extend the research on SEA.

11.1.1 Summary of Chapters [2-5]

In chapters [2-5] the main theory of SEA was derived. It started with an explanation what Statistical Energy Analysis means and then the historical development of the method was shortly described. Deriving an SEA model is always combined with discussing the energy relations of a simple linear resonator consisting of a mass, a stiffness element, a resistance and an exciting force. The equation of motion of a linear resonator was discussed for different excitation forces and it was found that displacement, velocity and acceleration are related in the same way for every case of excitation. Therefore one can change between different response variables without concern for excitation. Equations for the time averaged potential and time averaged kinetic energies of a linear resonator were found.

The system of a linear resonator was extended to a more complex system, in which the equations of motion were solved using eigenfunctions. The finding of this extension was that more complex dynamical systems can be treated as a group of linear resonators. Moreover it was shown that systems can be described by modal descriptions and wave descriptions and that at least in theory, both ways of describing the systems should lead to the same results. After the discussion of simple linear resonators the next step was to couple two linear resonators and describe the energy effects produced by these coupled systems. The energy exchange between coupled resonators was analysed and based on the energy flow the basic statements of SEA were derived.

The calculation of the mean and the variance of response variables was discussed and it was shown why the calculation of the variance makes sense in SEA. The variance in SEA is not a temporal variance but the variance of the response variables from one similar system to another. The confidence interval, which is another analysis tool in probability theory was also presented.

11.1.2 Summary of Chapters [6-10]

After discussing the basic theory of the method the procedures for applying SEA to real world problems were derived in chapter [6]. It was found that a complex system has to be divided into subsystems. The energy in the system decays, because of the coupling and damping loss factors of the subsystems. To analyse the energy in the complex systems, the coupling and damping loss factors have to be calculated. In case of many subsystems the equations are extended to matrix form and finally the energy matrix can be solved by knowing the energy of the external excitation and the loss factor matrix.

In chapters [7-9] a method based on the principles of SEA was used to calculate the energy decay curve of rooms. Starting with a single rectangular room, in a second step the method was used to calculate the energy decay curve of coupled rooms and in the last step the method was extended to the case where a room was coupled with plates. In the case of the single room, the

room is divided into seven subsystems, where each subsystem represents a mode group. The coupling loss factors, the damping loss factors and the initial energies were derived to finally solve a system of first order linear differential equations. The summation of the energies of the subsystems gives the total energy in the room. The energy of the subsystem can be described by an exponential function that decays by a factor that contains the energy losses due to damping, coupling and dissipation of air. The nice thing here is that the total energy of the room can be calculated depending on time. Based on this result the reverberation time of the room can be calculated. The energy decay curve predicted with SEA was compared with measurement results obtained in a real room and it was found that there is a perfect agreement between measurement and prediction.

The method used to calculate the energy decay curve of a single rectangular room was extended, resulting in a new method to calculate the energy decay curve of coupled rooms. For calculating the damping loss factor in the case of coupled rooms, the reverberation time of the rooms is needed. Here, this value was found by using the SEA method for calculating the energy decay curve (and based on this result the reverberation time) of a single rectangular room as described above. After determining the coupling and damping loss factors for coupled rooms, again a system of differential equations was solved, resulting in the energy decay curve. In this case the results were compared with a method presented in the literature [Bradley and Wang 2005] and it was found that the SEA method is also working very well in this case. Furthermore the method was used to describe the break point in the double slope of the decay curve that is typical for decay curves of coupled rooms.

The last step was to use SEA to derive the energy decay curve of a room that is coupled with plates. The damping loss factor of the plates is needed and the coupling loss factor room to plate and plate to room must be known to get the energy decay curve in this scenario. Equations for both, the coupling and damping loss factor, exist in the literature, where the loss factors can be calculated if the radiation factor of the plate is given. Calculations for the radiation factor were given and the meaning of the radiation factor was explained. Knowing the loss factor matrix again a system of differential equations was solved, resulting in the energy decay curve. For the case of a room coupled with plates the predicted energy decay curve was compared to measurements again, and by analysing the results it was found that measurement and prediction lead to the same results.

Based on all those findings in chapter [10] the SEA method was used to predict reverberation times in a non-rectangular reverberation chamber for different setups. The reverberation times obtained with SEA were compared to measurement results and the results were right if the radiation factor for the analysis frequency was not too low. In case of 4000 Hz the results of measurement and prediction agreed well, but for the 1000 Hz scenario SEA gives wrong results. The analysis frequency of 4000 Hz lies near the coincidence frequency of the used plate that means that the value of the radiation factor is quite large for this frequency and therefore also the damping and coupling loss factors that are directly proportional to the radiation factor give right values. For the 1000 Hz scenario the radiation factor is very low (nearly 0) and therefore also the damping and coupling loss factors are very low and the energy decay curves obtained with SEA are far too flat compared to measurement results.

11.1.3 Outlook

To sum it up it can be said that SEA prediction worked quite good for the analysed cases and is therefore an appropriate method to calculate energy decay curves for different room acoustical situations. Based on the energy decay curves the reverberation time (and other variables of acoustics) can be calculated. The main advantage of SEA to other prediction methods is that the calculations are very simple and can be executed very fast. The limitations of the method lie in the frequency range, for low frequencies the results obtained with SEA are not right. Moreover, in the case of rooms coupled with plates the radiation factor plays an important role.

In lower frequency ranges the calculation of loss factors leads to false values (they are too small) because the equations for calculating the radiation factor give very small values far below the coincidence frequency. The use of SEA in non-rectangular rooms can be further analysed, maybe for different rooms in the future. The method seems to work also in non-rectangular rooms but maybe improvements to the existing method in the case of non-rectangular rooms can be found in future works.

A remaining and very interesting topic is the analytical calculation of the radiation factor and therefore the calculation of the loss factors in case of a room coupled with a plate. It would be very nice if the equations for the damping loss factor and coupling loss factor of plates for frequencies that lie far below the coincidence frequency of the plate could be improved.

12

List of symbols

A	Area; Amplitude coefficient
\mathbf{A}	Acoustic admittance
a	Acceleration; General amplitude constant
B	Mechanical susceptance, $\text{Im}[\mathbf{Y}]$
\mathbf{B}	Bending rigidity
\mathcal{B}	Power flow coefficient for coupled modal energies
b	Normalised modal susceptance
C	General amplitude constant
CC	Confidence coefficient
c	Wave speed
d	Distance; Ordinary differential operator; Modal coupling parameter
E	Energy
\mathbf{E}	Young's modulus
\mathcal{E}	Modal energy
\mathbf{E}	Energy density
e	Exponential function
f	cyclical frequency [Hz]
G	Mechanical conductance
\mathbf{G}	Gain
g	Normalised modal conductance
H	Hankel function

h	Thickness
\mathbf{I}	Wave intensity
J	Bessel function
j	Imaginary number
K	Spring constant
k	Wave number
L	Length; Level on dB scale
\mathbf{L}	Force spectral amplitude
\mathcal{L}	Modal force
l	Force
M	Mass
N	Mode count
n	Modal density
$n(f)$	Modal density per Hertz
$n(\omega)$	Modal density per rad/sec
\mathbf{P}	Pressure spectral amplitude
\mathbf{P}	Wavenumber transform of pressure
p	Pressure; Distributed force excitation
R	Resistance, $\text{Re}[\mathbf{Z}]$; Dashpot constant
r	Radius; viscous resistance coefficient
S	Cross-sectional area
\mathbf{S}	Power spectral density function
T	Tension
t	Time
V	Volume
\mathbf{V}	Volume spectral amplitude

v	Velocity
X	Reactance, $\text{Im}[\mathbf{Z}]$
x	Coordinate position
\mathbf{Y}	Mechanical mobility
\mathcal{Y}	Modal displacement
\mathbf{Y}	Wavenumber transform of displacement
y	Displacement
\mathbf{Z}	Mechanical impedance; Acoustic impedance

α	Absorption coefficient
Δ	Damping bandwidth; Difference operator
δ	Delta function
$\overline{\delta f}$	Average modal frequency spacing, Hz
∂	Partial difference operator
ϕ	Probability density function
Γ	Gamma function
η	Coupling/damping loss factor
κ	Bending radius of gyration
Λ	Generalised spatial difference operator
λ	Wavelength
μ	Normalised inertia coupling coefficient
Π	Power
ρ	Mass density
σ	Standard deviation; Stress
τ	Transmission coefficient
ω	Radian frequency
ξ	Modal frequency ratio
Ψ	Eigenfunction; Mode shape

13

Bibliography

- [Bass et al. 1994] BASS, Henry E.; SUTHERLAND, Louis C.; ZUCKERWAR, Allen J.; BLACKSTOCK, David T.; HESTER, D. M.; *Athmosperic absorption of sound: Furhter Developments*. J. Acoust. Soc. Am. 97 (1), January 1995, pp. 680-683
- [Bradley and Wang 2005] BRADLEY, David T.; WANG, Lily M. ; *The effects of simple coupled volume geometry on the objective and subjective results from nonexponential decay*. J. Acoust. Soc. Am. 118 (3), Pt. 1, September 2005, pp. 1480-1490
- [Cremer et al.1982] CREMER, Lothar; MÜLLER, Helmut A.; SCHULTZ, Theodore J.; *Principles and Applications of Room Acoustics*. Applied Science, New York 1982, Vol. 1
- [Crocker 2007] CROCKER, Malcolm J; *Handbook of Noise and Vibration Control*. John Wiley & Sons, Inc., 2007, p. 94
- [Friesecke 2014] FRIESECKE, Andreas; *Die Audio-Enzyklopädie: ein Nachschlagewerk für Ton-techniker*. Second Edition. Gruyter Saur, 2014, p. 71
- [Kollmann et al. 2006] KOLLMANN, Franz G.; SCHÖSSER, Thomas F.; ANGERT, Roland; *Praktische Maschinenakustik*. Springer-Verlag Berlin Heidelberg, 2006, pp. 99-115
- [Lyon and DeJong 1995] LYON, Richard H.; DEJONG; Richard G.; *Theory and Application of Statistical Energy Analysis*. Second Edition. Newton : Butterworth-Heinemann, 1995
- [Lyon and Eichler 1964] LYON, Richard H.; EICHLER, E.; *Random Vibration of Connected Structures*. J. Acoust. Soc. Am., 36, pp. 1344-1354, 1964
- [Lyon and Maidanik 1962] LYON, Richard H.; MAIDANIK, Gideon; *Power Flow Between Linearly Coupled Oscillators*. J. Acoust. Soc. Am., 34, pp. 623-639, 1962
- [MATHWORKS]; <http://de.mathworks.com/help/matlab/ref/polyfit.html>; 24.07.2016, 21:30
- [Möser 2009] MÖSER, Michael; *Technische Akustik*. Springer-Verlag Berlin Heidelberg, 2009
- [Nilsson 2004] NILSSON, Erling; *Decay Process in Rooms with Non-Diffuse Sound Fields Part I: Ceiling Treatment with Absorbing Material*. Building Acoustics, Volume 11, 2004, pp. 39-60
- [Norton and Karczub 2003] NORTON, M. P.; KARCZUB, D. G.; *Fundamentals of Noise and Vibration Analysis for Engineers*. Second Edittion. Cambridge University Press, 2003, p. 410
- [Pfreundtner 2014] PFREUNDTNER, Felix; *Nachhallzeitprognosen in Räumen mit nicht-diffusem Schallfeld*. Bachelorarbeit, Technische Universität München, 2014

[Pfreundtner et al. 2015] PFREUNDTNER, Felix; MOMMERTZ Eckhard; SEEBER, Bernhard; *Statistische Energie Analyse: Ein Verfahren zur schnellen Prognose der Nachhallzeit in Räumen mit nicht-diffusem Schallfeld*. Fortschritte der Akustik – DAGA '15, Dt. Ges. f. Akustik e.V. (DEGA), 2015, pp. 959 - 962

[Sarradj 2004]; SARRADJ, Ennes; *Energy-based vibroacoustics: SEA and beyond*. CFA/DAGA'04, Strasbourg, 22-25/03/2004

[Smith 1962], SMITH, P. W., Jr; *Response and Radiation of Structural Modes Excited by Sound*. J. Acoust. Soc. Am., 34, pp. 640-647, 1962

[Weselak 2014] WESELAK, Werner; *Technische Akustik*. Lecture script, Version 10.0, 2014

[Wilmschurst and Thompson 2012] WILMSHURST, L.I. ; THOMPSON, D.J.; *A method for predicting the reverberation time and decay curves of rectangular rooms with non-uniform absorption distribution using Statistical Energy Analysis*. Proc. Acoustics 2012, Nantes Conference(2012), pp. 1435-1440.

[Zeitler 2006] ZEITLER, Andreas; *Untersuchung der Hubschrauberinnenakustik mittels der Methode der statistischen Energieanalyse*, Dissertation, Technische Universität München, 2006

14

Appendix

14.1 Description of Figures

In the following table, all the figures of the master thesis are listed.

<i>Figure number</i>	<i>Filename</i>
Figure 2.1	SEA_basic_system.jpg
Figure 3.1	linear_resonator.jpg
Figure 3.2	resonance_curve.jpg
Figure 3.3	frequency_response_rectangular_filter.jpg
Figure 3.4	frequency_response_2_filter.jpg
Figure 3.5	k1_k2_area.jpg
Figure 3.6	contour_for_evaluation.jpg
Figure 3.7	interaction_resonator_plate.jpg
Figure 3.8	plate_connection.jpg
Figure 3.9	direct_reverberation_field_plate.jpg
Figure 3.10	k_area.jpg
Figure 3.11	xs_area.jpg
Figure 4.1	energy_sharing_resonator.jpg
Figure 4.2	spectral_density_indirectly_excited.jpg
Figure 4.3	coupled_MDOF_system.jpg
Figure 4.4	connected_subsystems.jpg
Figure 4.5	energy_transfer_model.jpg
Figure 4.6	reciprocal_system_A.jpg
Figure 4.7	reciprocal_system_B.jpg
Figure 4.8	reciprocal_system_C.jpg
Figure 4.9	plate_point_force.jpg
Figure 4.10	plate_joined_plate.jpg
Figure 4.11	superposition_principle.jpg
Figure 4.12	transmission_two_systems.jpg
Figure 5.1	beam_plate_system.jpg
Figure 5.2	sum_of_pulses.jpg
Figure 5.3	upper_bound_estimation_intervals.jpg
Figure 7.1	decay_curve.eps
Figure 7.2	point_of_intersection_5.eps
Figure 7.3	point_of_intersection_65.eps
Figure 7.4	empty.jpg

Figure 7.5	comparison_empty_1000Hz.eps
Figure 7.6	comparison_absorber_1000Hz.eps
Figure 8.1	coupled_rooms.png
Figure 8.2	bradley_wang_early.eps
Figure 8.3	bradley_wang_final.eps
Figure 8.4	bradleywang_final_comparison.eps
Figure 8.5	bradleywang_final_comparison_exp2.eps
Figure 8.6	SEA1_SEA2_SEA3_5m2.eps
Figure 8.7	SEA1_SEA2_SEA3_1m2.eps
Figure 8.8	SEA1_SEA2_SEA3_1m2_2000.eps
Figure 8.9	SEA1_SEA2_SEA3_1m2_500.eps
Figure 8.10	SEA1_SEA2_SEA3_room2_0_1.eps
Figure 9.1	radiation_factor_example.eps
Figure 9.2	Room_plate_3panels_1000Hz_sigma.eps
Figure 9.3	Room_plate_3panels_4000Hz_sigma.eps
Figure 9.4	Room_plate_3panels_1000Hz_sigma_absorber.eps
Figure 9.5	Room_plate_3panels_4000Hz_sigma_absorber.eps
Figure 10.1	reverberation_chamber_1.png
Figure 10.2	reverberation_chamber_2.png
Figure 10.3	chamber_empty_1000Hz.eps
Figure 10.4	chamber_empty_4000Hz.eps
Figure 10.5	chamber_absorber_1000Hz.eps
Figure 10.6	chamber_absorber_4000Hz.eps

The .jpg files of chapter 2 up to chapter 5 are taken from [Lyon and DeJong 1995]. The pages of the book, where the figures can be found, are given in the descriptions of the figures. All the .eps files were produced with MATLAB. The codes for reproducing the figures are saved in the folder \Matlab.Figures that was submitted with the master thesis. Figures (8.1) and (10.1-10.2) were produced with Microsoft Word.

14.2 Description of Matlab Files

In this section a short description of the written MATLAB files is given, files are submitted in folder \Matlab.Code.

calc_edc.m: Function to calculate the energy decay curve of impulse response obtained by measurement for 1000 Hz case.

calc_edc_4000.m: Function to calculate the energy decay curve of impulse response obtained by measurement for 4000 Hz case.

calc_initial_energy.m: With this function the energy of a room can be calculated, based on the modes of the room.

calc_rad_factor.m: This function can be used to calculate the radiation factor of a plate.

calc_reverberation_time.m: With this function the values for the reverberation time T_{60} , T_{30} and T_{20} can be calculated.

calc_room_decay_DGL.m: MATLAB file to calculate the room decay of a single room as presented in chapter 7.

Comparison_Bradley_Wang_figure7_3.m: With this file it is possible to compare the energy decay curve of coupled rooms obtained with the SEA method with results obtained with the Bradley&Wang method.

Coupled_Rooms_DGL_function_comment.m: Calculation of energy decay curve of two coupled rooms based on the SEA method.

Coupling_Room_Plate_DGL_function.m: This function calculates the energy decay curve of a room that is coupled with a single plate based on SEA.

Coupling_Room_Plate_DGL_function_3plates.m: Determination of energy decay curve of a room coupled with 3 plates.

Coupling_Room_Plate_DGL_function_number_plates.m: Calculation of energy decay curve of a room coupled with an arbitrary number of plates. The number of plates is an input variable. Can be used in cases where all the plates have the same dimensions and are made of the same material.

Coupling_Room_Plate_DGL_function_chamber_setup1.m: Function to calculate the energy decay curve of reverberation chamber for setup1, 1000 Hz case.

Coupling_Room_Plate_DGL_function_chamber_setup1_4000.m: Function to calculate the energy decay curve of reverberation chamber for setup1, 4000 Hz case.

Coupling_Room_Plate_DGL_function_chamber_setup2.m: Function to calculate the energy decay curve of reverberation chamber for setup2, 1000 Hz case.

Coupling_Room_Plate_DGL_function_chamber_setup1_4000.m: Function to calculate the energy decay curve of reverberation chamber for setup2, 4000 Hz case.

Coupling_Room_Plate_DGL_function_chamber_setup3.m: Function to calculate the energy decay curve of reverberation chamber for setup3, 1000 Hz case.

Coupling_Room_Plate_DGL_function_chamber_setup3_4000.m: Function to calculate the energy decay curve of reverberation chamber for setup3, 4000 Hz case.

Coupling_Room_Plate_DGL_function_chamber_setup4.m: Function to calculate the energy decay curve of reverberation chamber for setup4, 1000 Hz case.

Coupling_Room_Plate_DGL_function_chamber_setup4_4000.m: Function to calculate the energy decay curve of reverberation chamber for setup4, 4000 Hz case.

damping_air.m: This function calculates the damping value of air.

damping_air_chamber.m: Calculation of the damping of air for chapter 10. Different values for the temperature and the humidity of air as in damping_air.m.

Room_decay_Hallraum_chamber.m: Calculation of the energy decay curve of the reverberation chamber, setup0.

Room_decay_Hallraum_chamber_setup1.m: Calculation of the energy decay curve of the reverberation chamber, setup1.

Room_decay_Hallraum_chamber_setup2.m: Calculation of the energy decay curve of the reverberation chamber, setup2.

Room_decay_Hallraum_chamber_setup3.m: Calculation of the energy decay curve of the reverberation chamber, setup3.

Room_decay_Hallraum_chamber_setup4.m: Calculation of the energy decay curve of the reverberation chamber, setup4.

Inputfile_energy_decay_curve_coupled_rooms.m: Inputfile for calculation of energy decay curve of coupled rooms.

Inputfile_energy_decay_curve_room_plate.m: Inputfile for calculation of energy decay curve of room coupled with plate.

Inputfile_energy_decay_curve_single_room.m: Inputfile for calculation of energy decay curve of a single room.

The figures were produced with the following MATLAB files (folder: \Matlab_Figures):

Room_decay_DGL_figure7_1.m: Starting this file Fig. (7.1) can be reproduced.

Room_decay_DGL_figure7_2.m: Starting this file Fig. (7.2) can be reproduced.

Room_decay_DGL_figure7_3.m: Starting this file Fig. (7.3) can be reproduced.

Room_decay_DGL_comparison_empty_figure7_5.m: Starting this file Fig. (7.5) can be reproduced.

Room_decay_DGL_comparion_empty_figure7_6.m: Starting this file Fig. (7.6) can be reproduced.

Early_late_Bradley_Wang_figure8_1.m: Starting this file Fig. (8.1) can be reproduced.

Early_late_Bradley_Wang_figure8_2.m: Starting this file Fig. (8.2) can be reproduced.

Comparison_Bradley_Wang_figure8_3.m: Starting this file Fig. (8.3) can be reproduced.

Comparison_Bradley_Wang_figure8_4.m: Starting this file Fig. (8.4) can be reproduced.

Room_Room_DGL_comparison_figure8_5.m: Starting this file Fig. (8.5) can be reproduced.

Room_Room_DGL_comparison_figure8_6.m: Starting this file Fig. (8.6) can be reproduced.

Room_Room_DGL_comparison_figure8_7.m: Starting this file Fig. (8.7) can be reproduced.

Room_Room_DGL_comparison_figure8_8.m: Starting this file Fig. (8.8) can be reproduced.

Room_Room_DGL_comparison_figure8_9.m: Starting this file Fig. (8.9) can be reproduced.

Radiation_factor_figure9_1.m: Starting this file Fig. (9.1) can be reproduced.

Radiation_factor_figure9_1.m: Starting this file Fig. (9.1) can be reproduced.

Coupling_Room_plate_DGL_main_inputbox_comparison_figure9_2.m: Starting this file Fig. (9.2) can be reproduced.

Coupling_Room_plate_DGL_main_inputbox_comparison_figure9_3.m: Starting this file Fig. (9.3) can be reproduced.

Coupling_Room_plate_DGL_main_inputbox_comparison_figure9_4.m: Starting this file Fig. (9.4) can be reproduced.

Coupling_Room_plate_DGL_main_inputbox_comparison_figure9_5.m: Starting this file Fig. (9.5) can be reproduced.

Room_decay_Hallraum_chamber_figure10_3.m: Starting this file Fig. (10.3) can be reproduced.

Room_decay_Hallraum_chamber_figure10_4.m: Starting this file Fig. (10.4) can be reproduced.

Room_decay_Hallraum_chamber_figure10_5.m: Starting this file Fig. (10.5) can be reproduced.

Room_decay_Hallraum_chamber_figure10_6.m: Starting this file Fig. (10.6) can be reproduced.